Morphological and Molecular Studies on Photoreceptors in Echinodermata

Dissertation
zur Erlangung des Grades
des Doktors der Naturwissenschaften
im Fachbereich Biologie, Chemie und Pharmazie
der Freien Universität Berlin

vorgelegt von
Esther Ullrich-Lüter
aus Berlin

März 2011

Gutachter

Erster Gutachter:	Prof. Dr. Klaus Hausmann Institut für Biologie Fachbereich Biologie, Chemie, Pharmazie Freie Universität Berlin
Zweiter Gutachter:	Prof. Dr. Thomas Bartolomaeus Institut für Evolutionsbiologie und Ökologie Mathematisch-Naturwissenschaftliche Fakultät Rheinische Friedrich-Wilhelms-Universität Bonn
Datum der Disputation:	15. April 2011

Erklärung

Hiermit erkläre ich, dass ich die vorliegende Arbeit ohne die unzulässige Hilfe Dritter und ohne die Verwendung anderer als der angegebenen Hilfsmittel angefertigt habe. Die aus anderen Quellen direkt oder indirekt übernommenen Daten und Konzepte sind unter Angabe der Quelle gekennzeichnet.

Die Arbeit wurde bisher weder im In- noch im Ausland in gleicher oder ähnlicher Form einer anderen Prüfungsbehörde vorgelegt.

Berlin, den 14. März 2011

Esther Ullrich-Lüter

Danksagung

Mein herzlicher Dank gilt Herrn Prof. Dr. Klaus Hausmann für die abschließende Betreuung dieser Dissertation und die Übernahme der Komissionsleitung des Promotionsverfahrens.
Ganz besonders bedanken möchte ich mich bei Herrn Prof. Dr. Thomas Bartolomaeus für die freundliche Aufnahme in seine Arbeitsgruppe und die Betreuung dieser Dissertation.
Mein besonderer Dank gilt ebenfalls Herrn Dr. Harald Hausen für seine fachliche Betreuung und für die inhaltliche Unterstützung bezüglich diverser Stipendien- und Finanzierungsanträge, ohne die diese Arbeit so nicht zustande gekommen wäre. In diesem Rahmen möchte ich mich ebenfalls bedanken für ein Auslandsforschungsstipendium, gewährt vom DAAD, und für die Unterstützung durch die DFG im Rahmen des Projektes HA 4443/4-1 innerhalb des SPP 1174 "Deep Metazoan Phylogeny".
Ich danke Herrn Dr. Thomas Stach für die freundliche Aufnahme in seine Arbeitsgruppe.
Desgleichen gilt mein Dank meinen Kollegen der ehemaligen AG 15, insbesondere Anne Zakrzewski, mit der mich fast mein gesamter Weg durch Studium und Doktorarbeit verbindet, Tobias Kaller, für dessen Unterstützung besonders während des letzten Jahres ich sehr dankbar bin, Sabrina Kaul für ihre große Hilfsbereitschaft, vor allem bei wiederkehrenden Schwierigkeiten mit Bildbearbeitungsprogrammen, sowie Alexander Ziegler für seine Unterstützung bei der Generierung und Auswertung der µCT Daten. Waltraud Brackwehr möchte ich sehr herzlich danken für die unermüdliche Unterstützung bei der Überwindung bürokratischer Hürden eines Universitätsalltags.

Prof. Dr. Johannes Müller vom Museum für Naturkunde, Berlin, sei gedankt für den extrem kurzfristigen Zugang zum µCT in seiner Arbeitsgruppe.

Meinen Kooperationspartnern M. Ina Arnone und Sam Dupont gebührt mein herzlichster Dank für eine anhaltend begeisternde und fruchtbare Zusammenarbeit.

Danken möchte ich ebenfalls ganz herzlich meiner Familie, die mich in den letzten Jahren mit fortwährendem Interesse an einem doch recht speziellen Forschungsthema begleitet, und mich in meiner Arbeit damit sehr bestärkt hat.

Mein spezieller und innigster Dank gilt meinem Mann Carsten Lüter. Ohne seine vorbehaltlose Unterstützung in allen wissenschaftlichen und nichtwissenschaftlichen Angelegenheiten wäre diese Arbeit so nicht zustande gekommen.

Table of contents

1. INTRODUCTION

1.1. Photoreceptors

Perception of light comprises one of the most important sensory capabilites in animals. Photoreception is deployed e.g. for vision, dial migrations, predator avoidance and circadian rhythms. These widely differing tasks can be accomplished through a vast amount of different photoreceptive organs, which evolved in the course of animal evolution. The structural organization of a photoreceptive organ used for a certain purpose is highly variable in both cell composition and arrangement. While e.g. vision in some phyla is achieved through very complex structures like a camera-type eye in vertebrates and cephalopods or a compound eye in arthropods, other animals manage to detect the direction of incoming light (although with a lower resolution) through much simpler organs consisting of just one photoreceptor cell shielded by some dark pigment (Gehring and Ikeo 1999, Land 2005, Fain et al. 2010). This huge divergence led to the hypothesis that eyes developed independendly between 40 and 65 times throughout the animal kingdom (Salvini-Plawen and Mayr 1977, Salwini-Plawen 1982). Other researchers focussed more on the cell types deployed as the functional units of the different “eye-like organs”. Eakin (1979, 1982) in opposition to Salwini-Plawen proposed two major evolutionary lines of photoreceptor cell evolution within Metazoa. The main reason to hypothesize this diphyletic origin of photoreceptor cell types was their distinct morphology. Most photoreceptor cells show a membrane enlargement to host the membrane-bound photopigment, a necessity to be able to sense light. Eakin concluded that deuterostomes retained the evolutionarily older photoreceptor cell type characterized by a ciliary membrane enlargement, whereas protostomes deployed a so-called rhabdomeric photoreceptor cell type, in which the apical cell membrane folds into numerous microvilli to enlarge the area for photopigment storage.

Due to molecular research of the last decade photoreceptor cell types can now be classified based not only on morphological characters but also on the expression of certain photopigment components (opsins) and other “eye-relevant” genes (see sections 1.2 and 1.4 of this chapter). Expression analyses of complex photoreception light transduction cascades established that indeed, ciliary photoreceptor cells express a distinct set of genes (among others the accordingly named c-opsin) whereas rhabdomeric photoreceptors express another distinct set (including the so- called r-opsin). But besides offering additional characters to morphological descriptions, photoreceptor cell “fingerprinting” methods provided some surprising discoveries within the last years. An r-opsin expressing photoreceptor was identified in the vertebrate retina which so far escaped attention due to its lack of microvillar membrane specialization (Provencio et al.

2000, Hattar et al. 2002, Rollag et al. 2003, Fu et al. 2005, Bellingham et al. 2006) and two protostome animals were shown to possess c-opsin expressing photoreceptors (Arendt et al. 2004, Passamaneck et al. 2011), a feature formerly believed to be restricted to deuterostomes. These findings have important implications for the present study. First, presence of ciliary as well as rhabdomeric photoreceptor cell types including their associated complex phototransduction cascades in both, Protostomia and Deuterostomia suggests that these taxa inherited both cell types from their last common Bilaterian ancestor (Arendt and Wittbrodt 2001, Arendt 2003, Koyanagi et al. 2005). Second, molecular methods can be used to investigate identity of photoreceptor cells, even if they lack typical morphological characters like prominent membrane enlargements or an associated screening pigment.

1.2. Opsins

Opsins (the protein part of animal photopigments) are essential components of the light transduction cascades of photoreceptor cells. It has been shown that different opsins are deployed by different photoreceptor cell types (Arendt 2003, Arendt et al. 2004, Land 2005, Terakita 2005) and that the presence of these photopigments can be used to (i) localize and (ii) identify photoreceptors in hitherto unknown structures or organisms.

The typical molecular structure of an opsin consists of a seven transmembrane alpha helix that has an intracellular carboxyterminal tail (C-terminus) and an extracellular amino-terminal segment (N-terminus). Opsin proteins are bound to a chromophore (in most cases a Retinaldehyde Vitamin A derivate) through a Schiff base bridge to a Lysine (Bellingham et al. 2006, Terakita 2005, Fain et al. 2010). When the chromophore is excited by photons it changes its configuration from the 11-*cis* form to an all-*trans* form, inducing a structural change on the opsin protein. The activated opsin then drives an intracellular cascade of enzymatic reactions involving the G-protein and different second messengers. These cascades are significantly different in the ciliary and the rhabdomeric photoreceptor cell type (Arendt 2003, 2008).

Classification of opsins has been performed starting from genome and expression analysis of many different organisms, leading to a somewhat puzzling variety of nomenclature and categorization (Frederiksson et al. 2003, Terakita 2005). The present thesis focusses on two out of (so far detected) six *S. purpuratus* opsins, namely the c-opsin and the r-opsin (see also section 1.4. of this chapter). The presented opsin phylogeny (Text-Fig. 1) displays these two *S. purpuratus* opsins clustering accordingly with r-opsin and c-opsin orthologs of other species.

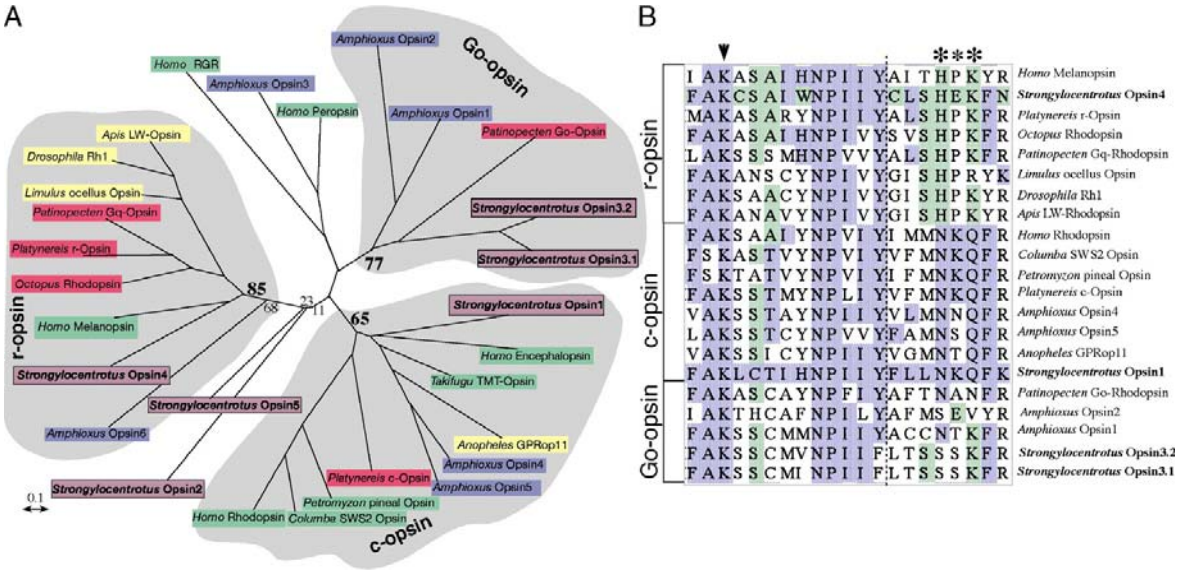

Text-Fig. 1: Phylogeny of opsins showing the position of photopigments used in the purple sea urchin *S. purpuratus* (adopted from Raible et al. 2006).

1.3. Photoreception in echinoderms

1.3.1. Photobehavior and proposed photoreceptive mechanisms

Photobehavior in echinoderms is well documented in many species representing all echinoderm classes. Yoshida (1966) compiled a list of 6 holothuroids, 10 asteroids, 10 echinoids and 6 ophiuroids that show photoelicited behavior reported by different authors which demonstrates that photoreception is obviously an important sensory feature for many echinoderm taxa. Photosensitivity thereby results in a variety of responses including color changes, reaction of single effector organs such as spines or podia, covering, directed phototaxis of the whole animal, spatial vision, diurnal migration and regulation of reproductive cycles (Yoshida 1966, Millott 1975, Pearse et al. 1986, Blevins and Johnsen 2004, Yerramilli and Johnsen 2010) Ecologically the photosensitive species might thus benefit from predator avoidance as well as from prey localization in carnivores, protection from UV-damage and enhanced feeding and reproductive success.

Crinoids are not explicitly listed in Yoshida's list of photosensitive echinoderms but are suspected to be responsive, too (Yoshida 1966). Feather stars are highly underexamined, but according to textbooks and diver´s observations they are well known to show diurnal migration, hiding in crevices over daytime and moving outside to filter feed in the dark.

Taking their vast amount of different photoreactions into account (Yoshida 1966, Millott 1975) it is astonishing that most echinoderms have so far been considered “eyeless” creatures. Apart from so-called optic cushions in Asteroidea (Vaupel von Harnack 1963, Eakin and Brandenburger 1979, Penn and Alexander 1980, Takasu and Yoshida 1983) and a proposed optic organ in the holothurian species *Opheodesoma spectabilis* (Yamamoto and Yoshida 1978) no distinct photoreceptors have been detected yet despite

more then a century of dedicated research. Diadematid sea urchins have once been mistakenly proposed to possess eyes (Sarasin and Sarasin, 1887), but later investigators characterized those structures to be iridiophores, which in fact represent the least photosensitive part of the diadematid sea urchin epidermis (Millott 1953, 1954, 1975, Millott and Manly 1961).

Missing structural evidence and behavioral observations since the late 19th century, therefore led to the hypothesis of a so called “dermal” or “neural” light sense in echinoderms, that was supposed to be the basis of the animals photosensory capabilities. This dermal light sense was thought to deploy unspecialized neurons of the epidermal nerve net as primary photoreceptors (for review see Yoshida, 1966). The onset of electrophysiological studies in echinoderms and the finding that parts of the animal's internal nervous system - namely the radial nerves - are intrinsically photosensitive (Yoshida and Millott, 1959) supported that view. But the unique organization of the echinoderm nervous system, which lacks a distinct centralized brain, hampered further in depht electrophysiological studies. Thus, it is important to note that although well excepted within the scientific community for a long time, the deployment of unspecialized epidermal nerve cells as primary photoreceptors in echinoderms has never been demonstrated by any researcher.

Several authors have demonstrated that the degree of photosensitivity varies depending on the investigated region of the echinoderm body surface. In some ophiuroids the aboral surface is more sensitive then the oral one (Mangold 1909, Aizenberg et al. 2001), and in the sea cucumber *Holothuria surinamensis* the photosensitivity is greatest at its anterior end and least in the midbody region (Crozier 1915). Millott (1954) by measuring spine movements after illumination and/or shading, observed that in the sea urchin *Diadema antillarum*, epidermal photosensitivity varies between different body regions of the animal. Photosensitivity is greatest at the ambulacral margins and decreases towards the ambulacral center, the interambulacrum being the least sensitive area of the body. Millot (1960) and Millot and Coleman (1969) later described the “podial pit” and the “podial ganglion”, i.e. an epidermal thickening near the bases of the podia where photosensitivity is greatest, and which they therefore assumed to correspond to their observations of photosensitivity. This unequal distribution of photosensitivity in *Diadema antillarum* was confirmed later with a more refined technique by Millott and Yoshida (1960a, 1960b), but the meaning of all this remained unclear.

Probably due to the intentionally careful interpretation through these and other early investigators, the results of some echinoderm body regions being more photosensitive then others seem to have been buried in obliviation regarding current publications on the issue. Blevins and Johnsen (2004) and Yeramilli and Johnsen (2010) e.g. do not take in

account these previous results on different regional sensitivity and propose a model for spatial vision in echinoids that only makes sense if an “overall” dermal light sense exists.

1.3.2. Photic reactions in respect to involved organs/body regions

Echinoderm photic reactions involve different organs and body regions and can, according to Yoshida (1966) be classified in three categories: direct responses, reflex responses of component parts of the animal and behavioral responses of the whole animal.

"Direct responses" include color changes due to photoreactivity of chromatophores expanding when illuminated and contracting in darkness (Kleinholz 1938, Millott 1952, Yoshida 1956) - a partly morphological and partly physiological phenomenon that will not be adressed further in the present study.

“Reflex responses” according to Yoshida (1966), include reactions of spines, tube feet, pedicellaria, tentacles and skin upon sudden increases or decreases in illumination. Spine reactions like the “jerk” in diadematids displayed upon sudden shading (Millot 1954), can be impressive and have been investigated in many different species including *Centrostephanus longispinus* (von Uexküll 1897a, 1897b, 1900, Hess 1915), *Arbacia punctulata* (Holmes, 1912), *Diadema antillarum* (von Uexküll 1897b, 1900, Millott and Yoshida, 1959), and *Arbacia lixula* (Mangold 1909).

Tube feet have also been shown to be photoreactive in a variety of species. Two reaction types can be observed. First, the bending reaction towards or away from the light as has been reported in the asteroid *Asterias rubens* (van Weel, 1935) and the echinoid *Strongylocentrotus purpuratus* (personal observation), and second an immediate withdrawel of tube feet upon changes in light intensity. *Arbacia punctulata* (see Holmes, 1912), and *Asterias sp.* (Moore, 1921) retract their tube feet upon illumination, whereas *Diadema antillarum* (see Millott, 1954) and *Psammechinus miliaris* (see Millott and Yoshida, 1956) do so upon shading.

Pedicellaria are another “organ-system” that has been proposed to play a role in photoreception (Yoshida 1966). These apomorphic echinoderm appendages have previously been demonstrated to function as defending and cleaning devices but also seem to play an important role in the animals sensory system (O`Connell et al. 1974, Burke 1980, Peters and Campbell 1987). Since pedicellaria have been demonstrated to bear different types of mechnical and chemical receptors (Campbell and Laverick 1968, Ghyoot et al. 1987) it is not surprising that they have also become candidates for hosting photoreceptive structures. However, direct evidence for this is scarce and only consists of random observations like those of Giese and Farmanfarmaian (1963) reporting spine and pedicellaria erection upon illumination in *S. purpuratus*.

Behavioral responses of the whole animal, the third category classified by Yoshida (1966), are especially interesting with regard to the investigation of photoreceptor systems. To react upon a light stimulus e.g. with a turning reaction, covering, or phototaxis, an organism needs photoreceptive cells, but equally important is a nervous interconnection between those receptors and the effector organs. The present thesis accounts for this by thoroughly investigating the connection of the photoreceptor cells with the animal's nervous system.

Most sea urchins will initiate a turning or “righting” reaction, to keep their oral surface in contact to the substratum and this reaction can be influenced by light (Diebschlag 1938, Yoshida 1966). Phototaxis has been reported for many echinoderm species (for review see Yoshida, 1966) and it is important to note that this complex photobehavior depends on the presence of the radial nerves. Yoshida and Ohtsuki (1966) observed that in *Temnopleurus toreumaticus* separation of a radial nerve from the oral ring nerve abolishes phototaxis in the referring ambulacral sector and Holmes (1912) reported that after dissection of the oral ring nerve, *Arbacia punctulata* no longer displays directed phototaxis.

1.4. Expression of opsins and other “eye-relevant” genes in *S. purpuratus*

Molecular data of photoreceptors in deuterostomes other then vertebrates and *Branchiostoma* have been missing so far. Echinoderms as the basal most recent deuterostome subgroup may thus provide important information regarding photoreceptor evolution in Deuterostomia despite their highly derived morphological organization. Additionally, data providing insight into photoreceptor evolution in Echinodermata may also shed light on the evolution of photoreceptors in the chordate/vertebrate lineage.

The genome sequencing of the purple sea urchin *Strongylocentrotus purpuratus* (see Sodergren et al. 2006) led to the surprising discovery of a large number of typical “eye” genes like *pax6*, *atonal*, *neuroD* and *barh1*, which in vertebrates are responsible for patterning early retina development (Burke et al. 2006). Moreover, six different opsins plus other essential components of the signal transduction cascade of photoreceptor cells were identified (Burke et al. 2006, Raible et al. 2006). RT-PCR showed that many of the discovered genes are expressed in adult *S. purpuratus* tube feet (Burke et al. 2006, Raible et al. 2006) suggesting the presence of a more elaborate light sensing apparatus in echinoids than previously assumed.

1.5. Aims of the present study

The novel molecular data arising from the sea urchin genome sequencing project and subsequent expression analyses provided a completely new start point for the quest of echinoderm photoreceptors. It was thus the primary aim of the present study to identify and characterize any photoreceptor cells in echinoids and other echinoderms using a combination of structural/morphological and molecular methods. Following cell type localization via detection of opsin expression by *in situ*-hybridization and antibody labelings, different electron microscopical methods were deployed to further characterize potential photoreceptor cells including their connection to the nervous system and their potential function.

When I started the experiments of the present work nobody had ever consciously seen an echinoid photoreceptor. Therefore, it was a great scientific challenge and pleasure - together with my collaboration partners - to step by step unravelling such a long-standing mystery.

2. MATERIALS AND METHODS

Animal supply and culture

A number of different species covering four out of five subgroups of Echinodermata were investigated during the present study. The species names and sources of supply are listed in the following table.

Table 1. List of echinoderm species investigated in the present study. For details see text. (MfN: Museum für Naturkunde, Berlin; DDU: "Deep Downunder"; CalTech: California Institute of Technology)

Subgroup	Species	Source
Crinoidea	*Antedon bifida* (Pennant, 1777)	The Lovén Centre, Kristineberg, Sweden
	Comatulidae spp.	DDU-Expedition, Bougainville Reef, Coral Sea, Australia
Echinoidea	*Strongylocentrotus purpuratus* (Stimpson, 1857)	Kerchoff Marine Laboratory (CalTech)
	S. droebachiensis (O.F. Müller, 1776)	The Lovén Centre, Kristineberg, Sweden
	Echinus melo Lamarck, 1816	The Lovén Centre, Kristineberg, Sweden
	Echinus esculentus Linnaeus, 1758	The Lovén Centre, Kristineberg, Sweden
	Echinometra lucunter (Linnaeus, 1758)	MfN, collection "Marine Invertebrates"
	Brissopsis lyrifera (Forbes, 1841)	The Lovén Centre, Kristineberg, Sweden
Asteroidea	*Asterias rubens* Linnaeus, 1758	The Lovén Centre, Kristineberg, Sweden
Ophiuroidea	*Amphiura filiformis* (O.F. Müller, 1776)	The Lovén Centre, Kristineberg, Sweden
	Ophiuroidea sp.	DDU-Expedition, Osprey Reef, Coral Sea, Australia

Strongylocentrotus purpuratus: Adult animals were collected by Patrick Leahy, Kerchoff Marine Laboratory (California Institute of Technology, USA) from a location at 25-30 m depth in the San Diego bay (San Diego, USA). The animals were maintained for a week in an open tank system and then shipped to the SZN in Naples, Italy, or Berlin, Germany, by Global Animal Transport, CA, USA. After arrival they were housed in seawater aquaria at 12°C under 12/12hrs day/night light cycle.

Comatulidae sp.: This hitherto undescribed comatulid was collected on 8 December 2009 by Andy Dunstan in a baited *Nautilus* trap deployed at Bougainville Reef, Coral Sea, Australia at a depth of 200 m during the DeepDownunder Expedition (DFG: LU 839/2-1).

Ophiuroidea sp.: The basket star-like ophiuroids were collected during ROV dive 7 on 13 December 2009 at Osprey Reef, Coral Sea, Australia at a depth of 365 m in the framework of the DeepDownunder Expedition (DFG: LU 839/2-1).

All other echinoderms were collected at the Sven Lovén Centre of Marine Science in Kristineberg, Fiskebäckskil, Sweden during several research stays between June 2008 and August 2010.

Phototaxis experiments

Experiments on photobehavior of adult *S. purpuratus* were performed using a goose neck (1 cm diameter) optic fiber light source (color temperature 3350 K, CRI 100Ra8).

Fertilization and larval culture

Strongylocentrotus purpuratus: Spawning was induced by vigorous shaking of ripe animals or by intracoelomic injection of 0.1M Acetylcholine or 0.5M KCl through the soft tissue around the mouth. Spawning females were placed topside down on a 50 ml beaker containing ultrafiltered seawater until releasing their eggs into the vial. Eggs were rinsed thoroughly in filtered seawater (FSW). Sperm was collected directly from the males using a 200 µl Eppendorf pipette and stored for use in Eppendorf tubes on ice. *In vitro* fertilization was carried out in FSW at 12°C using a 1:500 dilution of sperm. Fertilized eggs were rinsed twice to wash out remaining sperm and to avoid polyspermy. They were regularly checked for proper development under a stereo microscope for three hours. Subsequently, developing embryos were transferred to 2000 ml beakers filled with FSW containing Kanamycin/Ampicillin with a final dilution of 1:1000 mg/l. They were incubated with an acrylic paddle stirring device for 3 days at 12°C in a fridge exposed to a 12/12 hrs day/night light cycle using an OSRAM L36 W/865 Lumilux daylight lamp. From three days post-fertilization until completion of metamorphosis, embryos and larvae were cultured in 5000 ml Erlenmayr-flasks. The water medium was continuously oxygenated using an air hose bubbling system. Salinity of the seawater was maintained at the level of original spawning conditions, ranging around 1000 mosmol and water changes were performed twice a week. Larvae were fed with a mixture of the gold alga *Isochrysis galbana* and the red alga *Rhodomonas lens* from our own stock. Larvae were fed starting at day three of

development until metamorphosis. Postmetamorphic juveniles were fed with red algae growing on small pieces of rock in our aquaria.

Asterias rubens: Spawning was induced by intracoelomic injection of 2 ml of 0.1 mM 1-methyladenine. Fertilized eggs were rinsed in FSW. Once the embryos reached the two cell stage they were transferred to 5000 ml Erlenmayr-flasks with a final density of 10 embryos per ml. Cultures were maintained at constant temperature (12°C), a salinity of 32‰ and alkalinity of 2.12 ± 0.02 mM. After day 2, larvae were fed daily with the red alga *Rhodomonas lens* at a concentration of 50 to 200 µg of carbon/liter.

Adult tissue dissection

A variety of external appendages as well as sea urchin radial nerves were dissected for immunohistology, *in situ*-hybridization, scanning electron microscopy and transmission electron microscopy. After dissection under a stereomicroscope using micro surgical tools, tissues were immediately placed into the respective fixatives (see description of methods below). To extract *S. purpuratus* radial nerves, an equatorial sectioning of the whole animal was performed using scissors, separating the sea urchin into oral and aboral halves. Dissection of the radial nerve was achieved via extraction of the whole water vascular system of a single ambulacrum.

Immunohistochemistry

Prior to some immunostaining experiments, life animals were anesthetized and thus their muscles relaxed with 7% MgCl in a 1:1 mixture of FSW and destilled water. Specimens or dissected tissues were directly transferred to the fixative. Adult tissues and juvenile specimens were fixed in 4% paraformaldehyde in FSW or phosphate buffered saline (PBS: 0.05M PB/0.3M NaCl, pH 7.4) at room temperature (RT). Fixation times varied between different antibody treatments: all stainings involving anti-Synaptotagmin B (1E11, Nakajima et al. 2004) required a short fixation time of 15 min. and subsequent post-fixation with ice cold methanol for 1 min.; tissues prepared for other antibody treatments were fixed for 30-60 min. at RT. If necessary, decalcification was obtained by treatment with 2% ascorbic acid/0.15 M NaCl after initial fixation, for 2-6 days on a slow rotator at RT. Fixed specimens were rinsed in PBS and blocked in 0.25% bovine serum albumin containing 0.1% triton X-100 and 0.05% NaN_3 for 30 min. at RT. Anti-Synaptotagmin B, anti-acetylated α- tubulin (SIGMA) and anti-Sp-Opsin4 were diluted in PBS with final concentrations of 1:200, 1:250 or 1:50, respectively. After an overnight incubation at 4°C, tissues were rinsed in PBS and then incubated in a 1:500 dilution of Alexa Fluor488 conjugated goat anti-rabbit IgG and Alexa Fluor568 conjugated goat anti-mouse IgG (Molecular Probes) for 2 hrs at RT. Phalloidin labeling was performed in a one step

method deploying Alexa Fluor488 conjugated phalloidin (Molecular Probes). After several washes in PBS, specimens were mounted in an antifading medium containing a Glycerin/PBS mixture and examined using a Leica TCS-SPE, a Leica SP 5 or a Zeiss 510Meta confocal microscope, respectively. Projections shown in the present study were produced by recording confocal image stacks and projecting them in the z-axis using MacBiophotonics ImageJ or Fiji.

Whole-mount *in situ*-hybridization (WMISH)

Both antisense- and sense-digoxigenin-labeled RNA probes were kindly provided by the lab of M.I. Arnone, SZN, Naples, Italy. Fragments of *Sp-opsin4* were amplified from genomic DNA by PCR using specific primers (Op4IL: ATGCCATCTTCTGGTCCATC / Op4IR: AGCAGAAGCAGAAGCAGGAG) targeting exon4 of Sp-opsin4 (length: 871 bp). Probes were labeled using DIG-RNA labeling Kit® (Roche); for a detailed ribo probe preparation protocol see Arboleda (2008).

Whole-mount *in situ*-hybridizations (WMISH) were performed using a protocol modified after Arendt *et al.* (2004). *S. purpuratus* tube feet were fixed in 4% Paraformaldehyde in FSW for 2 hrs at RT. To stop the fixation process, the specimens were then rinsed three times (5' each) in PTW, followed by one wash in 100% MeOH at RT. After replacing the MeOH, samples were stored overnight at -20°C to provoke membrane perforation, thereby enhancing probe penetration during the following treatment. After transferring the tube feet to a 6-well culture dish containing 100% MeOH they were stepwise re-hydrated in 75% MeOH/PTW, 50% MeOH/PTW and 25% MeOH/PTW (5' each) using small nylon meshs for transfer between solutions. Two washes in PTW (5' each) finished the re-hydration procedure. ProteinaseK (100 µg/ml in PTW) digestion was applied to half of the samples to ease probe penetration, but turned out to be unnecessary in sea urchin tissues. Two short rinses in freshly prepared 2 mg/ml glycine/PTW were followed by a postfixation step applying 4% PFA/PTW for 20 minutes. Afterwards, samples were washed five times (5' each) in PTW. Hybridization was performed in a pre-heated waterbath at a constant temperature of 65°C. Tube feet were transferred into 2 ml Eppendorf tubes containing Hybridization Mix (see Arendt *et al.* 2004). Pre-hybridization took place for 2 hours at 65°C and the *Sp-opsin4* probes (4 µl/200 µl Hyb-Mix) were denaturated for 10 minutes at 80°C prior to use. Pre-hybridization solution was carefully removed and Hyb-mix containing the probe was added to the tube. Hybridization took place overnight at 65°C on a slow rotator. Two washes (30' each) in 1 ml formamide/2xSSCT at 65°C were followed by one wash (15') in 1 ml 2xSSCT at 65°C and two subsequent ones (30' each) in 1 ml 0.2xSSCT at 65°C. Detection for this non-fluorescent WMISH was initiated through a blocking step of two hours with 1 ml of 5%

sheep serum in PTW at RT. In the following, the tube feet were incubated in pre-absorbed anti-DIG-AP F_{ab} fragments diluted 1:2000 in PTW. The samples were transferred again to a 6-well dish and washed six times (10' each) in PTW on a shaker at RT. Equilibration in staining buffer (SB) was followed by staining in darkness with NBT (final concentration 337.5 µg/ml) and BCIP (final concentration 175 µg/ml) in SB overnight at RT without shaking. Three washes (5' each) in PTW were followed by an overnight postfixation step in 4% PFA in PTW. In order to obtain a better understanding of the "*in situ*" localization of the *Sp-opsin4* mRNA, an additional immunostaining using anti-acetylated-α-tubulin was performed. The *in situ*-hybridized tube feet were therefore briefly washed three times in PTW, followed three washes of 10', 20' and 30', respectively. Samples were blocked using 5% sheep serum in PTW at RT for 1 hour on a slow rotator followed by primary antibody incubation overnight at 4°C. 1 µl anti-acetylated α-tubulin was diluted in a 2.5% sheep serum/PTW mix and the tissues were slowly rotated. After several washes in PTW, tube feet were incubated in the secondary antibody Alexa Fluor488 conjugated goat anti mouse IgG overnight at 4°C. Three washes (10' each) in PTW finished the immunoprocedure. After staining, samples were mounted in glycerol and analyzed on a Leica SP5 confocal microscope.
Accuracy of the WMISH results was confirmed by (negative) control experiments using exactly the same procedure except deploying sense probes instead of antisense probes.

Scanning electron microscopy

Tissues were fixed in 2.5% glutaraldehyde in PBS (0.05M PB/0.3M NaCl, pH 7.4) and rinsed in PBS several times. After postfixation in 1% OsO_4 in PBS, tissues were dehydrated in a graded acetone series, transferred to 100% Ethanol and dried using a critical point dryer. After mounting the specimens on stubs they were sputter coated with gold and examined in a FEI Quanta 200 SEM operating at 15 KV.

Transmission electron microscopy

Tissues were fixed in 2.5% glutaraldehyde in PBS at 4°C for 1 hour and subsequently rinsed in PBS several times. After postfixation in 1% OsO_4 in PBS, specimens were dehydrated in a graded acetone series and embedded in plastic resin (Araldite M, Fluka, art. no.: 10951) for 48 hrs at 60°C. Serial sections were cut using a diamond knife and a Reichert ultramicrotome S and automatically stained with 2.0% Uranyl Acetate for 15' and Lead Citrate after Reynolds (1963) for 20' in a Phoenix ultrastain (Phoenix staining technologies, Berlin). Examination was carried out using a Philips CM 120 Biotwin TEM.

Immunogold labeling on TEM sections

For immunogold labeling on ultrasections, *S. purpuratus* tube feet were fixed in 0.5% glutaraldehyde/4% PFA in PBS plus Ruthenium red, pH 7.4 for 3 hrs at RT. Samples were thoroughly washed in PBS for 4 days and subsequently decalcified in 1% Ascorbic acid/0.15M NaCl on ice on a slow rotator. Samples were dehydrated in an alcohol series including 30%, 50%, and 70% EtOH (15' each). Tissues were then transferred into a 2:1 L.R. White/70% EtOH mixture slowly rotating for one hour. Embedding followed after two changes to 100% L.R. White after 1 hr and again after 24 hrs. Polymerization was carried out in small Eppendorf tubes (0.6 ml) within an UV-incubator for 48 hrs at RT. Sections were cut using a diamond knife and a Reichert ultramicrotome S. They were mounted on pre-treated nickel grids according to Hayat (2000). For the immunogold labeling and the gold enhancement single grids were placed on droplets of liquid solution placed on parafilm. The parafilm was mounted in plastic boxes containing wet cellulose tissue to avoid desiccation of the grids during overnight procedures. Between different staining steps, grids were moved from one droplet to the next using superfine forceps. Subsequent processing basically followed the protocol of Tan *et al.* (2001) including treatment with 50mM ammonium chloride for 15' and blocking with 5% normal goat serum/0.1% bovine serum albumin in PBS for 30', both at RT. Primary antibody incubation (anti-Sp-Opsin4) 1:50 in blocking solution overnight was followed by two brief PBS washes and incubation with anti-rabbit IgG Gold (Sigma Aldrich Cat. No.:G7402) 1:50 in blocking solution for 2.5 hrs at RT. A short PBS wash, three washes in blocking buffer (5' each) and three washes in MQ (5' each) were followed by the gold enhancement procedure. Gold enhancement was performed using the Nanoprobes GoldenhanceTM-EM kit (Cat. No.: 2113), following the manufacturers instructions, except that no postfixation step was applied. Enhancement was allowed to develop between 30'' and 3' at RT. After thorough rinsing with MQ, sections were automatically stained with 2.0% uranyl acetate for 15' and lead citrate after Reynolds (1963) for 20' in a Phoenix ultrastain (Phoenix staining technologies, Berlin). Examination was carried out using a Phillips CM 120 Biotwin TEM at 60 KV.

X-ray microtomography (µCT)

A small (ca. 3 x 5 mm) part of the skeleton of an adult specimen of *S. purpuratus* was scanned using a Phoenix Nanotom µCT scanner. The system uses a tungsten x-ray source and a CCD camera with a 2304 x 2304 pixel matrix. Scanning was accomplished using 1440 images at 360° rotation, resulting in a voxel size of 5.5 µm. Scanning parameters were as follows: 150 kV, 180 µA, 750 ms exposure time, and three averages. Image reconstruction was performed using the software provided with the µCT system. 3D visualization was accomplished using VGStudioMAX 2.0.

3. RESULTS

3.1. Photoreceptors in Echinoidea

As can be extracted from the literature, many sea urchin species show a variety of responses upon photic stimuli while others display no clear reaction upon light. At the start of my investigation, little was known about phototaxis and light-triggered reactions in the echinoid *S. purpuratus*. Besides preliminary observations of Giese and Farmanfarmaian (1963) reporting on negative phototaxis of this sea urchin species observed as a by-product of experiments on osmotic stress, no one had clearly demonstrated photosensitivity in these animals. It was thus essential, despite the excellent first time opportunity of having genomic information of an echinoderm at hand, to test *S. purpuratus* for photoreactions before chosing this species for studies on echinoderm photoreceptors. The observed phototaxis (see following paragraph) in combination with the documented expression of “eye-relevant” genes (Burke et al. 2006, Raible et al. 2006) finally led to the choice of *S. purpuratus* as a model organism with regard to the adressed questions.

3.1.1. New evidence for an echinoid visual response

Behavioral observations in my tank system showed that the sea urchin *S. purpuratus* starts migrating upwards as soon as light was switched off during the night cycle. When illuminated using a small white light dive torch (see Materials and Methods) following dark adaptation for one hour, the animals displayed intensive tube foot movement, including the typical “bending reaction” (Weel 1935) with subsequent negative phototaxis. To obtain further and statistically relevant data, one of my collaboration partners, M. I. Arnone (Stazione Zoologica, Naples), performed more sophisticated behavioral experiments using an artificial light source (with a continuous spectrum) on adult *S. purpuratus*. In this set up the animals were placed in a special tank with a small corridor that allowed for speed measurement during the experimental course. It could be demonstrated that, like other echinoderms (Yoshida, 1966), these sea urchins immediately react to illumination by intensifying tube foot and spine activity and rapidly (at the average speed of 4.6±1.8 cm/min, n=20) move away from the light source to the furthest side of the tank. These behavioral data thus confirm the preliminary observations of Giese and Farmanfarmaian (1963) on *S. purpuratus*.

3.1.2. R-Opsin positive PRCs in tube feet of *Strongylocentrotus purpuratus*

Adult echinoids possess a variety of external organs that have been debated to function in photoreception. In *S. purpuratus* the most immediate and striking reaction following illumination is an intense movement of tube feet. It was thus natural that in accordance

with a considerable number of publications reporting on light-triggered tube foot reactions in echinoderms (Cowles 1909, 1910, 1911, Hess 1915, Sharp and Gray 1962, Millott 1954, Yoshida 1957, Millott and Yoshida 1956) and the additional finding of the expression of several opsin genes within *S. purpuratus* tube feet (Burke et al 2006, Raible et al. 2006) these echinoderm specific type of podia where chosen as a first examination target. Presence of an opsin clearly indicates light sensing cells and thus can be used to localize the site of photoreception.

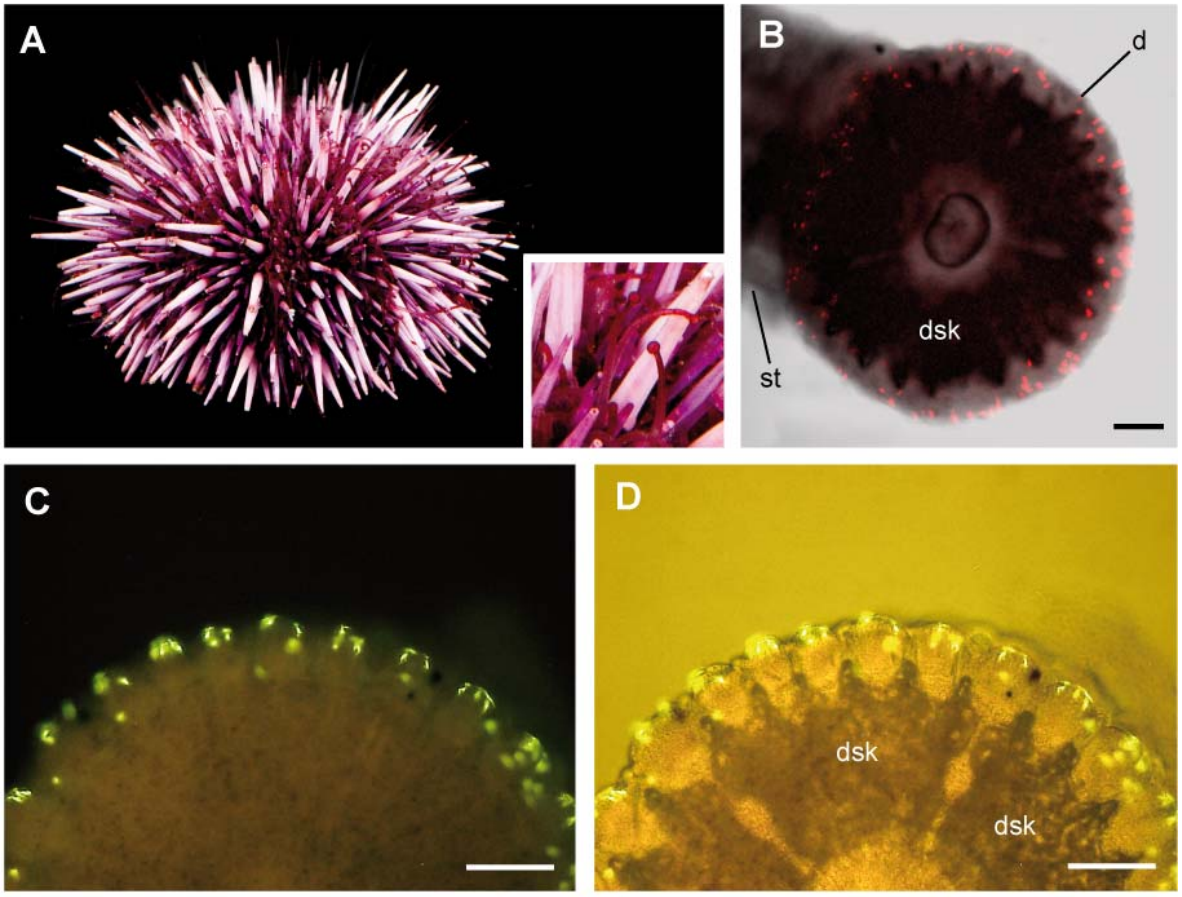

Fig. 1: R-opsin positive PRCs in the tube foot disc of *S. purpuratus*. **A.** Adult animal. Inset: tube feet. Photograph courtesy of M. Ormestad/KahiKai, Hawaii. **B.** Color merge of CLSM z-projections showing tube foot with stalk (st), disc (d) and disc skeleton (dsk). Anti-Sp-opsin4 immunolabeling shows single PRCs (red) located in the rim of the tube foot disc. **C.** Tube foot disc in top-view with r-opsin positive PRCs (yellow) grouped in epidermal bulges. **D.** PRC arrangement and calcite tube foot disc skeleton (rosette). Scale bars in B-D: 100 µm.

M.I. Arnone and co-workers had designed a sequence specific antibody against the c-terminal end of the *S. purpuratus* rhabdomeric opsin (Sp-Opsin4). To localize potential photoreceptor cells, the first approach was to determine the site of r-opsin expression in tube feet deploying immunohistological methods. Incubation of dissected locomotory tube feet (Fig. 1A and inset) of different body parts of the sea urchin with the Sp-Opsin4 antibody revealed distinct immunoreactive cells within the rim of the tube foot disc (Fig.1B). The labeled photoreceptor cells (PRCs) are regularly arranged around the terminal disc in

groups of 2-4 PRCs (Fig. 1C+D). Surprisingly, the morphology displayed by the r-opsin staining hints on an immunoreaction of a larger portion of the cell, which is not restricted to the apical membrane that would be expected to host the opsin photopigment molecules. The number of Sp-Opsin4 positive cells per tube foot disc varied betweeen 37 and 67 in tube feet of different individuals (n=5), keeping in mind that the confocal plane width is limited, i.e. a small amount of cells might have been overlooked due to large tissue size.

Unspecific cross-reaction of sequence-based designed antibodies can pose severe problems on the resulting reliability of the stainings. Opsin detection was therefore in the following performed at both the mRNA and protein levels using *in situ*-hybridization and the newly developed Sp-Opsin4 antibody, respectively. The resulting stainings indeed demonstrate high specificity of the r-opsin antibody as both, antibody and *in situ*-staining (against the mRNA target) of *Sp-opsin4* could be co-localized in single cells (Fig. 2 A-E). In accordance with the traditionally proposed “diffuse” dermal light sense in echinoderms, the photoreceptive tissue would be expected to be randomly scattered across the neurons of the diffuse nervous system. In contrast to this hypothesis, the r-opsin photopigment was found to be clearly expressed in PRCs in distinct regions of each sea urchin tube foot. These findings provide the first evidence for a distinct photoreceptor cell documented in an echinoid.

To further characterize the Sp-Opsin4 positive cells, different other cytological markers were applied. Phalloidin (as an f-actin marker) was used to determine whether the labeled cells possess a pronounced rhabdom-like structure, a feature often found in r-opsin positive photoreceptor cells the apical cellular membrane of which is enlarged by numerous microvilli. But despite varying the fixation time as well as applying different detergents to overcome tissue penetration problems due to echinoderm typical excessive mucus secretion during fixation, the phalloidin labeling experiment revealed no such structure. The resulting recording showed a low signal/noise ratio, suggesting that insufficient penetration of the phalloidin molecule might have been the causing factor. In the following, an anti-acetylated alpha-tubulin antibody was chosen to perform co-labeling experiments together with anti-Sp-Opsin4. The anti-acetylated alpha-tubulin antibody (for details see Materials and Methods) reacts with alpha-tubulin only in its stabilized form. The structures revealed by this antibody thus include stabilized microtubuli as present in cilia and neurotubuli of nerve cells. The anti-acetylated alpha-tubulin antibody co-applied with anti-Sp-Opsin4 allowed to localize the receptor`s connection to the nervous system. Anti-acetylated alpha-tubulin staining revealed an extensive nerve net pervading the tube foot disc (Fig. 3A). The r-opsin positive PRCs send their axons into branches of this disc nerve net (Fig. 3B). But co-application of the two antibodies revealed another interesting

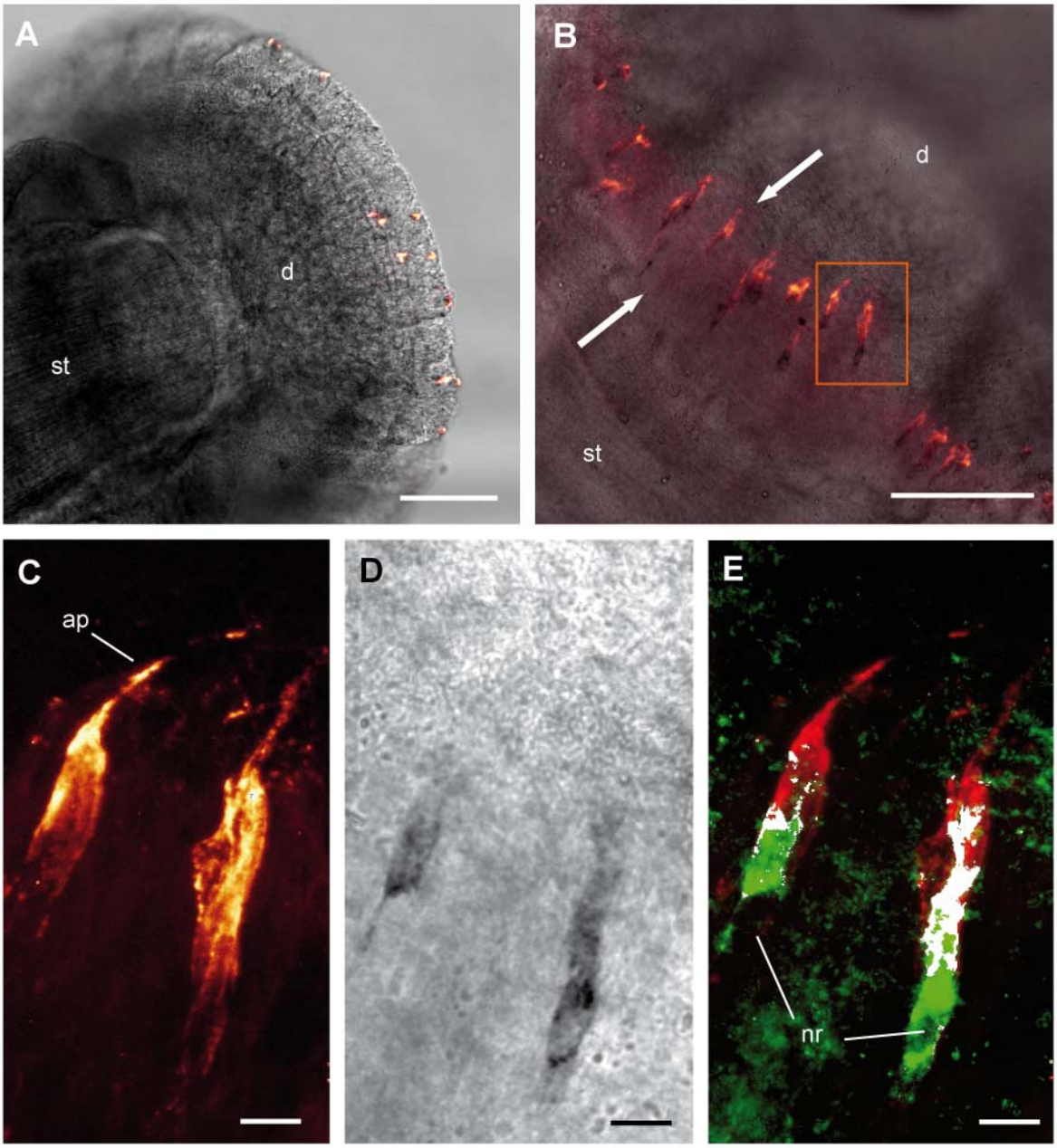

Fig. 2: Sp-Opsin4 protein and RNA co-localization in *S. purpuratus* tube feet discs. **A.** Whole mount *in situ*-hybridization against *Sp-opsin4* RNA and immunostaining against Sp-Opsin4 protein in a tube foot. CLSM z-projection with single cells double labeled (black: RNA, hot red: protein) within the rim of the tube foot disc (d). No PRCs were localized in the stalk region (st). **B.** Portion of the same tube foot as in A but view towards the disc rim (arrowed). **C.** High magnification of disc rim portion arrowed in B. Two PRCs showing strong Sp-Opsin4 antibody labeling (hot red). **D.** *Sp-opsin4* RNA (black) as detected by in situ-hybridization using NBT/BCIP. Note nucleus region (nr) with weaker or no RNA presence. **E.** Co-localization (white) of *Sp-opsin4* RNA (green) and Sp-Opsin4 protein (red) deploying MacBiophotonics ImageJ co-localization tool. Scale bars in A-B: 100 µm, C-E: 10 µm.

feature of the photoreceptor cells. Examining stacks of CLSM pictures, I found that the photoreceptors are not distributed randomly around the terminal disc but are grouped in 2-4 cells and accompanied by distinct pads of cilia (Fig. 3C). In rare cases a cilium projecting from an Sp-Opsin4-positive cell could be detected (Fig. 3D) but the resolution of the stainings recorded at these very high magnifications was too poor to allow for clear classification of the receptor cell type.

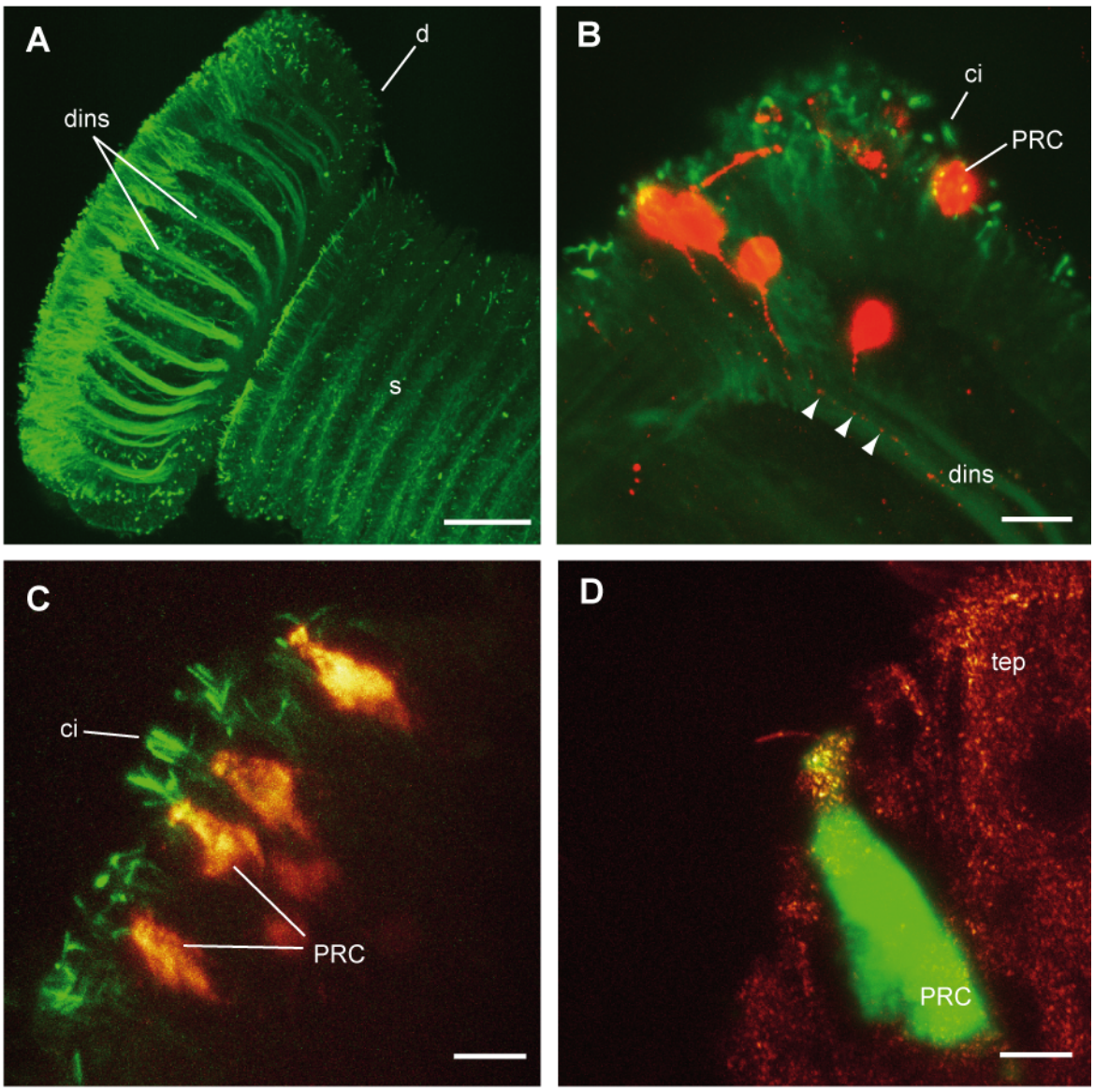

Fig. 3: Structure of *S. purpuratus* r-opsin positive PRCs and their connection to the nervous system. **A.** Anti-acetylated alpha-tubulin staining (green) of a locomotory tube foot with stalk (s) and disc (d). Notice the massive, branched nerve (dins) pervading the disc. **B.** Portion of the tube foot disc with cilia (ci), double-immunolabeled against acetylated alpha-tubulin (green) and Sp-Opsin4 (red). PRCs send axons (arrowheads) into a branch of the disc nervous system (dins). **C.** The same immunolabeling as in B shows presence of many cilia (ci) (green) in the PRC region (hot red). **D.** PRC (green) within the tube foot epidermis (tep) bearing a single cilium (red). Scale bars in A: 100 µm, B: 25 µm, C: 10 µm, D: 5 µm.

3.1.3. Structural examination of the r-opsin positive PRC type

Scanning electron microscopy (SEM) was deployed to localize the exact position of the photoreceptor cells and to gather more detailed information about the cell type´s morphology. The external tube foot surface is generally covered with microvilli, but around the bulbous enlargement of the terminal disc a number of distinct ciliary patches are positioned in vertical intermittent rows (Fig. 4A-D). This finding provided important positional information for the subseqent transmision electron microscopy (TEM) work. Based on the finding that ciliated cells were not randomly distributed over the entire disc

surface, but grouped in distinct patches, it became clear from the anti-acetylated alpha-tubulin staining that the photoreceptor cells had to be located within these patches, too. Thus, the SEM investigation allowed to considerably downsizethe investigation area for transmission electron microscopy, a valuable result given the relatively large size of an adult echinoid tube foot disc. But deploying SEM did not allow to say anything further regarding the examined photoreceptor cell type. As the overall microvillar cover is extremely dense (Fig. 4D) it is impossible to detect potential apical cell membrane enlargements of single cells. In this context it is all the more surprising that a phalloidin staining (see above) could not reveal any prominent microvillar structures in the epithelium.

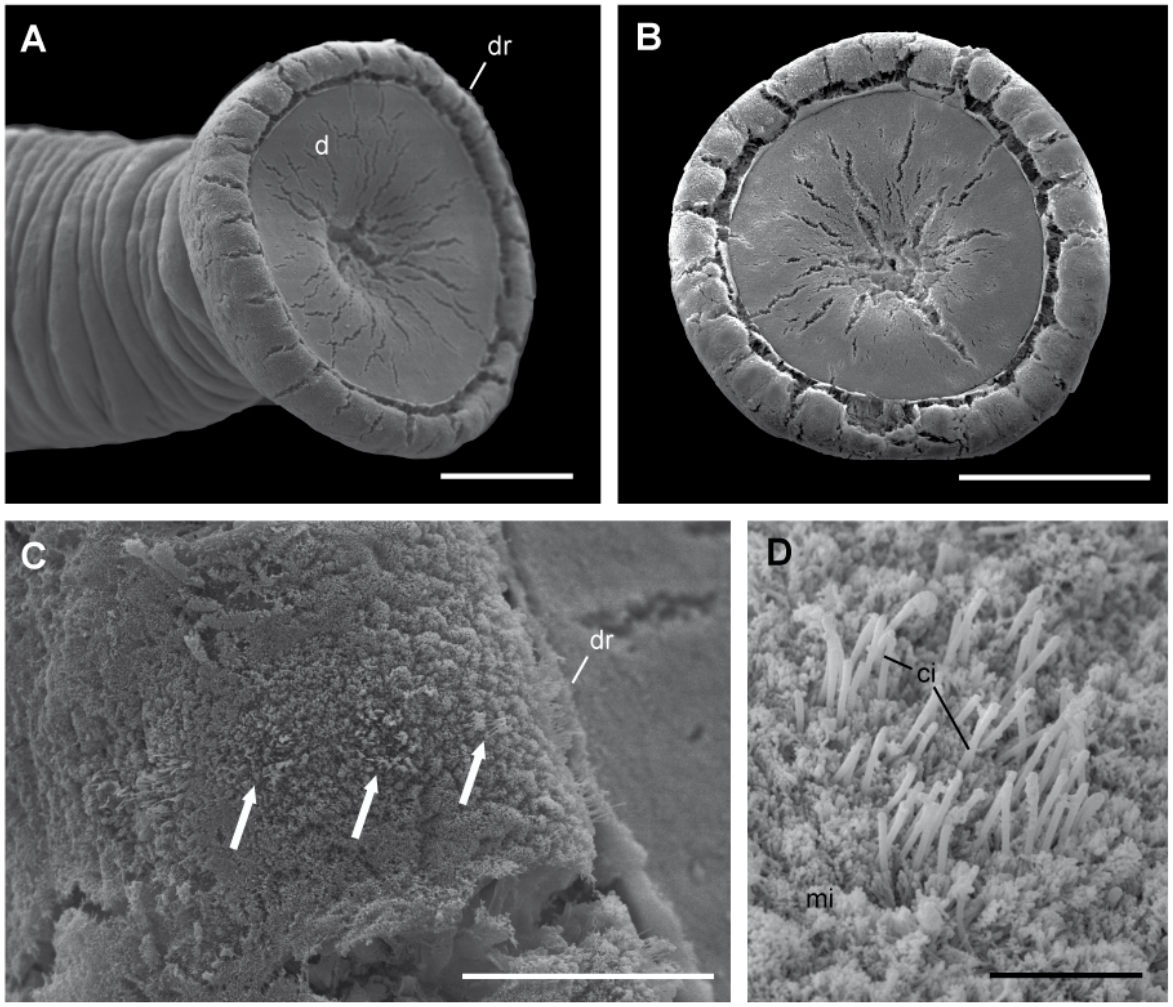

Fig. 4: SEM of *S.purpuratus* tube foot discs. **A.** Adult locomotory tube foot with showing disc (d) and disc rim (dr) in semi-lateral view. **B.** Same speciment, top view. **C.** Distinct patches of cilia perpendicularly arranged to the rim. **D.** High magnification of a single patch of cilia protruding from a dense layer of epidermal microvilli. Scale bars in A-B: 250 µm, C: 25 µm, D: 5 µm.

When examining serial sections with (TEM) it was easy to locate the ciliary patches within the tube foot disc epidermis. The tube foot discs of *S. purpuratus* locomotory tube feet are not exactly round in shape but show epithelial bulges (see Fig 1C+D and Fig. 4A-C) hosting the ciliary patches that are well recognizable in TEM as well (Fig. 5A). Nevertheless, it turned out to be difficult to locate distinct photoreceptor cells, since all cells comprising the ciliated patches morphologically resemble typical echinoderm sensory cells (Fig. 5B) by projecting their extensions towards the nervous system.

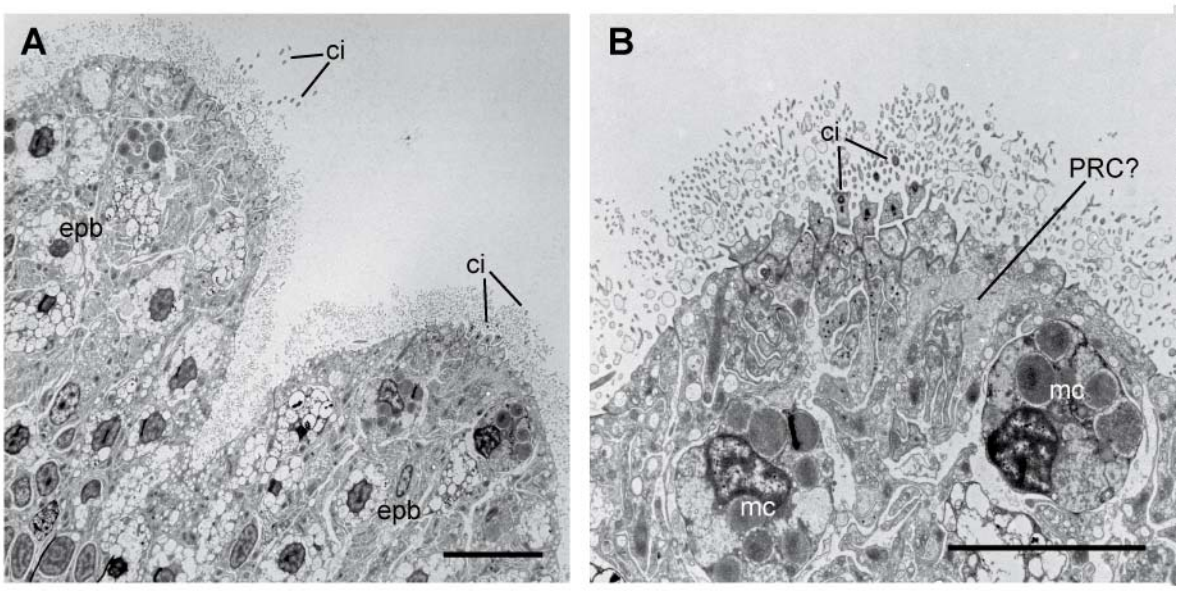

Fig. 5: TEM pictures of PRC region in *S. purpuratus* tube foot discs. **A.** Epidermal bulges (epb) of disc rim, where PRCs were detected by CLSM. Cilia (ci) of sensory cell patches can be clearly distuinghished. **B.** Patch of ciliated sensory cells in close vicinity to a PRC candidate cell (PRC?) and mucus cells (mc). Scale bars in A-B: 5 µm.

As from immunocytological and SEM results, the photoreceptors could not be expected to display extremely prominent microvillar structures, i.e. another methodological approach was needed. Application of an anti-Sp-Opsin4 immunogold staining on ultrastructural level allowed to gather direct evidence for cells containing the r-opsin photopigment. The method was performed with and without gold enhancement. Varying enhancement times were applied and combined evaluation of the obtained results allowed to clearly identify the stained cell type in conventional TEM sections. The cytoplasm makes the cells, which are immunoreactive to the anti-Sp-Opsin4 antibody, easily distinguishable from all surrounding nerve cell types by being completely filled with numerous clear vesicles of differing size (Fig. 6A-E). Interestingly, the r-opsin photopigment is thereby not restricted to the apical cell membrane but widely distributed within the membrane of intracellular vesicles (Fig. 6C+D). As the respective tube feet had been fixed within the daily illumination period of the aquaria, the large amount of PRC vesicles containing

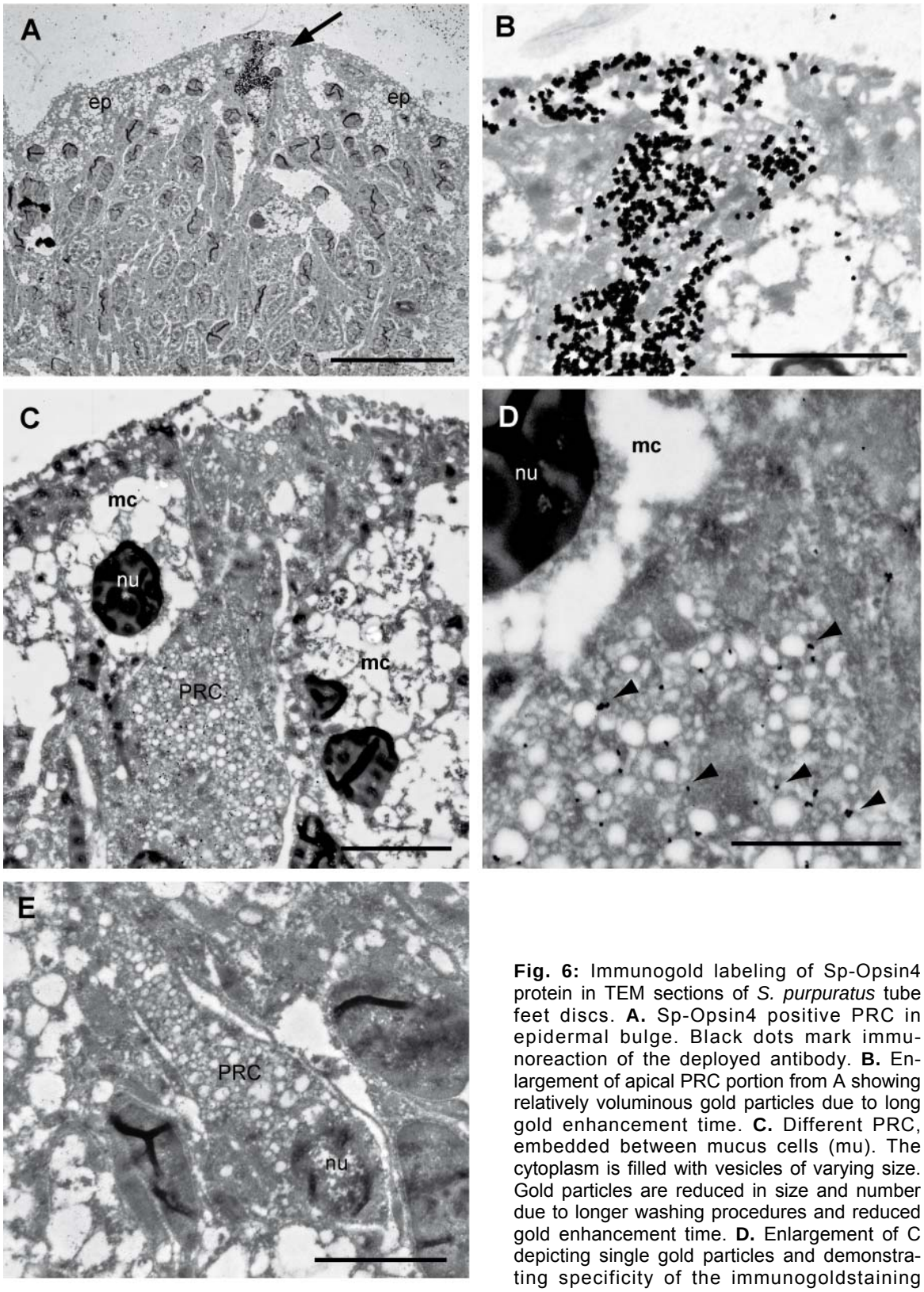

Fig. 6: Immunogold labeling of Sp-Opsin4 protein in TEM sections of *S. purpuratus* tube feet discs. **A.** Sp-Opsin4 positive PRC in epidermal bulge. Black dots mark immunoreaction of the deployed antibody. **B.** Enlargement of apical PRC portion from A showing relatively voluminous gold particles due to long gold enhancement time. **C.** Different PRC, embedded between mucus cells (mu). The cytoplasm is filled with vesicles of varying size. Gold particles are reduced in size and number due to longer washing procedures and reduced gold enhancement time. **D.** Enlargement of C depicting single gold particles and demonstrating specificity of the immunogoldstaining as neighboring cells show no gold labeling. **E**. Yet another PRC sectioned in a more proximal po-sition where the nucleus is located. Immunogold labeling performed without gold enhancement and thus not visible at the depicted magnification. Yet the picture allows for cell type comparison with PRC candidates in conventionally fixed tissues. Scale bars in A: 10 µm, B, C, E: 2 µm, D: 1 µm.

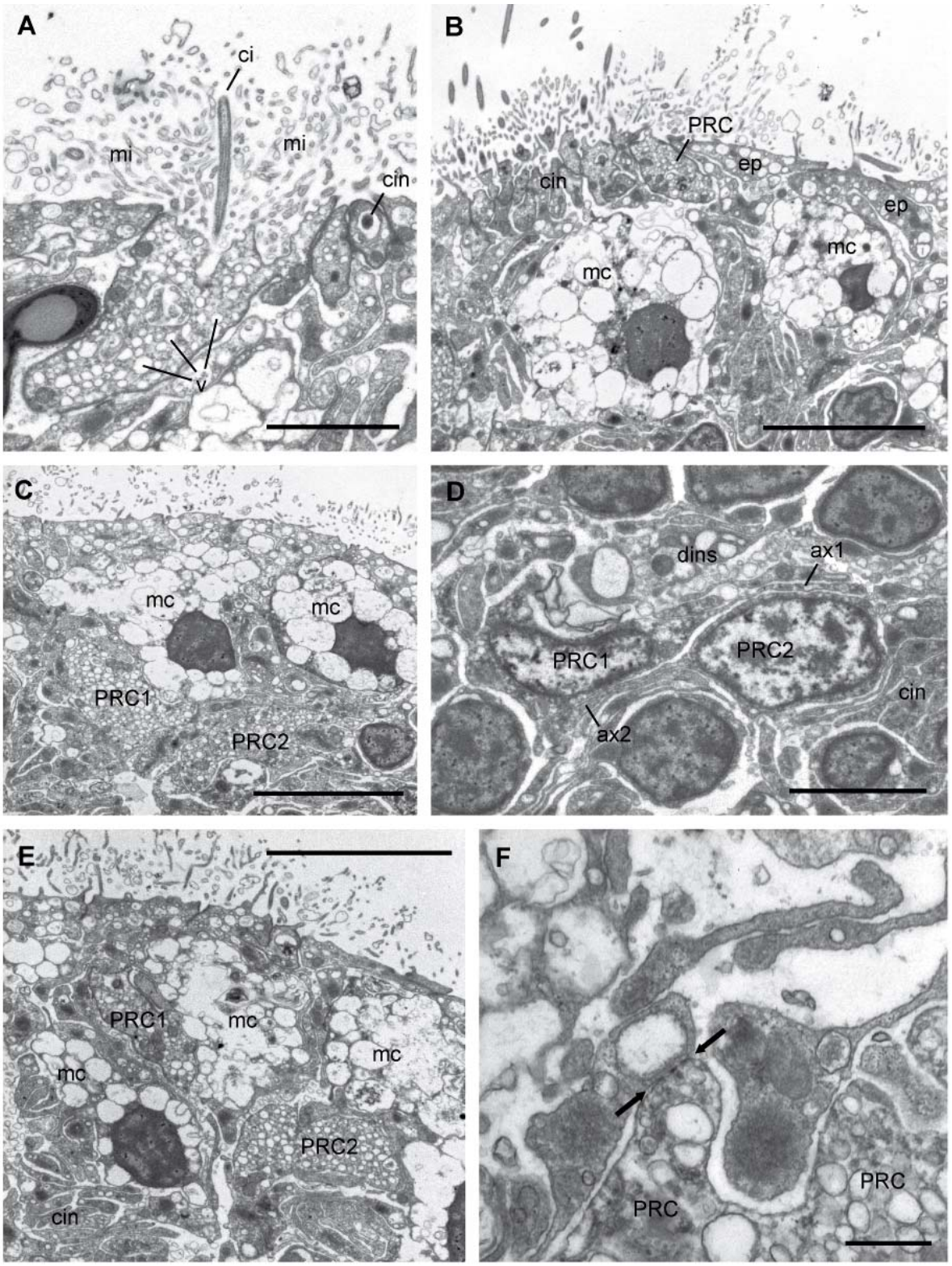

Fig. 7: Ultrastructure of *S. purpuratus* tube foot disc PRCs. TEM serial sections. **A.** Apical portion of r-opsin positive disc PRC showing many microvilli (mi) and an unmodified cilium (ci) arising from its apical membrane. The cytoplasm is filled with numerous vesicles (v) of different sizes that allowed for cell type determination from Sp-Opsin4 immunogold labeling. The PRC is flanked by a flat epidermis cell and ciliated sensory cells (cin). **B.** A more basal portion of the same PRC showing close vicinity to patch of ciliated sensory and epidermis cells (ep). Mucus cells (mc) neighbor the PRC within its proximal region. **C.** Proximal portion of PRCs with wider cell diameter. **D.** PRC region bearing nuclei and axons sent into disc nervous system (dins). **E.** Ciliated sensory cells flank the PRCs running proximad. **F.** PRC contacts neighboring cell projection (black arrows). Scale bar in A: 2 µm, B, C, E: 5 µm, D: 2.5 µm, F: 0.5 µm.

Sp-Opsin4 in their membranes might hint on storage or a recovery process of these vesicles as part of a membrane turnover cycle that has been postulated for many rhabdomeric PRCs (Blest 1988).

After identifying the PRC cell type deploying immunogold labeling, conventional TEM sections revealed the PRCs to possess an apical membrane enlargement bearing many microvilli (Fig. 7A), which are slightly longer than those of the neighboring epidermal cells. The microvilli-bearing cell apex of these PRCs is situated always in close vicinity to the described ciliary patches formed by flat mono-ciliated presumed sensory cells (Fig. 7B). The PRCs are surrounded by mucus cells typical for echinoderm tube feet (Coleman 1969b). Additionally, flat epidermis cells with empty vacuoles were observed (Fig. 7B). Following a “bottle-neck” of the apical cell part towards the basal membrane, the cell body widens proximally where it contains the nucleus (Fig. 7C+D). The cell finally extends into several axons (Fig. 7D). The PRCs are flanked by mucus cells and the presumed mono-ciliated sensory cells (Fig. 7E). The PRC axons could be followed until their topological integration into the tube foot nervous system but due to the echinoderm typical scarce occurence of chemical synapses (Cobb 1987, Peters and Campbell 1987, Byrne 1994) a structural connection to other nerve cells through this kind of cell-cell contact could not be demonstrated. The axons simply contact other cellular projections and sometimes inconspicious membrane thickenings lacking a synapse-typical accumulation of regular sized vesicles can be observed (Fig. 7F). Schematic 3D reconstruction of the overall PRC morphology using surface rendering of aligned TEM serial images revealed the PRCs to be elongated, flask shaped cells (Fig. 8A). Although not investigated any further, part of the PRCs` cell bodies notably run in direct neighborhood to skeletal elements of the tube foot disc (Fig. 8B+C). As can be seen by schematic TEM serial reconstruction (Fig. 8D) the PRC`s microvilli form a “crown-like” structure at the cell apex, that in some sea urchin species (see later sections of this chapter) even take the form of flower-like petals. A single unmodified cilium (schematic reconstruction of the serial sections Fig. 8D), is present in the investigated PRC type. As observed in TEM serial sections of different photoreceptor cells and different tube feet respectively, none of the investigated cilia showed signs of modification resulting in surface enlargement and thus the cilium of the investigated PRC seems very unlikely to be involved in photoreception. Many rhabdomeric photoreceptors do have a persisting cilium or at least a rudiment of such (Purschke et al. 2006). Resulting from the structural examination, the investigated PRC cells were classified as rhabdomeric (microvillar) photoreceptor cell type.

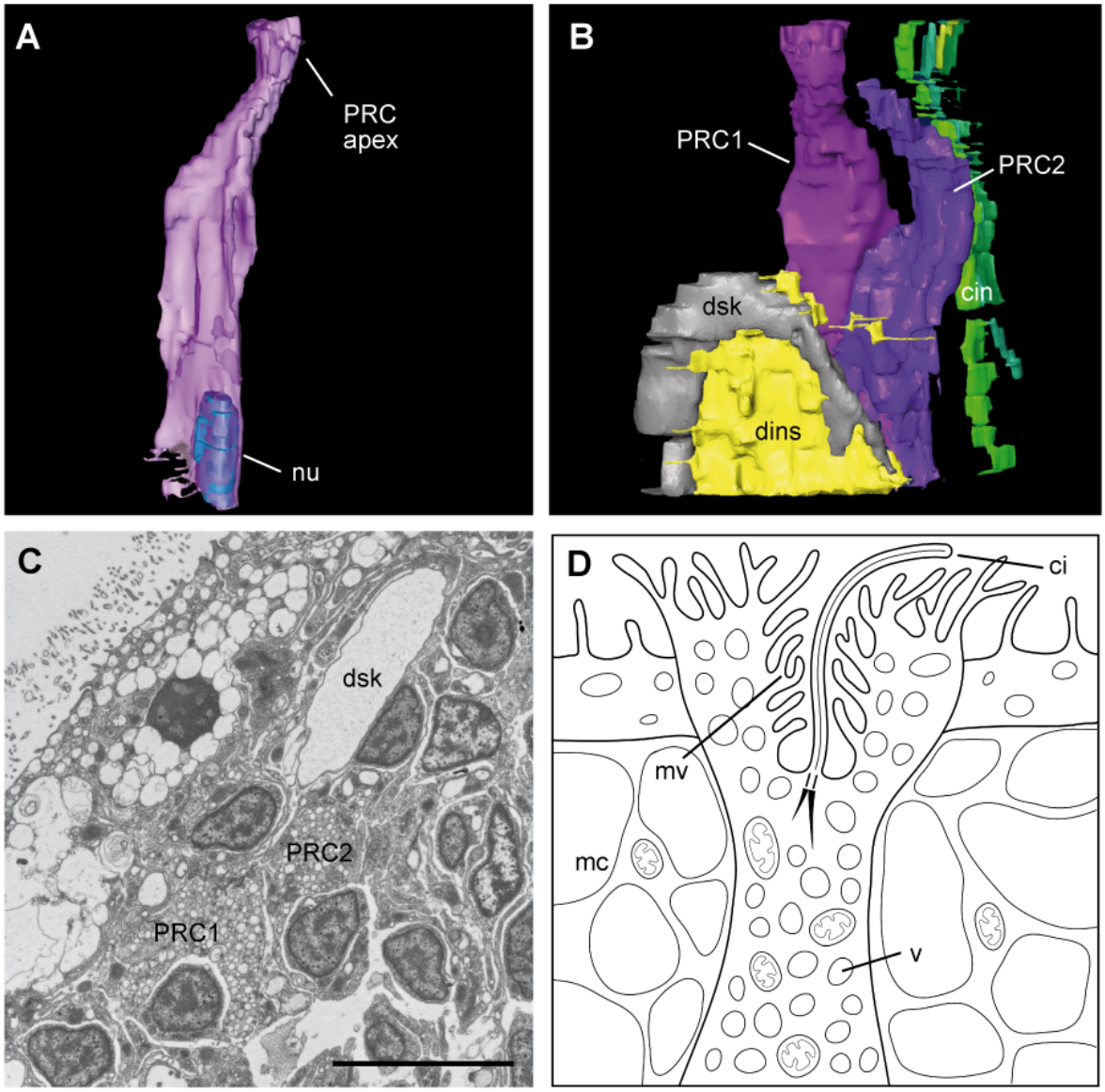

Fig. 8: Schematic reconstruction of *S. purpuratus* disc tube foot PRCs and associated tissues. **A.-B.** Surface rendered schematic 3D reconstructions from TEM serial sections. **A.** Single PRC showing an elongated flask-shaped morphology with the nucleus (nu) in a very basal cell portion. **B.** Two PRCs contacting the disc nervous system with their basal portions. The disc skeleton (dsk) is situated in close vicinity to PRCs and disc nervous system (dins). The ciliated sensory cells (cin) comprising the ciliary patches show a very thin and slender morphology and run in parallel to the PRCs. Mucus cells are not displayed in the reconstruction. **C.** TEM section showing close position of PRCs to the skeleton. **D.** Schematic reconstruction of TEM serial images of apical PRC portion showing the PRC to possess an unmodified cilium (ci) and many microvilli (mi) arranged in a “crown-like” structure. The vesicle (v) filled PRC apex slightly protrudes from the surrounding epidermis and the PRC body is flanked by mucus cells (mu). Scale bar in C: 5 µm.

Surprisingly, detailed TEM observations failed to detect the presence of any kind of dark screening pigment in the PRCs themselves and in their direct vicinity. This finding bears two important implications. First, it offers an explanation why former research failed to detect any photoreceptive structure in sea urchins. A dark screening pigment is a very common and easy to observe feature of PRC morphology. The lack of it has certainly hampered the former histological and electron microscopy studies trying to detect such photoreceptors. Second, the lack of any dark screening pigment results in the unavoidable need for an alternative PRC screening (or light-shielding) mechanism, given that the

organism has the ability to evaluate the direction of incoming light. This question will be adressed in one of the following paragraphs.

3.1.4. Sp-Opsin4 protein localization in juvenile *S. purpuratus*

With the novel finding of distinct PRCs that contrast to the long proposed overall dermal light sense, many new questions on echinoid photosensitivity arose. One of them concerned the onset of phototaxis and the required expression of the respective photopigment in the animal's life cycle. Since first experiments with *S. purpuratus* larvae had shown no or only diffuse reactions upon illumination (Arboleda 2008), our team of collaboration partners decided to examine larvae over the course of metamorphosis to adress the onset of phototaxis and opsin protein/RNA expression.

It turned out to be very difficult to successfully raise larvae until that stage and it was Sam Dupont (Sven Lovén Centre, Kristineberg, University of Gothenburg) who managed first to do so. His double-immunostainings in early juveniles using anti-Sp-Opsin4 together with anti-Synaptotagmin B (an echinoderm/deuterostome nervous system marker, see Nakajima et al. 2004, Burke et al. 2006) revealed the existence of two different r-opsin positive PRC clusters, one consisting of the formerly described PRCs in the tube foot disc and a second one residing at the base of the five primary tube feet (Fig. 9A). The primary podia are the first podia that develop in echinoderm juveniles. Interestingly, these primary podia later transform into the so-called terminal tentacles (Atwood 1973, Mooi et al. 2005, Morris et al. 2009) which in asteroids host the optic cushions at the tips of their arms (see below). Therefore the logical next step was to examine adult tissues to check whether the second PRC cluster is an exclusive feature of the primary podia and the terminal tentacles, respectively, or whether the locomotory tube feet also possess this kind of basal PRCs.

An additional important question deals with the connection of the investigated structures to the animal's nervous system. This is best examined in very young juveniles, since in adult echinoids the massive calcite corona hampers accessability of the internal nervous system for both molecular and morphological methods. It was thus very important regarding later functional evaluations that S. Dupont by anti-SynaptotagminB labeling of the internal juvenile nervous system observed that the basal PRC clusters project their axons as far as into the developing radial nerves (Fig. 9B)

R-opsin immunostainings of older *S. purpuratus* juveniles successfully raised by myself in Berlin (Fig. 9C), revealed no further labelings except for those in the two tube foot clusters (Fig. 9C+D). This finding is interesting in different respects. Exclusion of expression of

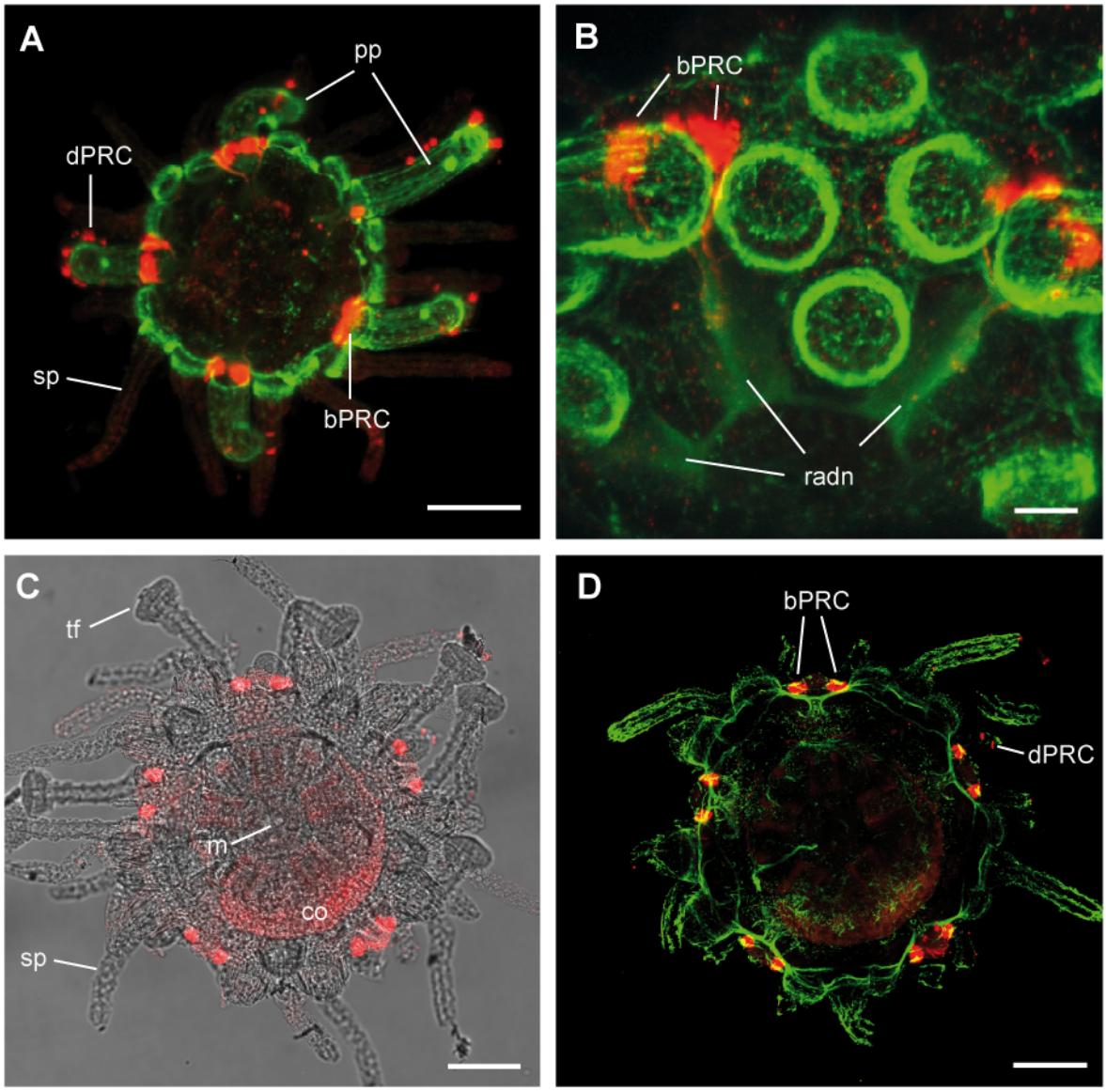

Fig. 9: Two clusters of r-opsin positive PRCs in juvenile *S. purpuratus* recorded by CLSM. Pictures A.-B. courtesy of Sam Dupont, Sven Lovén Centre for Marine Science, Sweden. **A.** Early juvenile with five primary podia (pp) showing Sp-Opsin4 localization within disc (dPRCs) and basal (bPRCs) PRCs (red). Nervous system stained with anti-Synaptotagmin B (green). **B.** Same immunolabeling applied as in A. Lateral view showing high magnification of basal PRC cluster projecting axons into the developing radial nerves (radn). **C.** Oral transmission view (m=mouth) of later juvenile with incomplete corona (co), tube feet (tf) and spines (sp). R-opsin labeling exclusively present in bPRCs and dPRCs (red). **D.** Same specimen showing localization of the nervous system in regard to basal PRCs via anti-acetylated alpha-tubulin staining. Scale bars in A, C, D: 100 µm, B: 25 µm.

Sp-opsin4 in other *S. purpuratus* organs than tube feet (like e.g. pedicellaria) is essential while looking for a potential mechanism to enable the animals to perform phototaxis. But the experiments turned also out to be important regarding the time of onset of phototaxis. As can be seen from Fig. 9D, the specimen clearly shows expression of Sp-Opsin4 protein in both tube foot clusters, but skeletogenesis is not complete with a roundish closed skeleton still missing (Fig. 9C). Section 3.1.6. of this chapter will deal with the interrelation between skeletogenesis, r-opsin expression and onset of phototaxis.

3.1.5. Basal r-opsin positive PRC cluster in echinoid tube feet

After discovering Sp-Opsin4 positive cells in the proximal (basal) part of the first few emerging juvenile tube feet, ambulacral pieces of adult *S. purpuratus* bearing several tube feet were dissected from live animals and fixed for immunohistochemistry. To check whether all adult locomotory tube feet host these Sp-Opsin4 positive cells at their bases, the fixed tissues were decalcified and stained with anti-Sp-Opsin4. The staining confirmed the existence of this second immunopositive PRC cluster residing in the very basal portion of each tube foot stalk, at a position where the tube foot attaches to the animal's skeleton (Fig. 10 A-E). Unlike the PRC's in the tube foot disc, up to 70 basal PRCs cluster closely together at the base of each echinoid tube foot. Some more scattered PRCs also appear along the lateral nerve that constitutes an extension of the basal portion of the tube foot nerve into the radial nerve (Fig. 10D-F), and rarely within the spine nerves. In later experiments, fractions of radial nerves from different ambulacra were dissected from freshly opened animals by extracting them together with the radial water vascular system. Anti-Sp-Opsin4 and anti-acetylated alpha-tubulin incubation of the dissected radial nerve revealed no r-opsin positive cells within this part of the internal nervous system of the sea urchin. Only in the very distal portion of the radial nerve branches where they contact the tube foot ampullae, some weak stainings might indicate presence of single Sp-Opsin4 positive cells (Fig. 11A+B). It could thus be shown that all r-opsin positive PRCs do connect to the nervous system of *S. purpuratus* (see also scheme Fig. 11C+D).
Absence of Sp-Opsin4 positive cells in the sea urchin radial nerves also hints on another type of photoreceptor cell being present there, as the radial nerves have been demonstrated to be intrinsically photosensitive (Yoshida and Millott 1959, for review see also Millott 1975).

3.1.6. Tube foot photoreceptors and the echinoid skeleton

Since the investigated PRCs do not possess any associated shielding pigment, the position of the basal photoreceptors at the margin of the tube feet and thus directly on top of the sea urchin's skeleton (also termed corona or test) attracted my attention. For a PRC to determine the direction of illumination, there has to be a shading mechanism or device that restricts the angle of the incoming light. The tube foot disc PRCs with their distal position in the extremely mobile tube feet seemed no good candidates to fulfill the requirements for such a scenario. However, the PRCs at the base of the tube feet are not subjected to such intense movements making the underlying opaque sea urchin skeleton a possible candidate to provide shielding for these receptor cells.

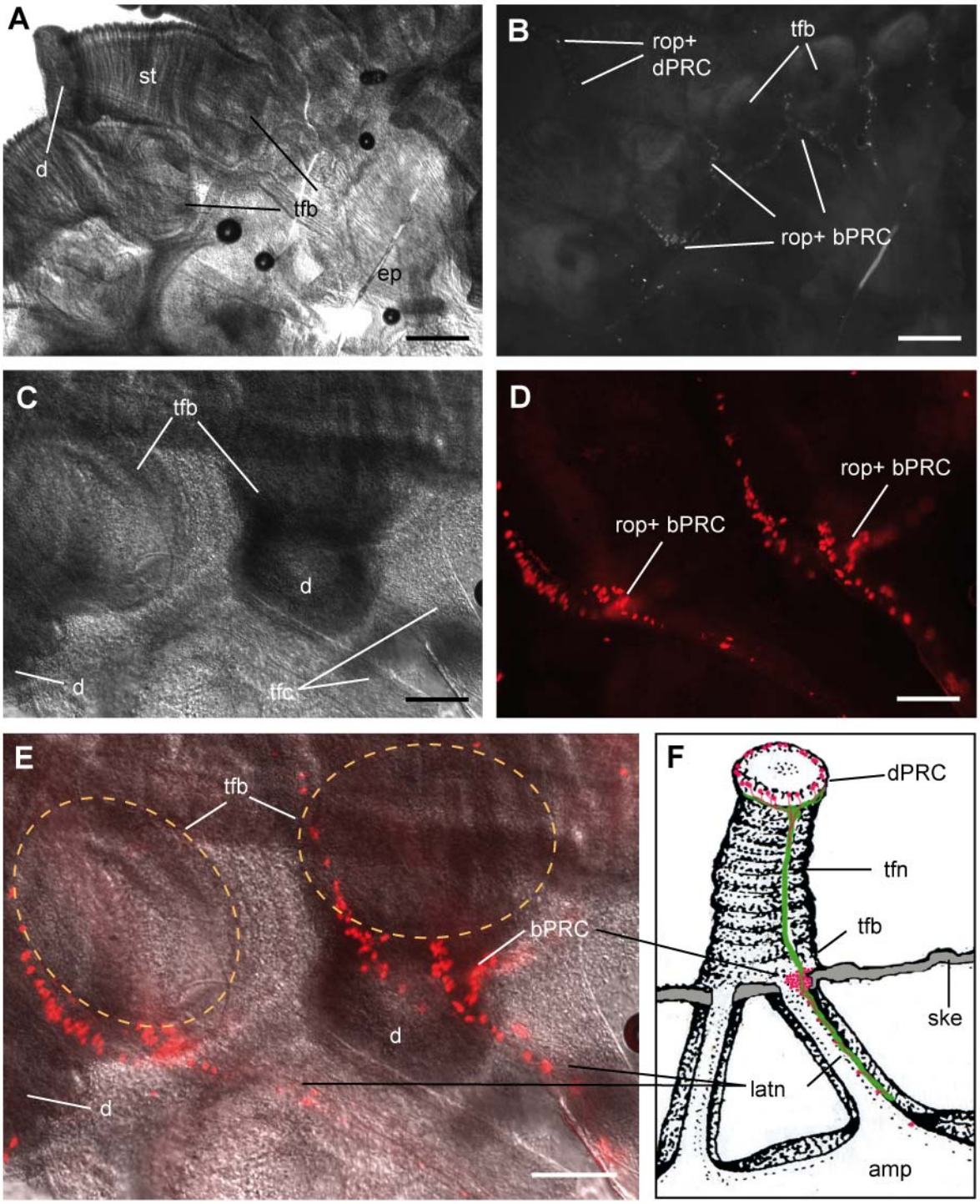

Fig. 10: Basal r-opsin positive PRC cluster in adult *S. purpuratus* tube feet. **A.-E.** DIC and fluorescence photographs of decalcified adult tissue. **A.** Row of tube feet with stalk (st), tube foot base (tfb), and disc (d) and neighboring epidermis (ep). **B.** Fluorescence image of the same region as in A, bPRCs and dPRCs in white. **C.** Two tube feet of another tissue portion mounted invertedly. View from former inside of corona towards external. Tube foot coelom (tfc) projects from tube foot towards ampulla. **D.** Fluorescence picture of same region as in C showing basal PRC cluster. **E.** Projection of C and D showing localization of basal PRCs at the base of tube feet (tfb) illustrated through orange dotted lines. Some PRCs are located within the lateral nerve (latn). **F.** Scheme of tube foot with nervous system and two PRC clusters. (amp:tube foot ampulla, ske:skeleton, tfn:tube foot nerve). Scheme of tube foot modified from Goldschmid 2007). Scale bars in A-B: 200 µm, C-E: 100 µm.

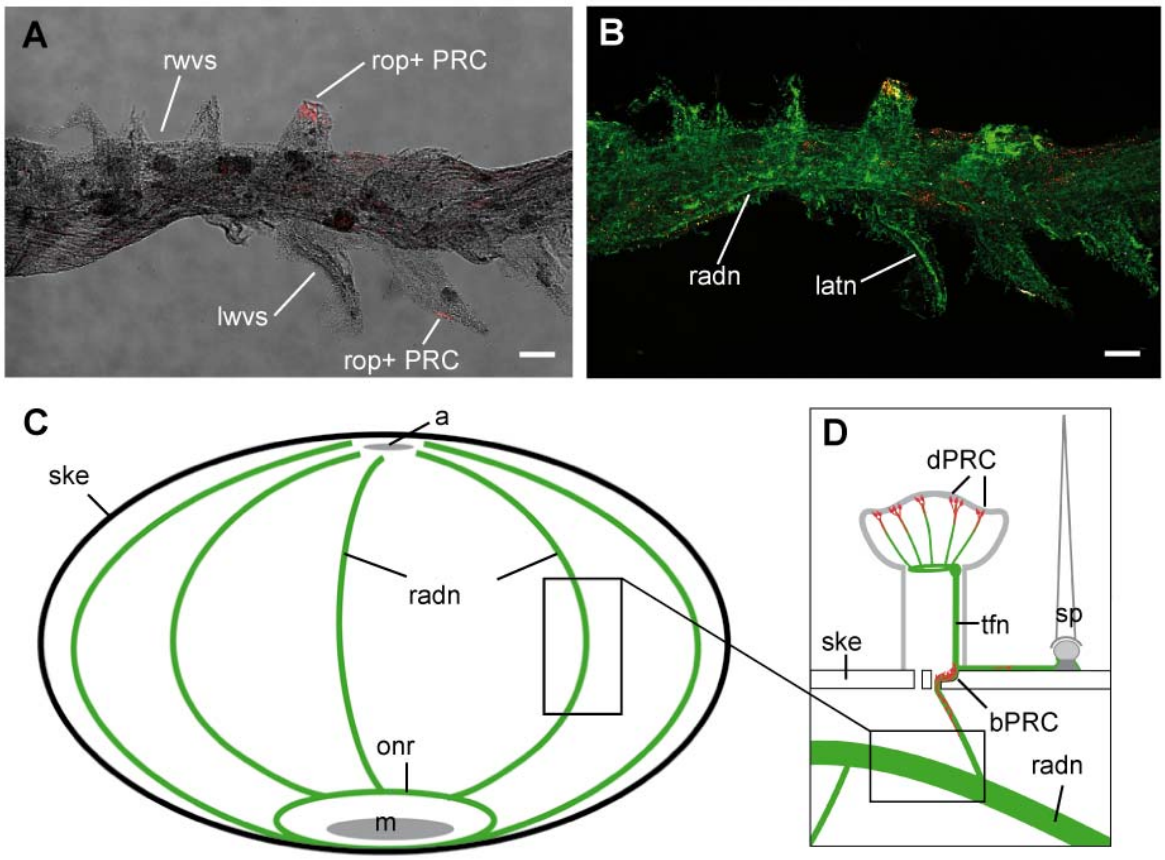

Fig. 11: R-opsin protein localization in *S. purpuratus* radial nerves and schematic depiction of PRCs within the echinoid nervous system. **A.-B.** Extracted radial water vascular system (rwvs) bearing radial nerve (radn). **A.** Transmission view showing radial water vascular system with alternating branches to lateral water vascular system. Sp-Opsin4 positive cells (rop+PRC) at distal region of lateral water vascular system (red). **B.** Co-labeling with anti-acetylated alpha-tubulin reveals radial nerve and lateral nerves as well as presence of many cilia within the water vascular system. Sp-Opsin4 positive PRCs in hot red. **C.** Scheme of echinoid internal nervous system with oral nerve ring (onr) and radial nerves, (a:anus, m:mouth, ske:skeleton). **D.** R-opsin positive PRCs and the echinoid nervous system (s:spine, bPRCs: basal tube foot PRCs, dPRCs: tube foot disc PRCs, tfn:tube foot nerve). Schemes C+D adapted from Burke et al. (2006). Scale bars in A-B:100 µm.

Using SEM it was possible to detect potential corresponding morphological structures in the sea urchin skeleton, which may function as a shielding device. The corona of sexually mature *S. purpuratus* shows an arrangement of 7-8 neighboring tube foot double-pores in a row, with (depending on skeletal size) some 20-30 of these rows vertically arranged in two columns following each ambulacral margin (Fig. 12A+B). Each tube foot resides on a characteristic double pore in the corona that is lined by a thin, ring-like depression where in the living animal connective tissue fibrils of the tube foot stalk attach to the skeleton. One pore of each pair has an additional small channel that accomodates the tube foot nerve on its way through the skeleton (Smith 1978, 1980) (Fig. 12C). Where this tube foot nerve channel meets the skeleton's outer surface it widens into an invagination (Fig. 12C). Closer examination of this structure which so far had been neglected in the context of echinoid photobehavior, led to the idea that in the living animal the basal tube foot PRC cluster might possibly be located in this skeletal depression. When projecting a picture of the Sp-Opsin4 immunostaining of a decalcified specimen (Fig. 12D) onto the SEM picture

of another specimen (Fig. 12C), the cells, despite potential deterioration effects of decalcification and size differences between the different specimens, fitted relatively well inside the depression of the skeleton (Fig. 12F). The counted number of tube foot double pores in skeletons of five sexually mature animals varied between 1260 and 1760. Approximated over the average number of counted disc and basal photoreceptors, each tube foot thus possesses up to 140 PRCs resulting in some 200.000 PRCs per animal, depending on its size and tube foot number.

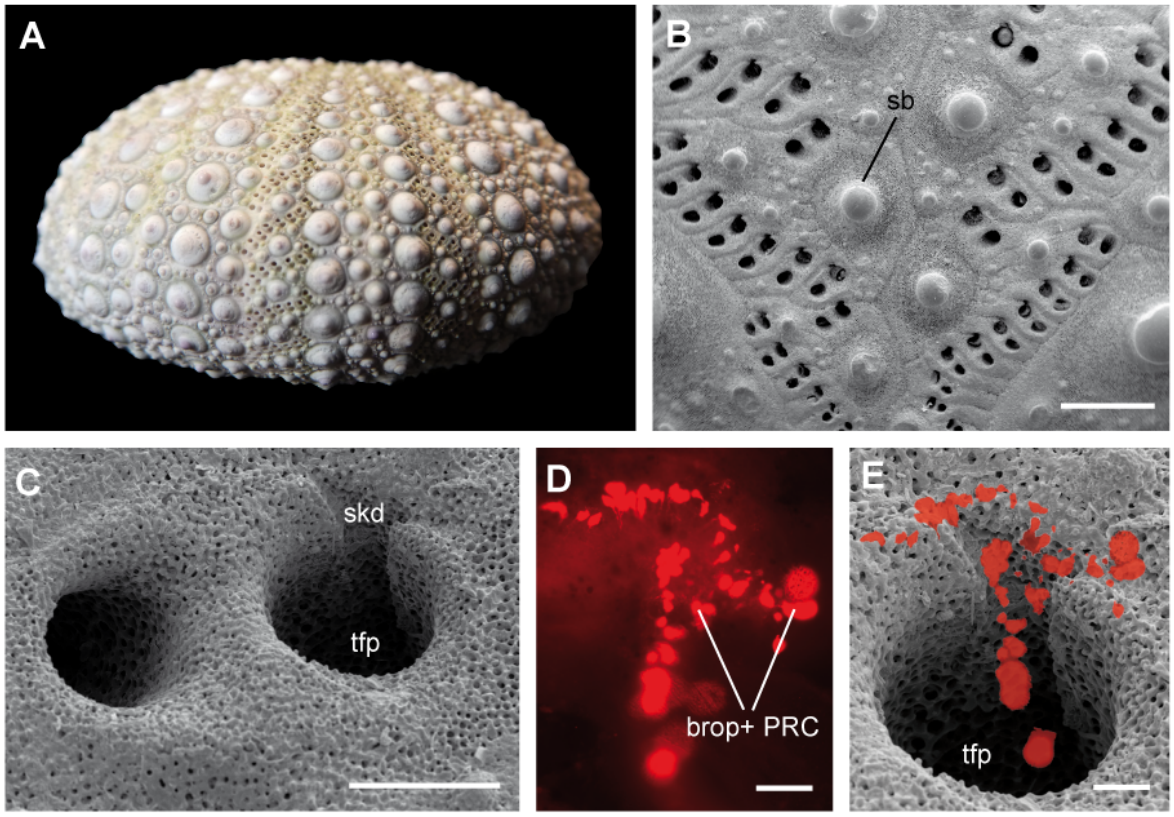

Fig. 12: Morphological arrangement of *S. purpuratus* basal tube foot PRCs in relation to the skeleton. (A) Photograph of a whole calcite skeleton, showing 7-8 neighboring tube foot double pores in a row with those rows vertically arranged in two columns following each ambulacral margin. **B.** SEM preparation of an ambulacral suture showing tube foot pore rows along both sides (sb:spine base). **C.** SEM preparation of double tube foot pore (tfp) corresponding to one tube foot attached within intact specimen. One of the pores bears an extra channel to acomodate the tube foot nerve, its apical portion widening into a roundish skeletal depression (skd). **D.** High magnification fluorescence picture of basal Sp-Opsin4-positive tube foot PRC cluster (red). **E.** projection of tube foot pore with extra nerve channel from C and basal PRC cluster from D. Size adapted and PRCs clipped out via Photoshop CS2. The basal PRC cluster fits inside the skeletal depression. Scale bars in B: 1 mm, C: 250 µm, D-E: 100 µm.

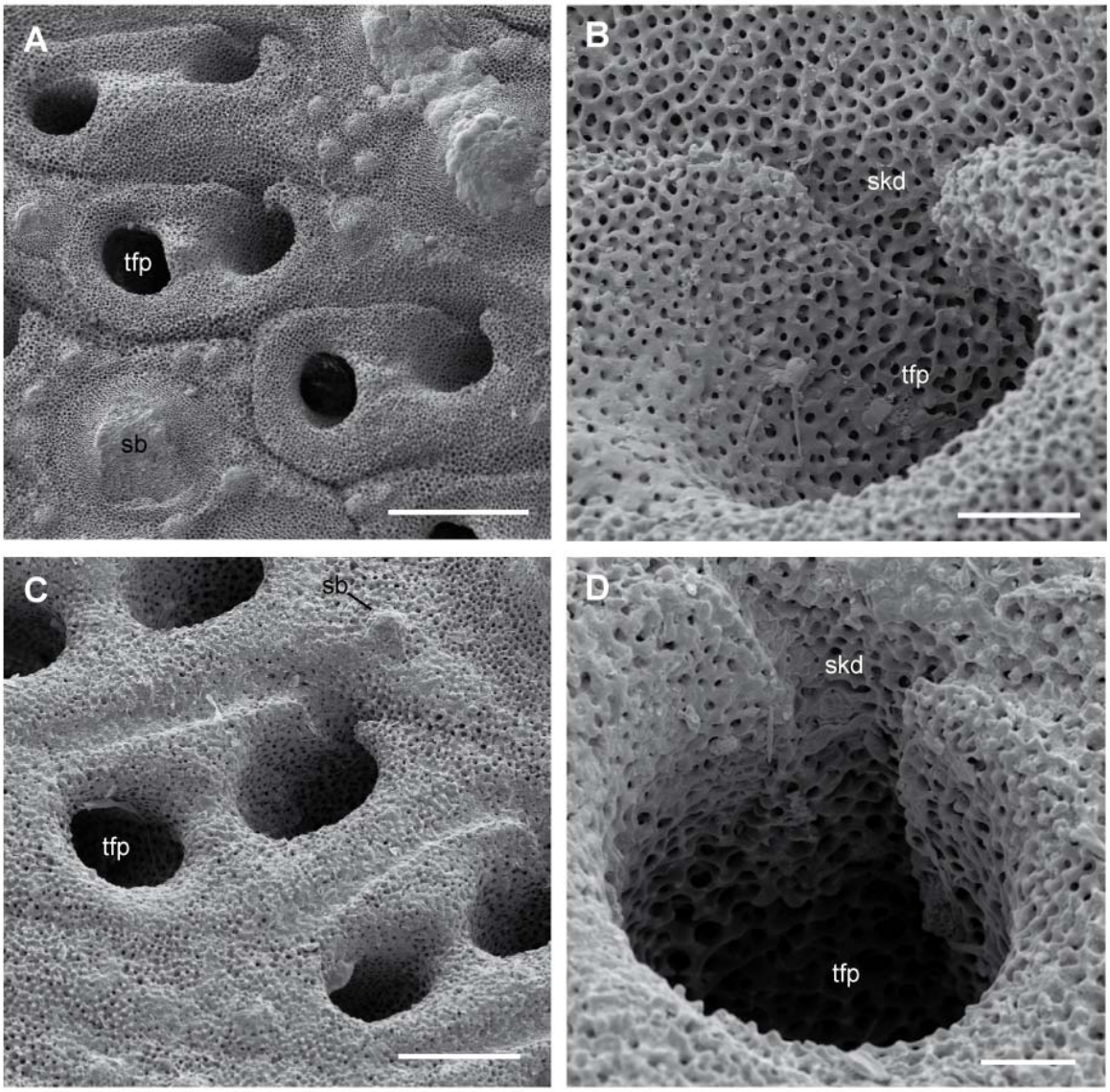

Fig. 13: Skeletal differences between *S. purpuratus* and *Echinometra lucunter* examined by SEM. **A.** Overview of ambulacrum portion of *E. lucunter*, showing three tube foot double pores (tfp:tube foot pore). **B.** In high magnification, the skeletal depression (skd) hosting the tube foot nerve in the skeleton of *E. lucunter* is visible. **C.** Overview of ambulacrum portion of *S. purpuratus*, also showing three tube foot double pores. The thin, ring-like depression surrounding each double pore is less prominent than in *E. lucunter*. **D.** High magnification of *S. purpuratus* tube foot pore shows stereom trabeculae to be more solid than in *E. lucunter*. Scale bars in A: 500 µm, B, D: 100 µm, C: 250 µm.

With these results on skeleton examination at hand, my collaboration partner M. I. Arnone performed phototaxis experiments with freshly metamorphosed juveniles of *S. purpuratus* and *Paracentrotus lividus* which had not yet developed a complete skeleton. Deploying a similar experimental phototaxis design as with adults (except for reduction of the seawater chamber size), she found that freshly metamorphosed juveniles of either species do not display any phototactic reactions. After the experiment, some of the tested animals were fixed for immunohistochemistry and sent to Berlin, where I checked Sp-Opsin4 protein presence. Sp-Opsin4 protein was indeed localized in all juveniles despite their documented lack of phototactic reactions in the illumination experiment. To exclude the

possibility that a different (and later expressed) opsin protein might be responsible for mediation of phototaxis, M. I. Arnone also tested the expression of Sp-Opsin1, the ciliary opsin, which is known to occur in *S. purpuratus* and of which an ortholog in chordates is deployed in the context of vision. Although a later paragraph of this section will deal more extensively with opsin1 expression in echinoderms, it can already be stated here that Sp-Opsin1 was also clearly expressed in the non-phototactic juveniles. A lack of Sp-Opsin1 expression as the reason for non existing phototactic behavior can thus be excluded.

Additional juveniles reared in the same fertilization experiment, were further cultivated until they developed a complete, closed skeleton (see Märkel 1975, 1976, David et al. 1995, for development of skeleton). Progress in skeleton formation was regularly checked by detecting auto-fluorescence of calcitic skeletal elements via CLSM microscopy. Both species, *S. purpuratus* and *P. lividus*, showed skeleton completion after approximately one month and when tested again under the same conditions all juveniles now displayed clear (negative) phototaxis (Arnone et al., personal communication). The obvious independence of displayed phototaxis from opsin protein expression plus the finding that only juveniles with a complete skeleton do show phototaxis strongly suggest that the sea urchin skeleton has a hitherto unknown functional role in phototaxis.

Recent publications (Blevins and Johnsen 2004, Yerramilli and Johnsen 2010) have revealed differing maximum spatial resolutions regarding photoreception in different sea urchin species, namely *S. purpuratus* and two species of the genus *Echinometra*. Given a possible involvement of the echinoid skeleton in visional processes (or PRC shielding, respectively), also a corona of *Echinometra lucunter* was examined by SEM to look for morphological differences between the species, which may account for the observed physiological discrepancies. The general morphology of the tube foot pore hosting the tube foot nerve differs slightly between *S. purpuratus* and *E. lucunter* (Fig. 13A+C) but the two skeletons also show differences in the stereom structure as can be observed in higher magnification (Fig. 13B+D). Compared to *E. lucunter,* the stereom of *S. purpuratus* is more solid, comprising massive trabeculae and thereby resulting in a reduction of intercalcite spaces. If the skeleton plays a role in shielding as suggested above, one could assume that the shielding properties of the coronae of both species are different.

3.1.7. X-ray microtomography (µCT) of the *S. purpuratus* skeleton

The assumption of a potential involvement of the sea urchin endoskeleton in phototaxis plus the unusual position of the basal PRC cluster embedded in the skeletal depression (see above), provoked the question how these elements might work together to

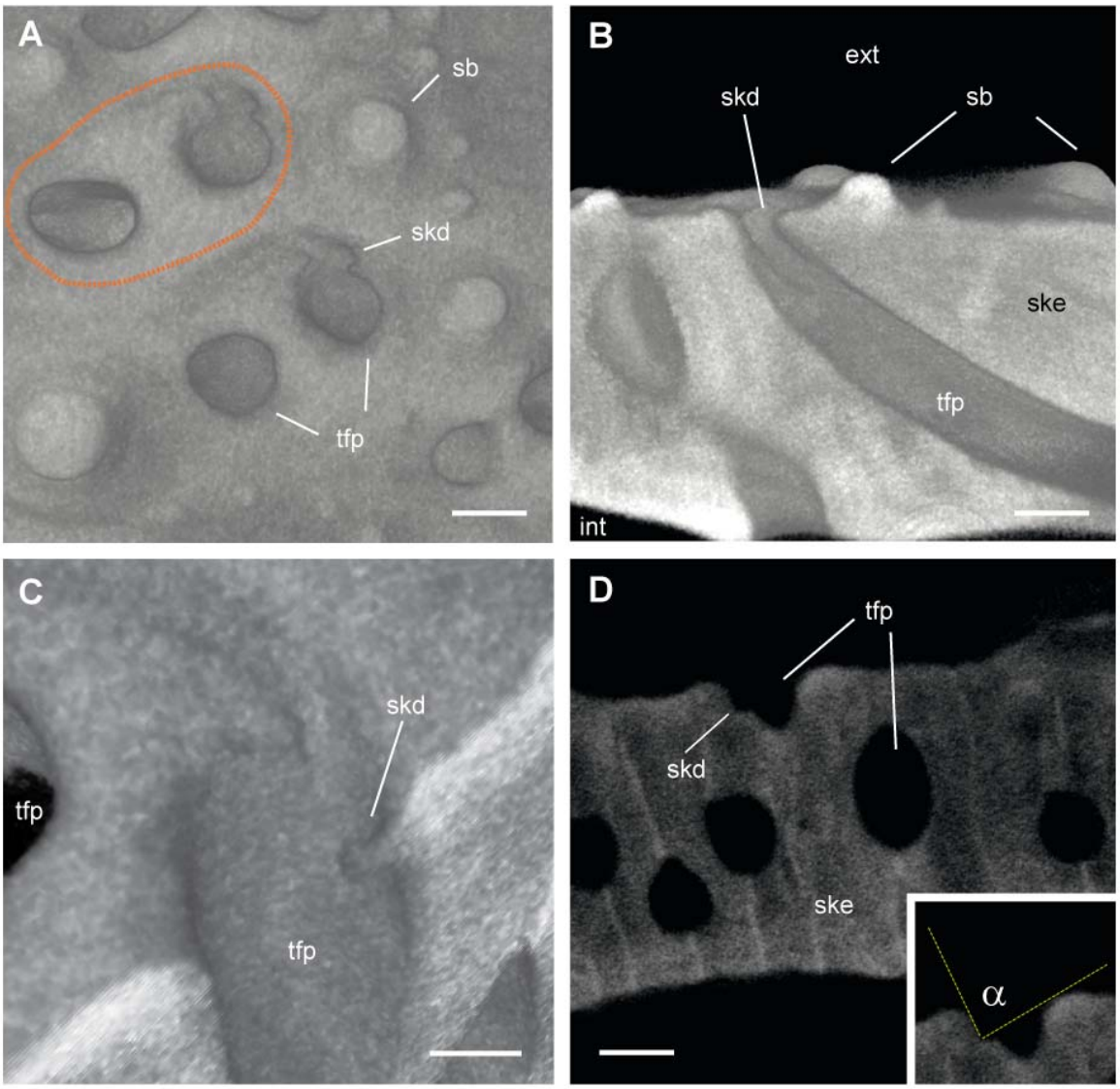

Fig. 14: The skeleton of *S. purpuratus* examined via X-ray microtomography. **A.** Virtual reconstruction of the skeletal surface showing tube foot double pores of locomotory tube feet (tfp) with skeletal depression (skd) and primary spine bases (sb). Orange dotted line corresponds to insertion of tube foot tissue in intact specimen. **B.** 3D reconstruction of virtual cross section of an ambulacral portion of the skeleton (ske). The tube foot pore bearing the tube foot nerve channel runs longitudinally through the skeleton. The apical portion of the tube foot pore widens into a depression (skd). **C.** Different 3D reconstructed virtual cross section depicting lens-shaped morphology of apical tube foot pore depression. Note that the second tube foot pore of the same tube foot runs straight vertically through the skeleton. **D.** Virtual skeleton cross section showing several tube foot pores and the skeletal depression of the lens-shaped apical widening. The insert depicts the smallest measured opening angle α = 88° towards the skeleton's external resulting in a maximum corresponding shading angle of 272°. Scale bars in A, B, D: 300 µm, C: 150 µm.

sufficiently restrict the angle of incoming light to allow for directed phototaxis. Another question was how to measure and visualize the 3D structure of this skeletal/nerve cell complex. X-ray microtomography combined with a 3D visualization software helped to overcome the limits set by the 2D perspective of the SEM technology. This technique allowed to perform the first measurement of the opening angle (and thus shading angle, respectively) of the skeletal structure in which the basal tube foot PRCs were shown to be embedded. Surface rendered virtual 3D reconstruction for the µCT data allowed to obtain

a better resolved picture of the sea urchin outer skeletal surface showing the exact 3D morphology of the tube foot pores (Fig. 14A). Deploying µCT furthermore allowed to produce virtual cross sections at every scanned plane in the 3D reconstruction. It could thus be visualized that in each pair of tube foot pores, the pore bearing the extra channel for the tube foot nerve does not run vertically through the stereom. On the contrary, this pore shows an extreme longitudinal transversion angle compared to the parallel outer and inner skeletal surface (Fig. 14B). With regard to the potential involvement of the skeleton in shielding of deployed PRCs, this is an important finding, because it shows that penetration of light through this pore into the animals interior is highly unlikely. Analysis of the µCT data corroborated the former SEM finding that the apical part of the pore, which accompanies the tube foot nerve channel, widens into a depression. It´s exact shape could be determined as lens- or drop-shaped (Fig. 14C). Measuring several of these depressions from a 90° (coss-section) angle to their widest opening, the smallest observed opening angle was 88° towards the external of the skeleton (Fig. 14D+inset).

3.1.8. R-opsin positive PRCs in other Echinoidea

Having a sea urchin specific r-opsin antibody at hand, I investigated tube feet of other echinoids to obtain comparative data for r-opsin positive PRCs in other species. The choice of species, however, was primarily driven by availability rather than phylogenetic relationsship of the tested species. All investigated regular echinoids showed r-opsin positive PRCs in their tube foot tips (Fig. 15A-D). The number of PRCs clearly varies between species (*S. purpuratus*, *Echinus esculentus*, *Strongylocentrotus droebachiensis*) but also shows minor variation between conspecific specimens. The experiments regarding the statistical evaluation of these differences are still ongoing, including two additional Mediterranean species (*Paracentrotus lividus* and *Arbacia lixula*) that are currently tested by M. I. Arnone and co-workers at SZN.

The irregular echinoid *Brissopsys lyrifera* showed no r-opsin positive cells in any of its different tube feet types. Preliminary phototaxis experiments performed by the lab of Sam Dupont in Kristineberg showed no detectable reaction upon illumination with a continuous light spectrum. Although these findings seem to correspond with the infaunal lifestyle of these animals, the behavioral experiments were cancelled due to the extremely slow overall reaction of this sea urchin species, which hampers the determination of distinct reactions upon any specifically given stimuli.

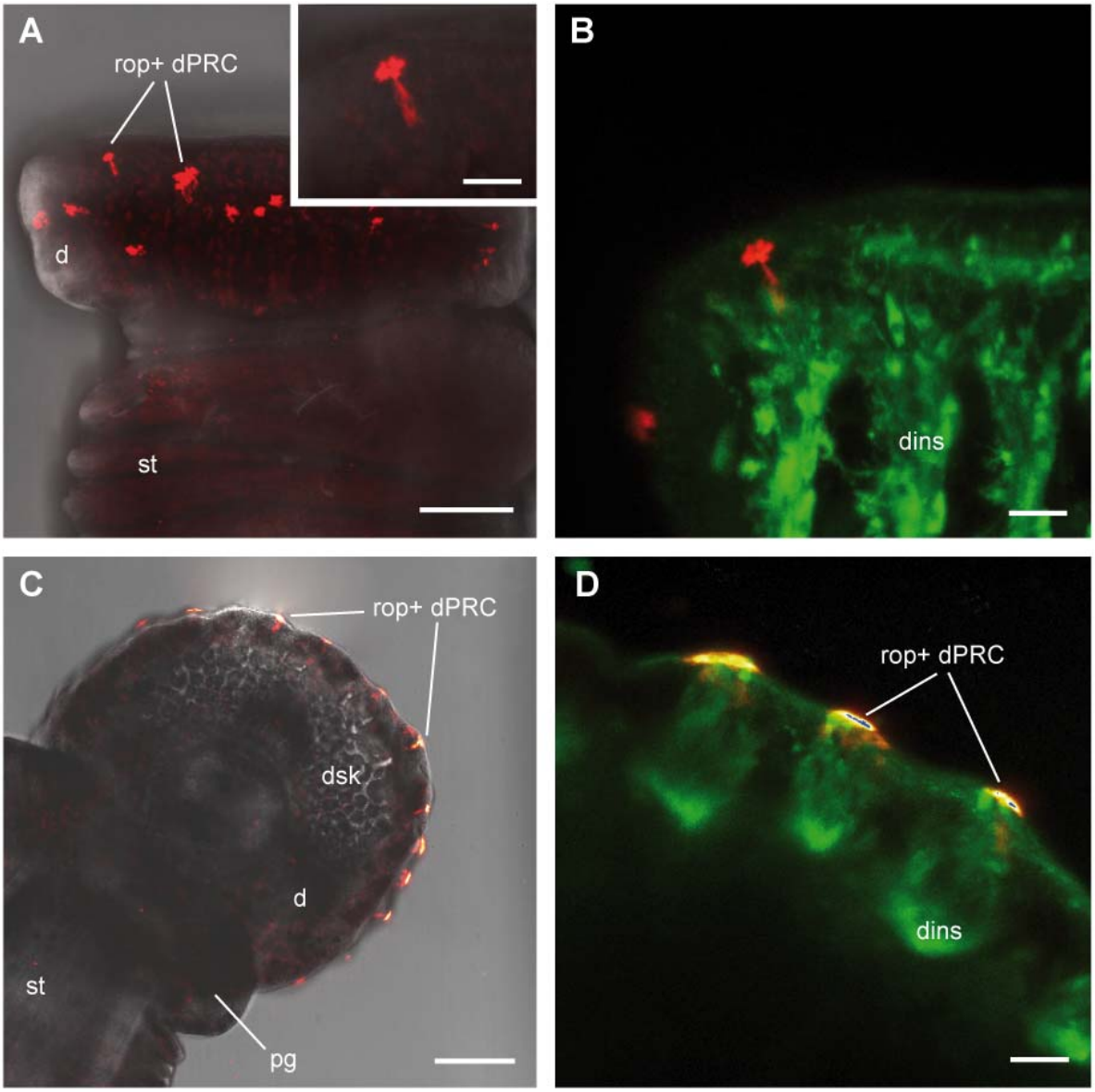

Fig. 15: R-opsin localization in tube foot disc PRCs of *Echinus esculentus* and *Strongylocentrotus droebachiensis* by CLSM. Z-stack projections of different immunostainings. **A.** Adult locomotory tube foot of *E. esculentus* bearing several r-opsin positive PRCs (rop+) (red) in the disc region (d). The stalk (st) shows no r-opsin localization. Insert shows "petal-like" morphology of apical PRC portion. Color merge depicting transmitted light and antibody labeling against Sp-Opsin4. **B.** Color merge displaying one PRC (red) in connection to the tube foot disc nervous system (dins) stained with anti-acetylated alpha-tubulin (green). **C.** Transmitted light projection of *S. droebachiensis* adult locomotory tube foot. View towards ventral portion of tube foot disc with disk skeleton (dsk), podial ganglion (pg) and stalk. R-opsin positive PRCs line the rim of the tube foot disc (hot red). **D.** Three PRCs arranged within an epidermal bulge of the tube foot disc in close connection to the disc nervous system (dins) immunolabeled via Synaptotagmin B (see Materials and Methods). Scale bars in A, C: 100 µm, B, D and inset in A: 20 µm.

3.1.9. Detection of c-opsin in *S. purpuratus* and *Echinus melo*

Expression analyses revealed up to six different expressed opsin genes in the purple sea urchin *S. purpuratus* (Raible et al. 2006). Although focussing on Sp-Opsin4 expressing (rhabdomeric) photoreceptors, investigations of photoreceptors deploying the ciliary opsin Sp-Opsin1 are included in this thesis, too. In the beginning, experiments on Sp-Opsin1 expressing cells were primarily conducted to exclude interference of these PRCs with the

emerging model scenario hypothesized for the rhabdomeric photoreceptors. But towards the end of the practical work of this study, a reasonable amount of data on ciliary opsin expressing photoreceptors in different echinoderm subgroups had been accumulated. In sea urchins, the most striking labelings deploying the designed anti-Sp-Opsin1 antibody derived from experiments on pedicellaria. In the juvenile echinoids, strong r-opsin labeling is visible in so called “tridentate” pedicellaria, the biggest type of pedicellarium present in *S. purpuratus* (Fig. 16A+B). The tridentate pedicellaria are composed of three “compartments”, (a) a slender stalk that attaches to the skeleton, followed by (b) the neck region that contains a mucus cylinder, connective tissue and the flexor muscles (Fig. 16C composit transmission) and finally (c) a head region bearing three calcite “valves” that can be opened and closed via a system of flexor, adductor and abductor muscles. The tridentate pedicellarium possesses an extensive nervous system, with a neuropil at the inner side of each of the three valves to and from which many nerve tracts branch and connect (Fig. 16D). The nerve tracks deriving from this neuropil often bifurcate and run down the neck and stalk region (Fig. 16E) integrating into a nerve ring at the base of the pedicellarium. Immunostaining against Sp-Opsin1 yields a relatively dispersed staining pattern in the head region (Fig. 17A). Although it is hard to evaluate the relation between background and specific staining at the present state without co-localization of the expressed RNA, some fibrillar structures clearly show Sp-Opsin1 labeling. This becomes especially evident within the neck region, where those Sp-Opsin1 “fibres” can be observed to run in parallel to the nerve tracts stained by anti-acetylated alpha-tubulin (Fig. 17B+D). The stalk shows no immunoreactivity to Sp-Opsin1. Z-projections of the two different antibody labelings show that whereas Sp-Opsin1 and acetylated alpha-tubulin in the head region are present within the same area (Fig. 17C, yellow) the two proteins clearly localize separately within the neck of the pedicellaria (Fig. 17D). High magnification of Sp-Opsin1 labeling reveals a morphology that reminds on mesodermal tissue like muscle cells or collagen fibres. (Fig. 17E). This finding is supported by the fact that Sp-Opsin1 is located deeper inside the pedicellarian tissue compared to the nerves stained by anti-acetylated–alpha-tubulin (Fig. 17F).

A second target for initial experiments on Sp-Opsin1 localization was its potential presence in the sea urchin radial nerves. As mentioned earlier in the context of lacking Sp-Opsin4 localization within *S. purpuratus* radial nerves, it has been shown electro-physiologically that sea urchin radial nerves are intrinsically photosensitive (Yoshida and Milott 1959, Millot 1975). Thus a photoreceptive pigment has to be present. Incubation with anti-Sp-Opsin1 indeed showed localization of the ciliary opsin within *S. purpuratus* radial nerves. The radial nerves were extracted together with the radial water

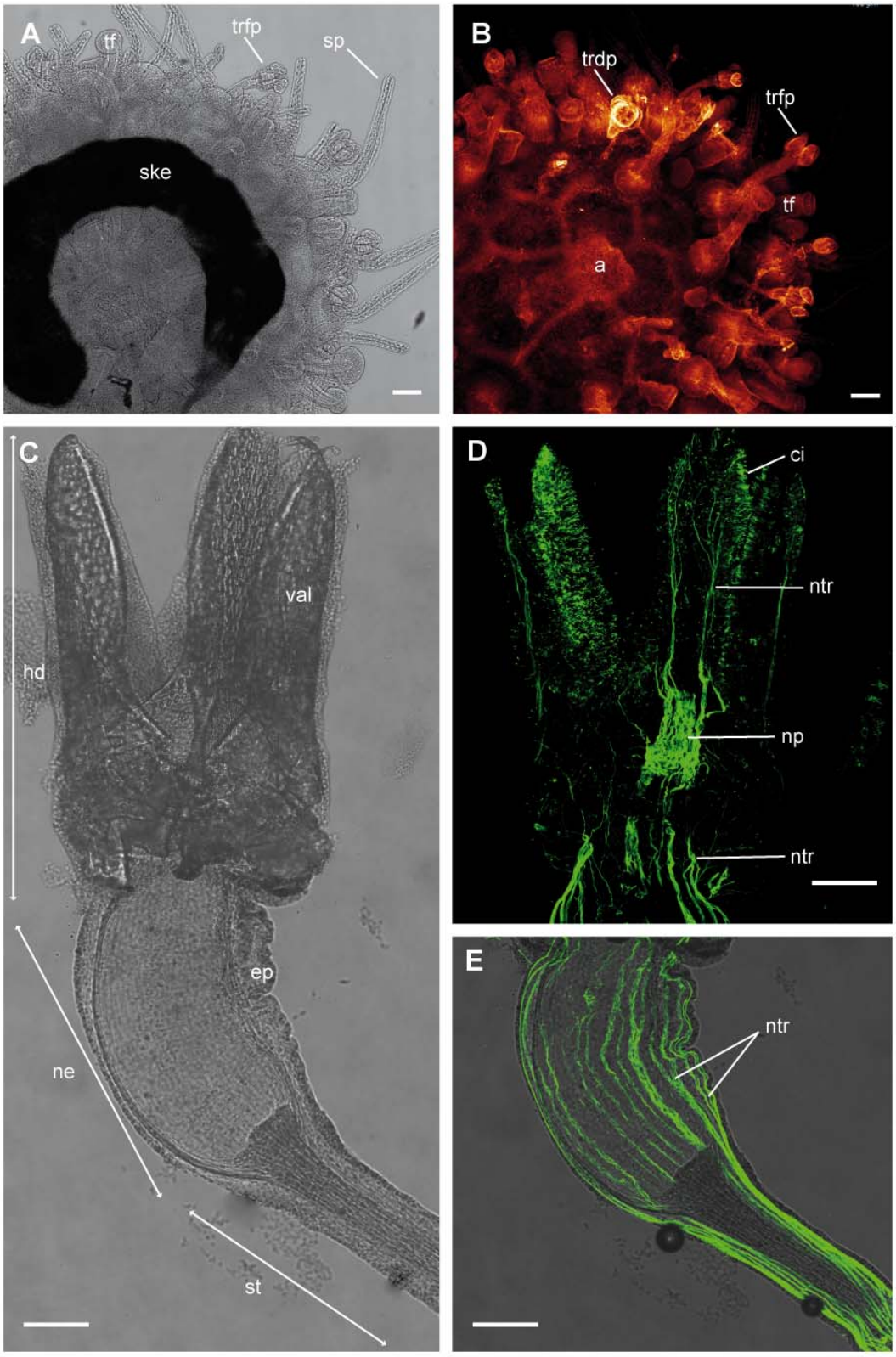

Fig. 16: Localization of ciliary opsins in *S. purpuratus* pedicellaria. **A.** Transmission view of whole mount juvenile with developing skeleton (ske), tube feet (tf), spines (sp) and trifoliate pedicellaria (trfp). **B.** Z-stack projection of anti-Sp-Opsin1 immunolabeling showing c-opsin protein present in tridentate pedicellarium (trdp) (hot red). **C.** Transmission view of adult tridentate pedicellarium. Composit from separate scans of “head” region (hd) with three ossicle bearing valves (val) and “neck (ne)/stalk (st)” region with epidermis (ep). **D.-E.** Z-projections of acetlyted alpha-tubulin staining. **D.** Head region showing prominent neuropil (np) of one of the valves. Prominent nerve tracts (ntr) connect the cilia (ci) bearing distal valve region to the neuropil that also sends bifurcating nerve tracts into the neck/stalk region (green). **E.** Neck/stalk region showing strongly labeled nerve trackts (green). Scale bars in A-E: 100 µm.

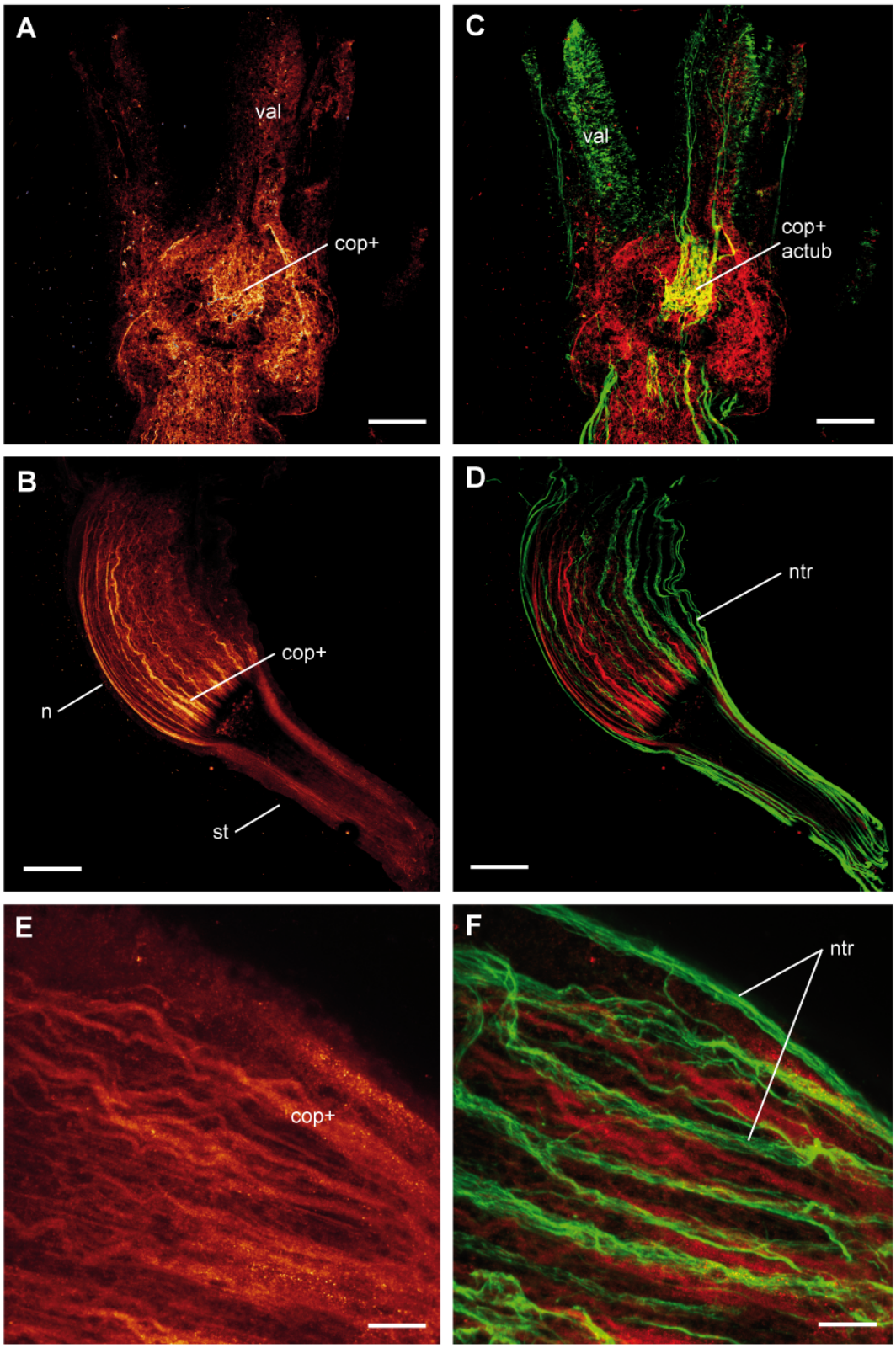

Fig. 17: C-opsin positive cells in *S. purpuratus* tridentate pedicellariae examined by CLSM. C-opsin protein localization (red) and acetylated alpha-tubulin (green) via color merge of z-stack projections. Projections and color merges from CLSM z-stacks. **A.** Head region with c-opsin protein localization in basal portion of all three valves (val). **B.** Neck (n)/stalk (st) region with c-opsin protein localization in fibre-like structures. **C.** Color merge both immunolabelings showing presence of both, c-opsin and nerve cells within basal portion of one valve. **D.** Color merge in the neck/head region showing c-opsin positive "fibres" running parallel to the nerves. **E.** High magnification reveals c-opsin protein presence in distinct single "fibres" resembling muscle cells. **F.** Same area as in E, c-opsin protein being localized deeper inside the neck tissue compared to nerves. Scale bars in A-D: 100 µm, E-F: 20 µm.

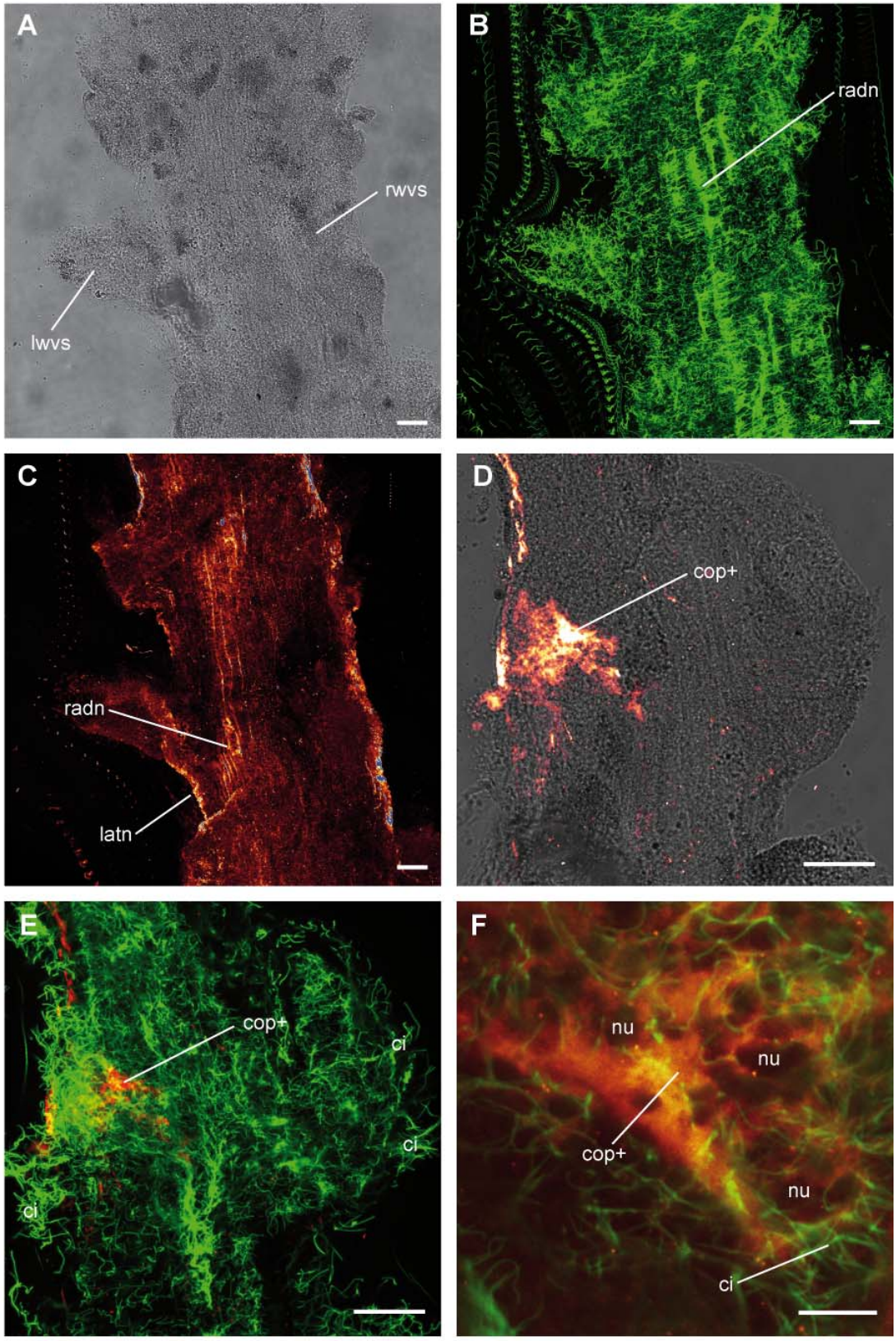

Fig. 18: C-opsin protein localization within *S. purpuratus* radial nerves examined by CLSM. C-opsin protein localization (red) and acetylated alpha-tubulin (green) via color merge of z-stack projections. **A.** Transmission view of dissected radial water vascular system (rwvs) and lateral water vascular system (lwvs). **B.** Radial nerves (radn) are hardly visible in projection due to massive presence of cilia. **C.** Sp-Opsin1 immunoreactivity within the radial nerve and the lateral nerve (latn). **D.** Massive c-opsin (cop+) protein presence within portion of the radial nerve. **E.** Region of c-opsin expression is densely ciliated (ci). F. High magnification of c-opsin positive area with dark areas possibly representing nuclei (nu) and cilia protruding from c-opsin positive area. Scale bars in A-E: 50 µm, F: 10 µm.

vascular system that shows a diffuse pigmentation pattern (Fig. 18A). A huge amount of cilia functioning in coelomic fluid transport was made visible via anti-acetylated alpha-tubulin staining (Fig. 18B). The radial nerves of *S. purpuratus* show a “segmentation” pattern (Burke et al. 2006) with a ganglion-like arrangement of neurons in defined distances. In between these neuronal accumulations, Sp-Opsin1 staining is present, but again, like in the case of pedicellaria, an evaluation of specificity is difficult regarding the performed experiments (Fig. 18C). Nevertheless, within those “ganglionated” nerve cell arangements a strong Sp-Opsin1 signal indicates presence of this photopigment protein (Fig. 18D). Compared to the rest of the water vascular system an accumulation of cilia was detected in the expression area (Fig. 18E). With high magnification, single cilia could be observed, protruding from the Sp-Opsin1 positive cells, and also darker areas most certainly indicating location of the nuclei (Fig. 18F). Expression of a ciliary opsin within radial nerves that are completely shielded from any natural light source by the sea urchin's skeleton is by itself an interesting observation which opens a wide field of opportunities for further experiments.

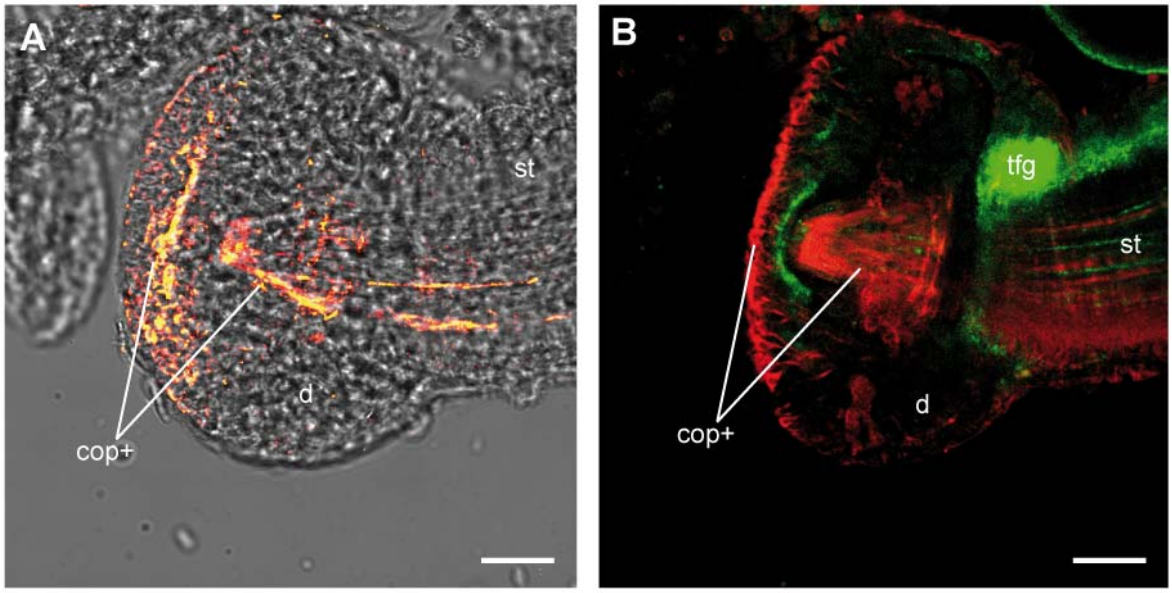

Fig. 19: C-opsin positive cells in adult *S. purpuratus* tube feet examined by CLSM. Double immunolocalization of Sp-Opsin1 (hot red/red) and acetylated alpha-tubulin (green) via color merge of z-stack projections. **A.** C-opsin staining (cop+) in tube foot disc (d) region where muscles connected to the skeleton (dsk) are located. Further c-opsin presence within muscular regions of tube foot disc and stalk (st). **B.** Thin striated c-opsin labelings in stalk region, interspersed by thin nerve fibres. (tfg:tube foot ganglion). Scale bars in A-B: 20 µm.

Reported expression of Sp-Opsin1 within adult *S. purpuratus* tube feet (although on relatively low levels) (Burke et al. 2006, Raible et al. 2006) initiated further immunostaining experiments. As can be seen in the processed specimen, Sp-Opsin1 is not detectable in juvenile tube feet of *S. purpuratus* (see Fig. 16B). In adult tube feet the antibody yields a relatively high background, but also shows some regions of distinct protein localization

within the tube foot disc and stalk. Within the disc region, Sp-Opsin1 positive cells occur corresponding to two different muscle groups present (Fig. 19A) (Flammang and Jangoux 1993). The tube foot stalk shows c-opsin positive cells with a striated pattern like in pedicellaria (Fig. 19B). Co-labeling against acetylated alpha-tubulin interestingly also shows a striated pattern of nerve tracts in the tube foot stalk, that, similar to that observed in the tridentate pedicellaria, do not co-localize with the Sp-Opsin1 staining (Fig. 19B).

For comparative reasons I also applied the Sp-Opsin1 antibody to pedicellaria of *Echinus melo*, collected in Kristineberg. Three types of pedicellaria were examined, namely the tridentate, the trifoliate and a third type belonging either to the globiferous or ophiocephalic type. In contrast to *S. purpuratus*, c-opsin positive photoreceptors within the head region of tridentate pedicellaria of *E. melo* could not clearly be identified. There are labelled cells within the neck and stalk regions, but their morphology is completely different from that of the striated Sp-Opsin1 positive cells in *S. purpuratus*. The cells are dispersed over the whole stalk and neck region of the tridentate pedicellaria (Fig. 20A) and show a simple oval form (Fig. 20B). They are located in the epidermis and co-labeling with anti-acetylated alpha-tubulin showed them to be nested between ciliated cells (Fig. 20C) and to possess a connection to the nervous system (Fig. 20D). *E. melo* trifoliate pedicellaria possess c-opsin positive cells within the head and stalk/neck region. The immunopositive cells within the stalk/neck region mirror the c-opsin positive cell morphology of the tridentate pedicellaria and are therefore not displayed separately. From the immunohistological experiments alone it is hard to further characterize the stained cells within the trifoliate pedicellarian head. They seem to be located within the epidermis and neighbor densely ciliated areas (Fig. 20E). A ciliary opsin is usually embedded in a ciliary structure, as its transport from the cell body into the ciliary membrane requires a mechanism deploying Myosin and Kinesin components of cilia (Wolfrum and Schmitt 2000, Williams 2002). Thus, the expectation was to find a co-localization of Sp-Opsin1 and acetylated-alpha-tubulin in a cilium. However, this co-localization could not be found in any c-opsin positive cell neither in *E. melo*, nor in any other echinoderm species investigated so far. Fig. 20F displays a close-by localization of c-opsin and acetylated–alpha-tubulin also observed within the head of a trifoliate pedicellarium.

The third type of examined pedicellarium shows strongly labeled c-opsin positive cells within its calcified head region. In one of the “claws” protruding from the valves (Fig. 21A+inset) a cell with a very unusual branched morphology is labeled (Fig. 21B+C). Co-labeling with anti-acetylated–alpha-tubulin again shows cilia in the direct neighborhood of the cell, maybe even arising from it (Fig. 21D).

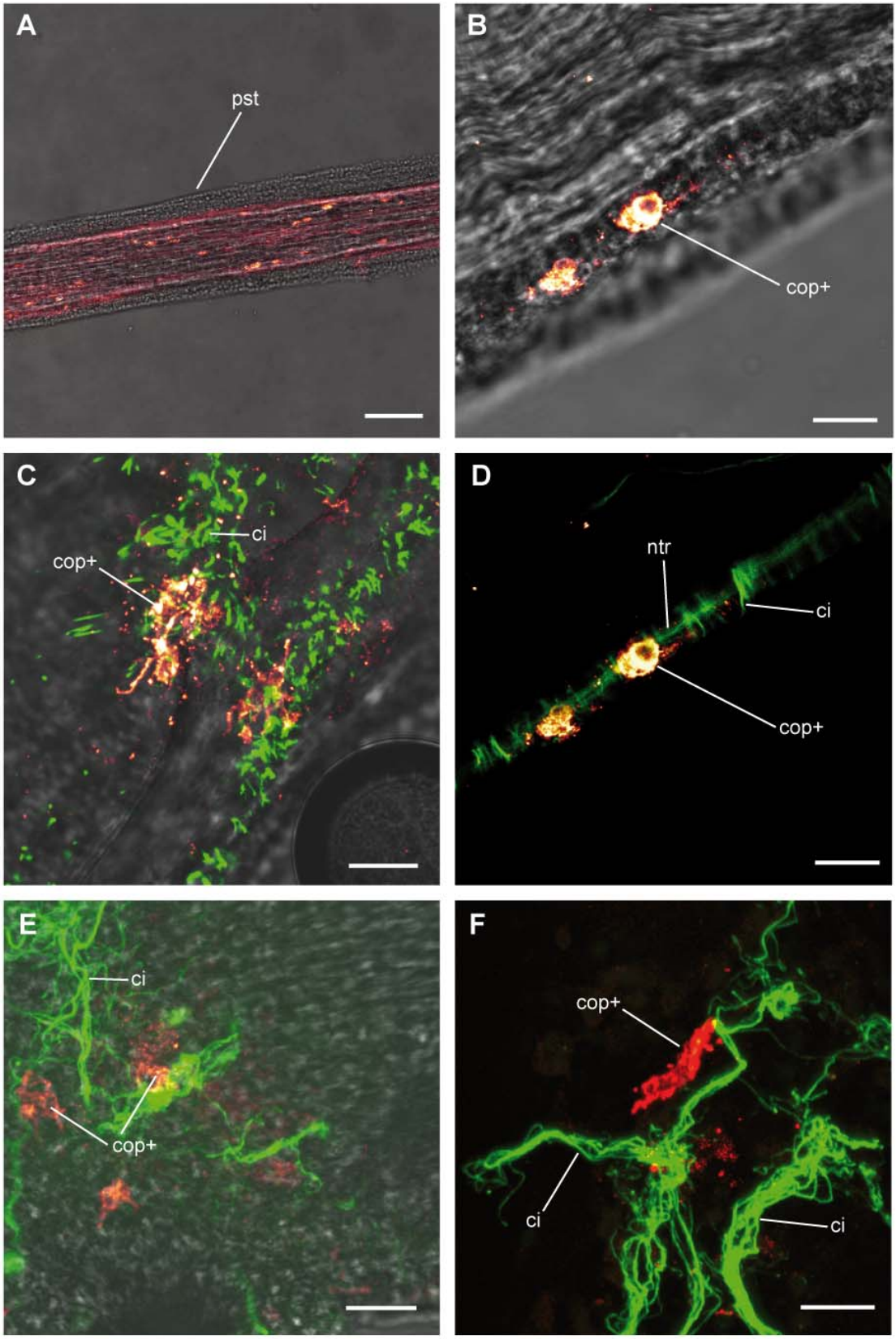

Fig. 20: C-opsin positive cells in *Echinus melo* pedicellaria examined by CLSM. Double immunolocalization of c-opsin (hot red/red) and acetylated alpha-tubulin (green) via color merge of z-stack projections. **A.** Stalk region of tridentate pedicellarium (pst) showing single c-opsin positive cells. **B.** Two c-opsin+ cells within stalk epidermis. **C.** High magnification of two c-opsin+ cells accompanied by cilia (ci) protruding from the epidermis. **D.** C-opsin+ connect to nerve tracts (ntr). **E.** Head region of trifoliate pedicellaria. C-opsin+ cells in the epidermis neighboring densely ciliated areas. **F.** C-opsin+ cell with possible protruding cilium. Scale bars in A: 100 µm, B-F: 20 µm.

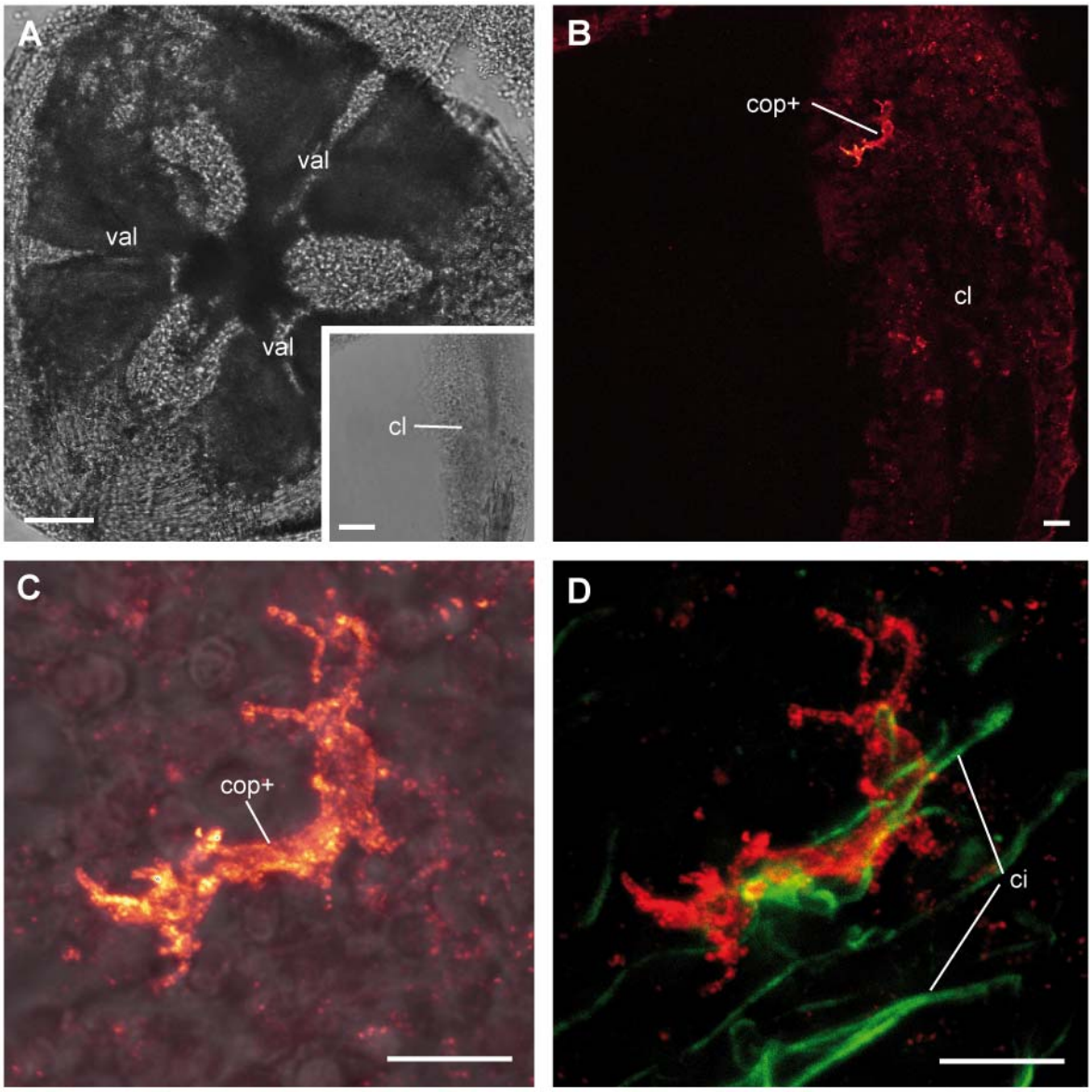

Fig. 21: C-opsin positive cells in *Echinus melo* pedicellaria examined by CLSM. Double immunolocalization of c-opsin (hot red/red) and acetylated alpha-tubulin (green) via color merge of z-stack projections. **A.** Transmission view of globiferous or ophiocephalus pedicellarium bearing calcified ossicles in its valves (val). Insert showing slender distal portion of valve forming a claw (cl). **B.** C-opsin positive cell (cop+) within the claw. **C.** High magnification depicting peculiar branched morphology of c-opsin+ cell. **D.** Cilia arise from/are in close vicinity of the c-opsin+ cell. Scale bars in A: 100 µm, A inset: 40 µm, B-D: 10 µm.

3.2. Photoreceptors in Asteroidea

After the first positive immunoreactions of Sp-Opsin4 in *S. purpuratus*, one question arose regarding the possible function of this photopigment in these animals. As previously mentioned, starfish optic cushions represent the only echinoderm optic organs which have clearly been demonstrated to play a role in phototaxis (Yoshida and Ohtsuki 1966, 1968, Takasu and Yoshida 1983). Thus a positive reaction of starfish optic cushion PRCs with the echinoid-specific Sp-opsin4 antibody would provide indirect evidence for the sea urchin r-opsin to function in phototaxis, too.

3.2.1. R-opsin positive PRCs in asteroid optic cushions and other cells

Optic cushions in asteroids are located at the base of the terminal tentacle in the tips of the arms and are visible from early development on, due to their red pigmentation in live animals (Fig. 22A). In adult asteroids a row of tube feet follows the terminal tentacle hosting the optic cushions, and spines embed those tube feet in the ambulacral grooves (Fig. 22B). Immunostainings of juvenile *A. rubens* optic cushions (Fig. 22C) clearly show presence of an r-opsin (Fig. 22D-E). Within the optic cushions the microvillar PRCs are arranged forming a cup-like structure with interspersing pigmented support cells. Cilia protrude from the PRCs and a multicelular “lens” covers the optic cushion to the external (Eakin and Brandenburger 1979). The obtained stainings correspond with the described photoreceptor cell arrangement although cellular borders between single PRCs can not be seen as clearly as in sea urchins, most probably due to the “lens” covering the PRCs, which contain the r-opsin. The r-opsin is situated within a cup-like structure and many cilia protrude from the terminal tentacle (Fig. 22E). Deployment of an ImageJ software co-localization tool shows almost no co-localization of r-opsin protein and dark shielding pigment (Fig. 22F), thus corroborating the results of Eakin and Brandenburger (1979), that the shielding pigment is not present within the PRCs but in distinct pigment cells. Anti-acetylated alpha-tubulin labeling shows the cilia protruding from the optic cushion PRCs (Fig. 23A) as also described by the above mentioned authors. Due to the size of the examined juveniles (wholemount preparations) the nerve net accompanying the optic cushion could only be recorded with low resolution (Fig. 23B) using CLSM.

Apart from the PRCs detected in its optic cushions, *A. rubens* possesses additional r-opsin positive photoreceptors. Similar to sea urchins, they have PRCs in their tube foot discs, although smaller and less in number (Fig. 23C+D). The aboral epidermis of *A. rubens* juveniles also bears r-opsin positive cells, integrated in a web-like neuronal network labeled by anti-acetylated alpha-tubulin (Fig. 23 E+F). Although these dispersed r-opsin positive PRCs occur along the whole aboral surface of the starfish juveniles, they

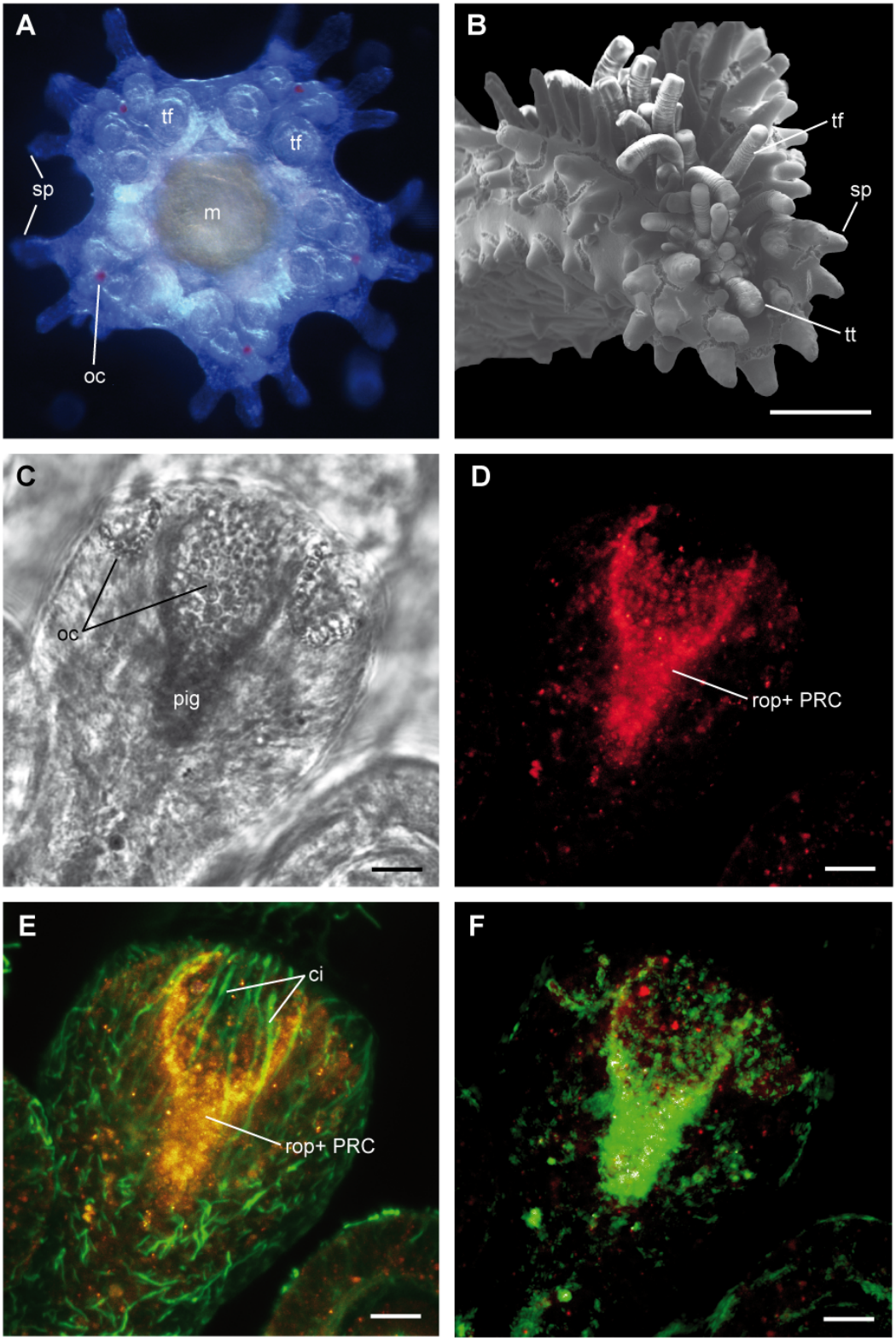

Fig. 22: R-opsin positive PRCs in *Asterias rubens* optic cushions, examined by CLSM. Double immuno-localization of r-opsin (hot red/red) and acetylated alpha-tubulin (green). **A.** Juvenile (oral view) with optic cushions (oc) visible as red pigment dots, developing tube feet (tf) and spines (sp) (m:mouth). Photograph courtesy of Sam Dupont, Sven Lovén Centre for Marine Science, Sweden. **B.** SEM preparation of adult armtip bearing terminal tentacle (tt) hosting optic cushions, tube feet and spines. **C.** Transmission view of juvenile terminal tentacle with (developing) optic cushions, on of which with dark pigmentation (pig). **D.** R-opsin protein localization within optic cushion. **E.** Color merge of both antibody stainings showing presence of cilia (ci) on the terminal tentacle. **F.** Colocalization (via MacBiophotonics ImageJ) of R-opsin and dark pigment (color transformed to green) demonstrates separate focal planes for recorded signal, correlating with dark pigment in supportive cells. Scale bars in B: 500 µm, C-F: 10 µm

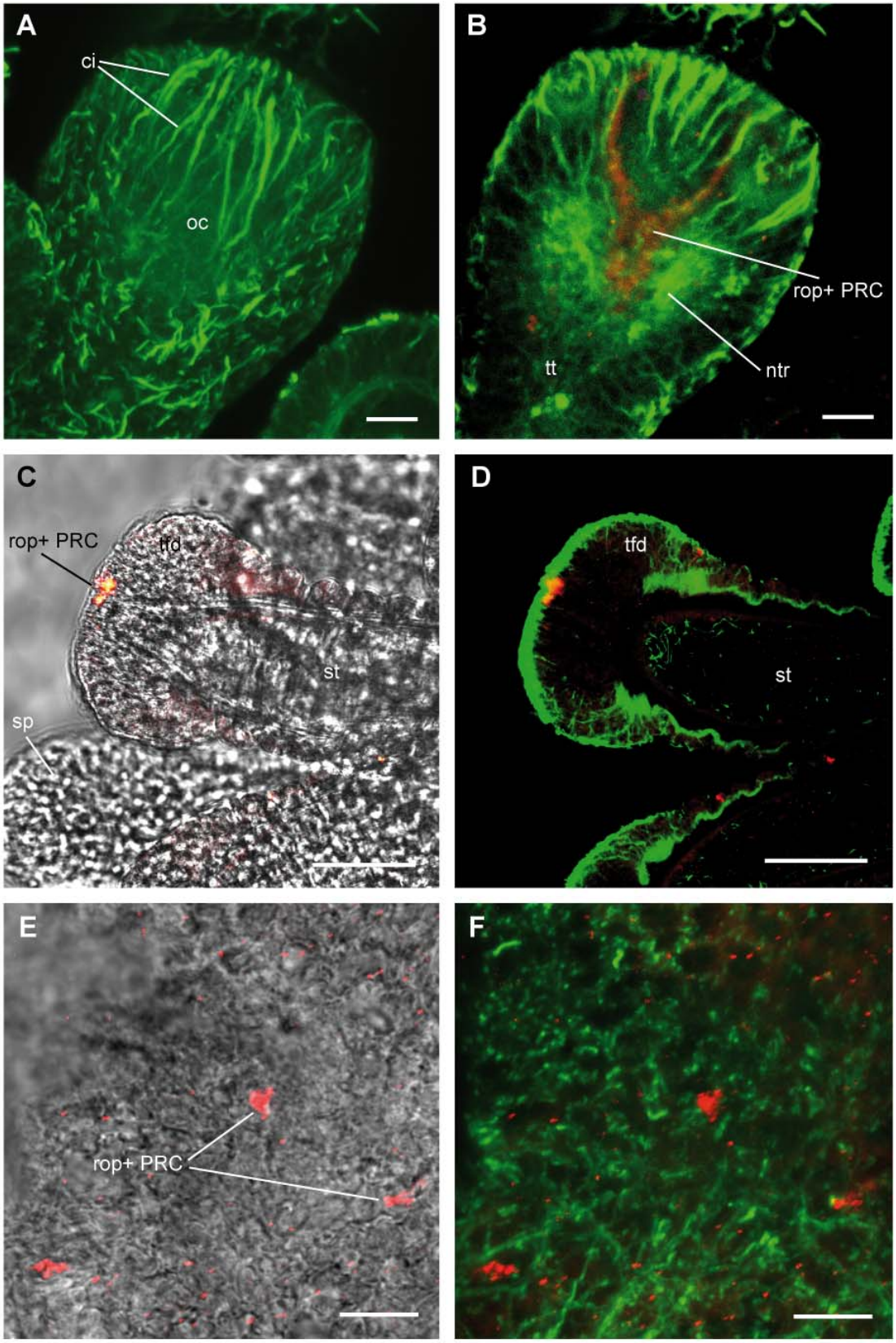

Fig. 23: R-opsin positive PRCs in juvenile *Asterias rubens* optic cushions and other cells, examined by CLSM. Double immunolocalization of r-opsin (hot red/red) and acetylated alpha-tubulin (green). **A.** Cilia (ci) protruding from optic cushion (oc) region of terminal tentacle. **B.** Neuronal tracts (ntr) underneath the optic cushion on terminal tentacle (tt). **C.** Tube foot with R-opsin+ PRC in disc region (tfd). Tube foot stalk (st) and spines (sp) show no r-opsin+ cells. **D.** Same tube foot as in C displaying heavily ciliated surface and epidermal PRCs. **E.** R-opsin+ cells within aboral epidermis. **F.** R-opsin+ cells embedded in epidermal web-like nerve net. Scale bars in A-B, E-F: 10 µm, C-D: 50 µm.

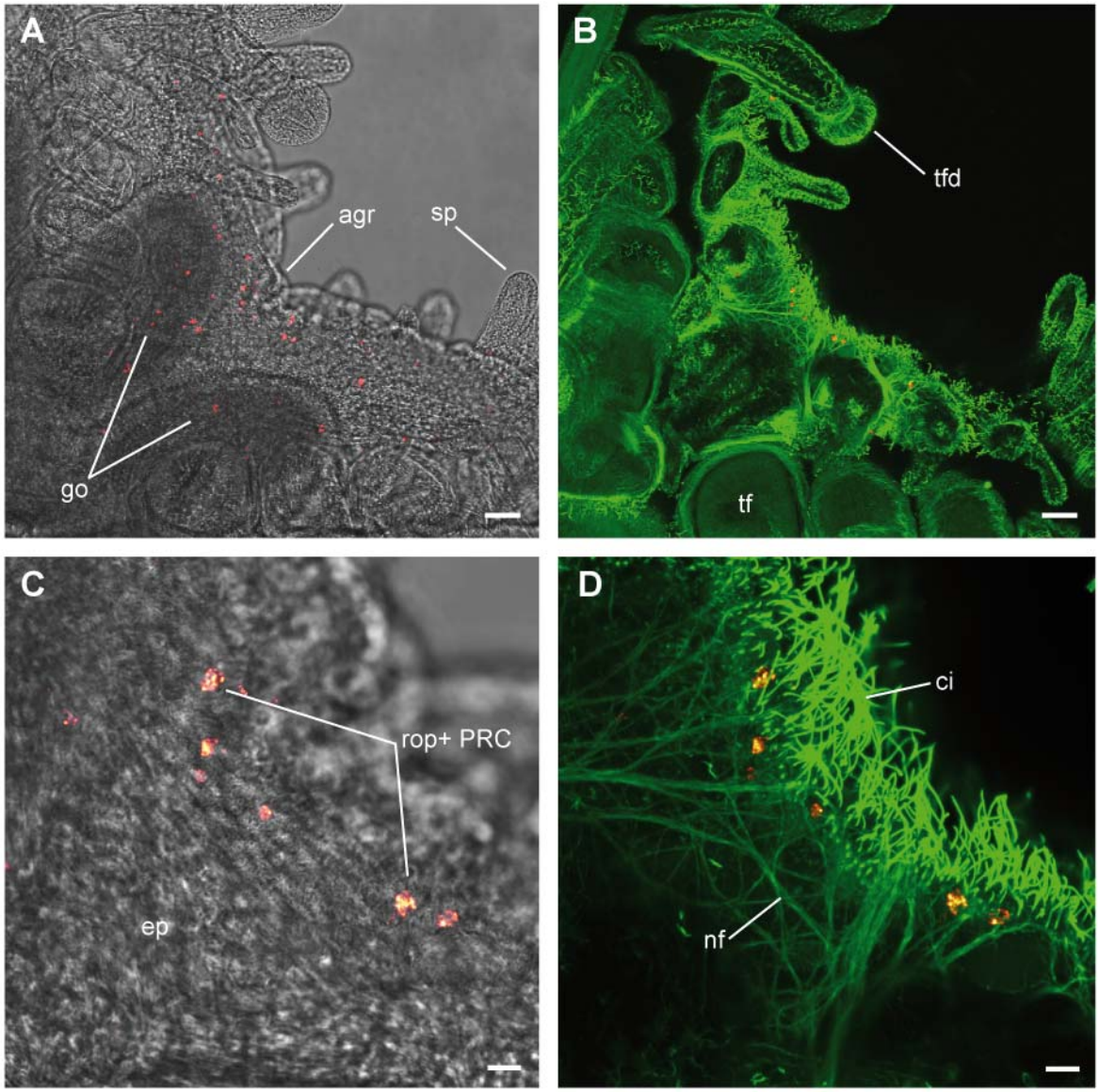

Fig. 24: R-opsin positive PRCs in aboral epidermis of juvenile *Asterias rubens*, examined by CLSM. Double immunolocalization of r-opsin (hot red) and acetylated alpha-tubulin (green). **A.** Aboral transmission view showing dispersed r-opsin+ PRCs in the aboral epidermis (agr: arm groove, go:gonads, sp:spine). **B.** Nerve net of armgroove region showing embedded r-opsin positive PRCs (tf:tube foot, tfd:tube foot disc). **C.** PRCs are located within the epidermis (ep). **D.** The epidermis shows an enormous amount of cilia and densely branching nerve fibres (nf) surrounding the PRCs. Scale bars in A-B: 50 µm, C-D: 10 µm.

are more numerous in the grooves between the animal's arms (Fig. 24A+B). The aboral epidermal PRCs are embedded in an impressively extensive nerve net stained by anti-acetylated-alpha-tubulin (Fig. 24B+D). The finding of distinct additional PRCs outside the optic cushion is important to notice with regard to the later discussed persisting phototactic behaviour in *A. rubens* after optic cushion removal (Yoshida and Ohtsuki, 1968).

3.2.2. C-opsin positive PRCs in *Asterias rubens*

The first relevant observation concerning ciliary opsin expression in *A. rubens* was its absence from the optic cushions. This experiment ensured that it is in fact the rhabdomeric opsin mediating starfish phototaxis via its deployment in the optic cushion.

In *A. rubens* juveniles, c-opsin presence could be demonstrated so far only within spines (Fig. 25A). The antibody specifically labels single cells within the the spine epidermis (Fig. 25 B+C).

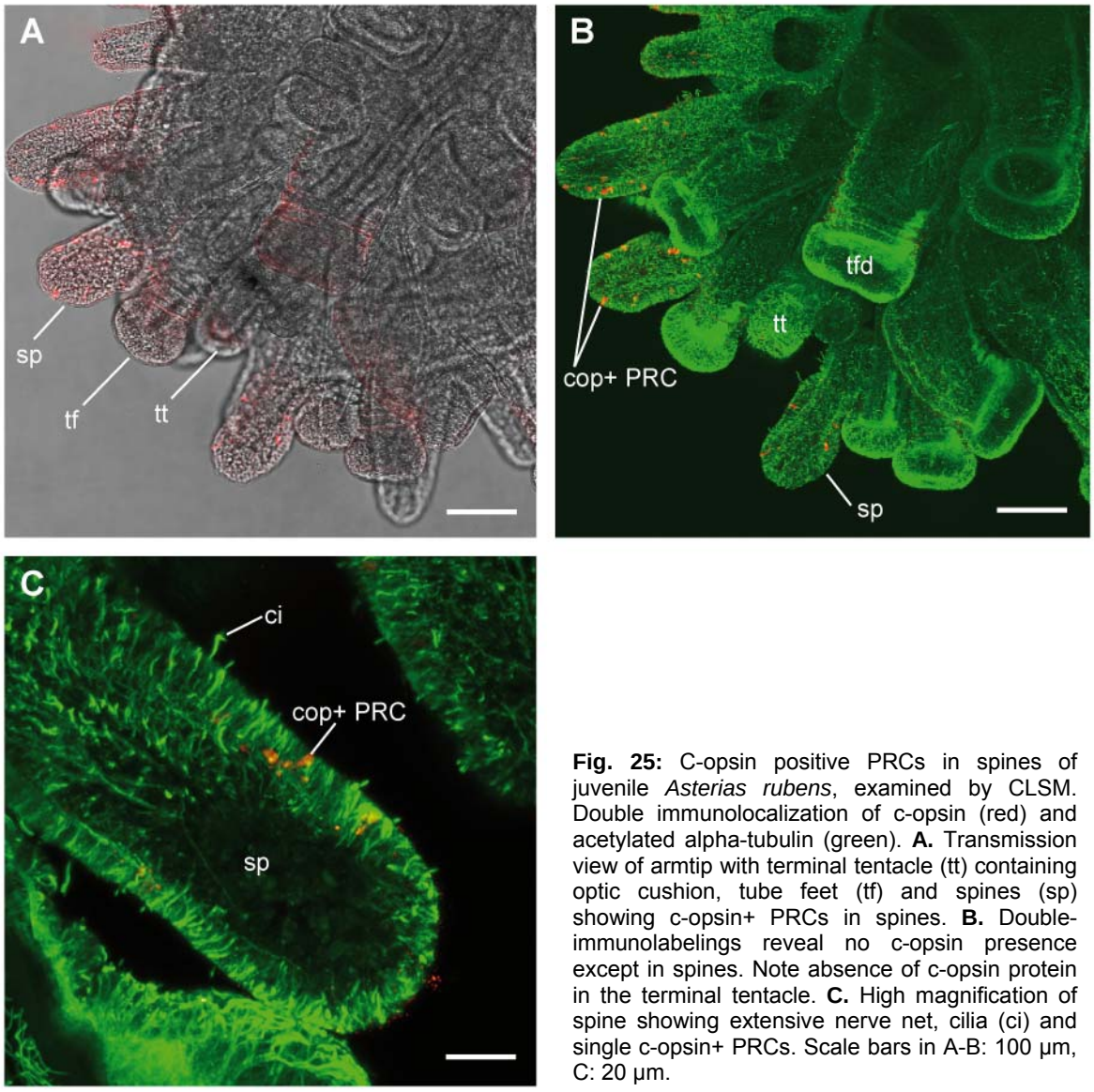

Fig. 25: C-opsin positive PRCs in spines of juvenile *Asterias rubens*, examined by CLSM. Double immunolocalization of c-opsin (red) and acetylated alpha-tubulin (green). **A.** Transmission view of armtip with terminal tentacle (tt) containing optic cushion, tube feet (tf) and spines (sp) showing c-opsin+ PRCs in spines. **B.** Double-immunolabelings reveal no c-opsin presence except in spines. Note absence of c-opsin protein in the terminal tentacle. **C.** High magnification of spine showing extensive nerve net, cilia (ci) and single c-opsin+ PRCs. Scale bars in A-B: 100 µm, C: 20 µm.

3.3. Photoreceptors in Ophiuroidea

Many ophiuroid species have been documented to be photosensitive and different experimental settings were used to determine (a) the most sensitive body regions (Mangold 1909), (b) the wavelenghts or light conditions triggering the most prominent reactions (Johnsen 1994, Johnsen and Kier 1999, Moore and Cobb 1985) as well as (c) the potential mechanisms accounting for the demonstrated behavior (Hendler 1984, Hendler and Byrne 1987, Aizenberg et al. 2001). None of these investigations revealed information about the exact position or structure of the photoreceptors in these different brittle stars. It was thus challenging to investigate whether the antibodies designed against the sea urchin specific r-opsin and c-opsin would be able to specifically bind to the brittle star ortholog and if at all present, where the respectively labeled cells would be found. The examination of different brittle star species is still ongoing and hence only the results concerning *Amphiura filiformis* are included here. Due to the life cycle of *A. filiformis*, no early juvenile stages were available at the time of experiment performance and thus parts of adult animal bodies had to be used for experimental purposes. Since brittle stars show massive calcite skeletal elements in the vertebral ossicles of their arms and because adult animals of the examined species are relatively large, it was necessary to decalcify the investigated specimens prior to antibody incubation. This methodological drawback has to be kept in mind when looking at the observed c-opsin expression present in spines, which structurally deteriorated due to the decalcification procedure.

A. filiformis is a brittle star with an infaunal lifestyle, burrowed in the mud over daytime with two or three armtips hold above the substratum swobbing for detritus particles at night. Those armtips constitute the body region most likely to be reached by light and were therefore chosen for the experiment.

3.3.1. R-opsin positive PRCs in *Amphiura filiformis*

The arms of *A. filiformis* show segmental pairs of relatively unspecialized, cone shaped tube feet, each of them accompanied by a triplet of spines (Fig. 26A). The skeletal depression in which the radial nerve runs in living specimens is visible in the midline of the arm, showing regular bulbs in between each tube foot pair and set of spines. Immunohistochemical labelings using anti-Sp-Opsin4 antibodies revealed r-opsin positive cells in the animal's tube feet and within the bulb region of the radial nerve (Fig. 26B). The arms of *A. filiformis* show an impressive innervation. Each tube foot is innervated by nerve fibres originating from/leading into the radial nerve and has a nerve ring surrounding its proxi-mal portion. Another nerve strand connects each spine triplet to the radial nerve. (Fig. 26C).

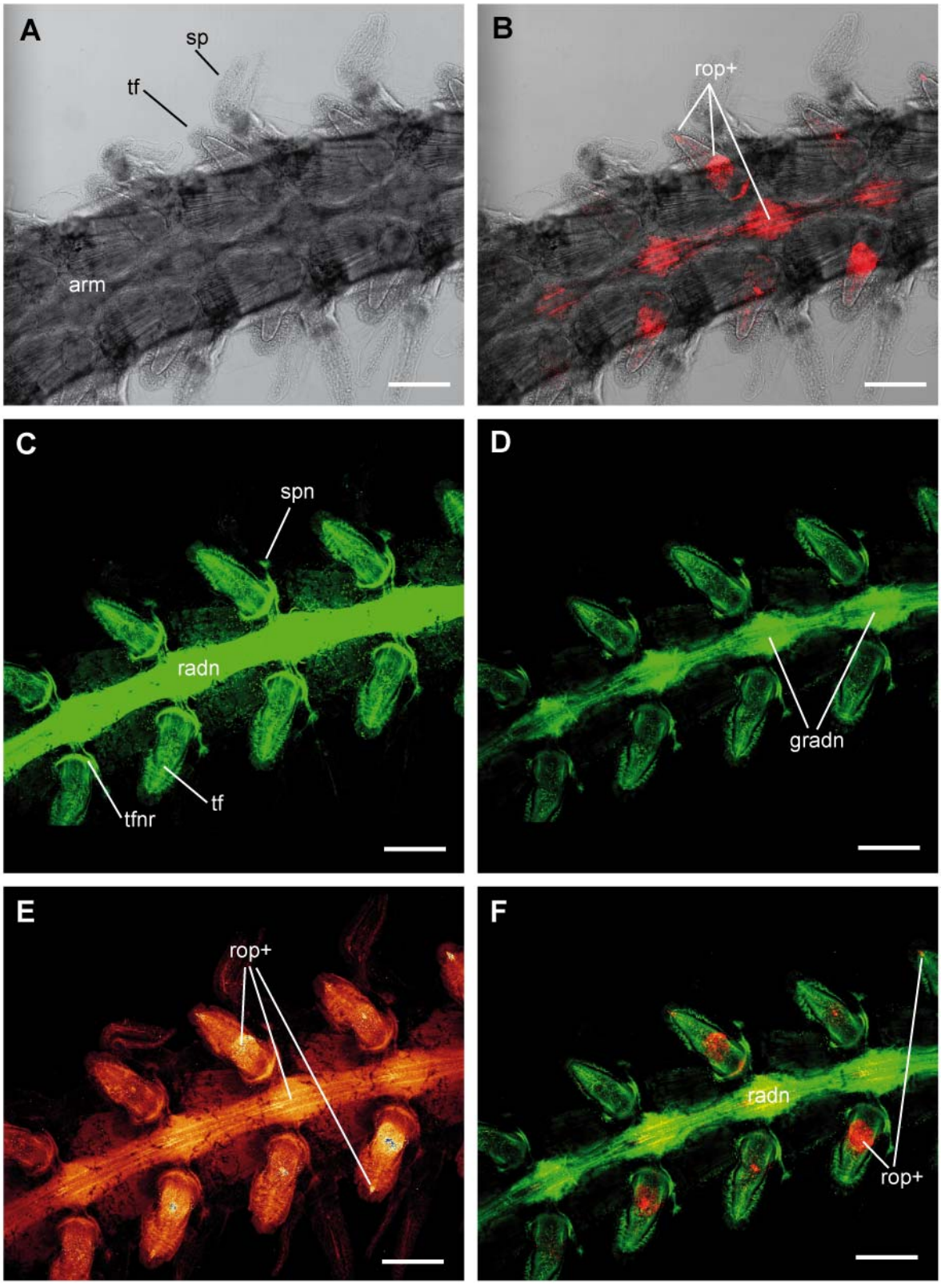

Fig. 26: R-opsin positive PRCs in decalcified arms of *Amphiura filiformis*, examined by CLSM. Double immunolocalization of c-opsin (red/hot red) and acetylated alpha-tubulin (green). **A.** Transmission view of arm (arm) with tube feet (tf) and spines (sp). **B.** R-opsin+ cells reside in tube feet and radial nerve. **C.** Innervation of arm showing connection of the radial nerve (radn) to each tube foot nerve ring (tfnr) and spine nerve (spn). **D.** Partial z-stack projection reveals the radial nerves to be organized in a "segmented" pattern with "ganglion-like" aggregations of nerve tracts (gradn). **E.** Tube feet show R-opsin protein (rop+) presence within middle and tip region. R-opsin is also detected within radial nerves. **F.** R-opsin+ cells within the radial nerve hint on axonal/dendritic projections due to lack of stained cell bodies. Scale bars in A-F: 200 µm.

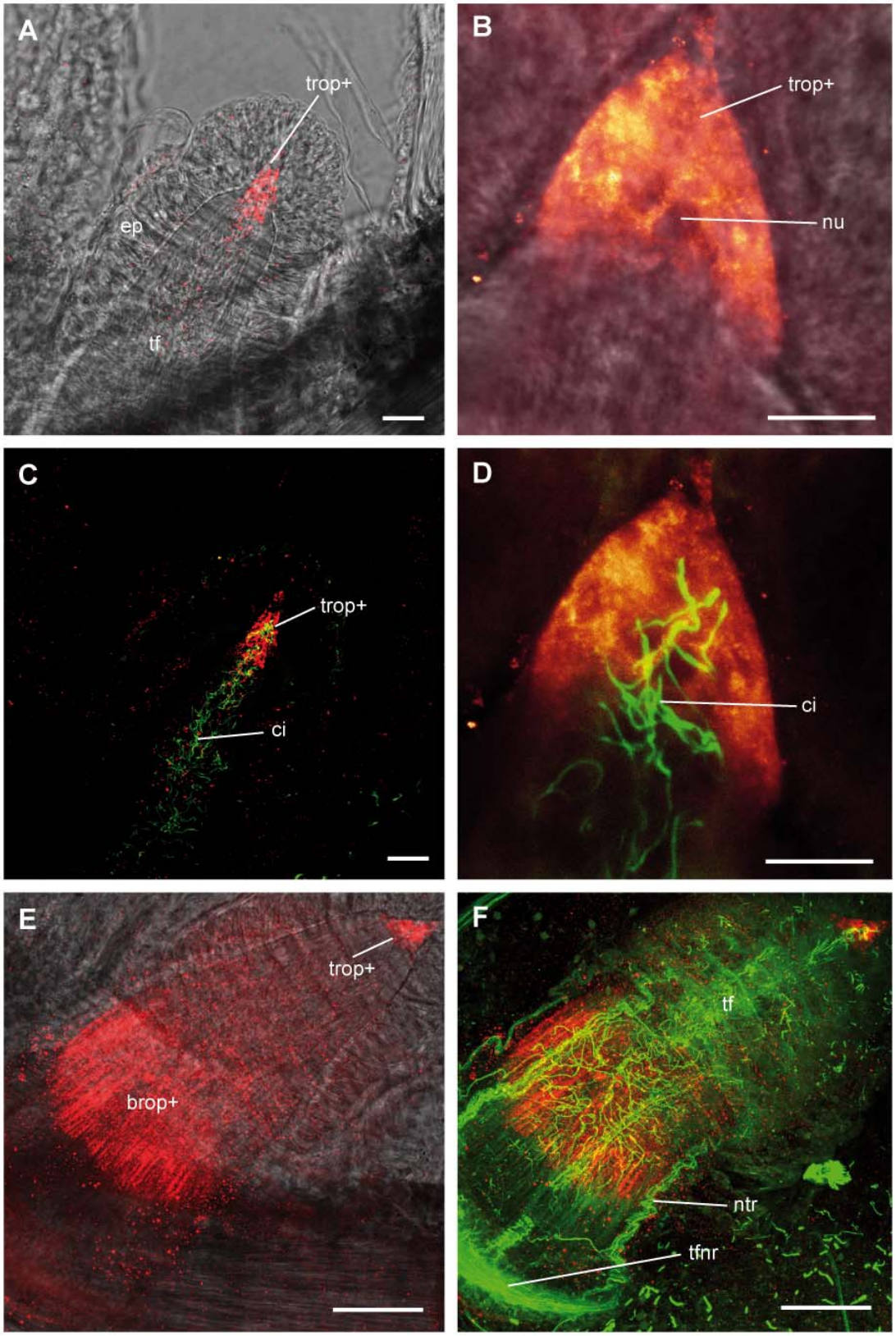

Fig. 27: R-opsin positive PRCs in decalcified arms of *Amphiura filiformis*, examined by CLSM. Double immunolocalization of c-opsin (red/hot red) and acetylated alpha-tubulin (green). **A.** Transmission view of tube foot (tf) with epidermis (ep) and r-opsin+ tip cells (trop+). **B.** R-opsin staining shows cone shaped morphology (nu:nucleus). **C.** Cilia (ci) are present along the longitudinal axis of the tube foot. **D.** Dark areas within R-opsin+ region indicate location of nuclei. Cilia protrude from the r-opsin+ cells. **E.** Tube foot proximal r-opsin+ (brop+) cells showing a striated pattern. **F.** Color merge of both immunostainings reveal dense nerve tracts (ntr) but also fine nerve fibres connecting to the tube foot nerve ring (tfnr) in the area of proximal r-opsin+ cells. Scale bars in A-D: 10 µm, E-F: 50 µm.

The most prominent r-opsin stainings could be observed in two distinct regions of the tube feet and within thin striated structures in the thickened portions of the radial nerve cord. The first staining within tube feet is located in a middle portion of the podium but, in contrast to the sea urchin basal PRC cluster, clearly separated from the site of tube foot origin and the nerve ring surrounding it (Fig. 26E). These Sp-Opsin4 positive cells are clearly located within the tube foot epidermis. The second cluster of Sp-Opsin4 positive cells resides in the distal-most portion of the tube foot tip that has a cone shaped structure distinct from the rest of the tube foot (Fig 26E). The r-opsin staining in the thickening of the radial nerve is less clear than the previously described ones (Fig. 26E). The shape of the immunostained cells or cell components hint on axonal/dendritic projections rather then whole cell bodies, but it is also possible that the r-opsin protein is localized in nerve cells that show a slender morphology without prominent cell bodies present. In a projection view of both antibody stainings it can be observed that within the two r-opsin positive tube foot regions only small portions show co-expression of the two proteins, whereas within the radial nerve both seem to be present within the stained striated structures (yellow stripes) (Fig. 26F). High magnification examination of the tube foot tips revealed the r-opsin positive area to be cone shaped (Fig. 27A) with darker areas, most presumably hosting the cell nuclei (Fig. 27B). Cilia, visualized by the anti-acetylated alpha-tubulin staining, are present along the longitudinal axis of the whole tube foot (Fig. 27C) and also emerge from the area of the r-opsin staining (Fig. 27D). In the second r-opsin positive area, the more proximal portion of the tube foot, the immunostaining shows a striped pattern contrasting to the voluminous staining in the tip region.

3.3.2. C-opsin localization in *A. filiformis*

Antibody labeling with anti-Sp-Opsin1 revealed staining in the spines, consistent to the stainings in the starfish *A. rubens* (Fig. 28A). Higher magnification shows the c-opsin protein to reside in an obviously inner portion of the *A. filiformis* spine (Fig. 28B). Nerve tracts, detected by acetylated alpha-tubulin staining, run longitudinally through the spines and contact the c-opsin positive cells (Fig.28 C+E). Caution is necessary as decalcification of the spines influences the maximum resolution achievable with CLSM technology. However, high magnification clearly reveals association of c-opsin positive cells with the spine's nervous system. At the base of the spines and in close vicinity to ciliary opsin protein localization *A. filiformis* shows a dark pigmentation (Fig. 28F). Whether this pigmentation is somehow related to the opsin protein presence remains unclear.

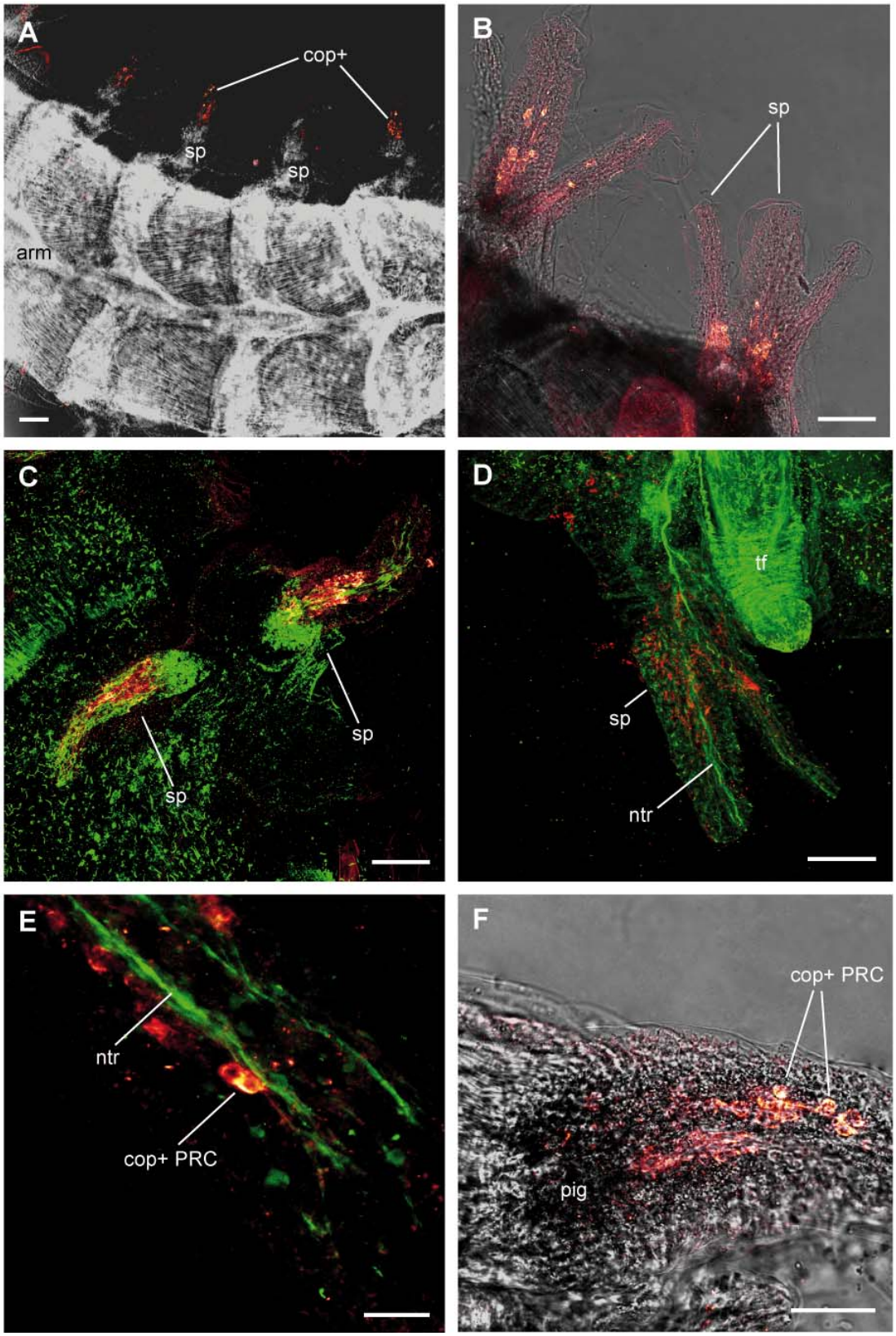

Fig. 28: C-opsin positive PRCs in decalcified arms of *Amphiura filiformis*, examined by CLSM. Double immunolocalization of c-opsin (red/hot red) and acetylated alpha-tubulin (green). **A.** Inverted transmission picture of arm (arm) showing c-opsin+ cells (cop+) in spines (sp). **B.** C-opsin protein seems to be localized in an inner portion of the spines. **C.** Massive nerve tracts are present at the spine bases. **D.** Nerve tracts (ntr) partially also seem to run through an internal portion of the spines. Tube feet (tf) show no c-opsin+ cells. **E.** High magnification reveals connection of the c-opsin+ PRCs to the nerve tracts (ntr). **F.** Transmission view showing spine internal c-opsin+ PRCs and dark pigment (pig) at the spine base. Scale bars in A-D: 100 µm, E: 20 µm, F: 50 µm.

3.4. Photoreceptors in Crinoidea

To obtain a comprehensive picture on opsin expression in echinoderms I also tested three different species of crinoids. The comatulid *Antedon bifida* was collected at the Sven Lovén Centre in Kristineberg, Sweden, and freshly fixed with standard immunocytological methods (see Materials and Methods). Labeling with anti-Sp-Opsin4 revealed no specific r-opsin staining. The co-applied anti-acetylated alpha-tubulin showed specific and clear reactivity, thus tissue preservation was adequate for immunostaining. Two deep-sea (and so far undescribed) comatulid crinoids also showed no specific immunoreactivity neither to the rhabdomeric opsin nor the ciliary opsin antibody. However, in this case also the anti-acetylated tubulin staining showed no specific signal. The collecting procedure included a rather long transport of the samples through warm surface water which may thus have resulted in a bad tissue preservation and hence the failure of the experiment.

4. DISCUSSION

This thesis presents an integrated study combining molecular and structural data to characterize distinct photoreceptor cells (PRCs) in echinoderms. In negatively phototactic *S. purpuratus* I found PRCs arranged in clusters at the base of the echinoid tube feet and in the rim of the tube foot disc. These PRCs express an r-opsin type photopigment and have a microvillar structure. The basal PRC cluster is embedded in a depression of the opaque echinoid skeleton that shields the PRCs against incoming light with an angle of up to 272°. The basal PRC axons connect to the radial nerves of the developing NS. Rhabdomeric opsin expression was furthermore detected in asteroid optic cushions mediating phototaxis in these animals, as well as in asteroid tube feet and aboral epidermis cells. Ophiuroids were also shown to possess rhabdomeric opsin positive cells within their tube feet. Localization of ciliary opsin in different echinoderm tissues including spines and pedicellaria complements the presented studies on echinoderm photoreceptors. The presented findings allow a reconsideration of the evolution of form and function of echinoderm PRCs from a new perspective.

4.1. Expression of opsins and other “eye-relevant” genes in echinoids

The molecular experiments on echinoderm photoreceptors presented in this thesis focus on expression patterns of two different opsin genes, namely a rhabdomeric and a ciliary opsin, in echinoids, asteroids and ophiuroids. The design of the performed experiments followed the previous finding of six different opsin proteins that are encoded in the *S. purpuratus* genome and expressed in different tissues (Raible *et al.* 2006, Burke *et al.* 2006). Both research teams deployed qRT-PCR to determine the relative abundance of expressed opsins and other “eye-relevant” genes within the sampled tissues. Burke et al. (2006) found the rhabdomeric opsin (Melanopsin) Sp-Opsin4 to be most abundandly expressed in tube feet of adult *S. purpuratus* (compared to different larval stages), whereas expression of the ciliary opsin (Rhodopsin) Sp-Opsin1 was almost 10 fold lower in adult tube feet and much higher in late larvae. These findings mirror those of Raible et al. (2006) also demonstrating a relatively high amount of *Sp-opsin4* in tube feet, compared to a relatively low expression level of *Sp-opsin1* in these locomotory appendages. Those two opsin genes and their gene products respectively are relevant for different aspects examined in the present study. Opsin genes act relatively downstream in the molecular cascade of photoreceptor-related gene expression. Their gene products comprise an essential component of the photopigment necessary for its function in light perception. Presence of an opsin protein thus always indicates presence of a light sensitive cell. This makes the opsin protein such a useful marker for localization of so far undiscovered

photoreceptor cells (and their further characterization). Due to their functional role, opsin proteins have to be continuously expressed (and translated) in fully differentiated photoreceptors, a feature that allows to investigate their localization not only in developmental studies but also in adult animals.

The finding of distinct *Sp-opsin4* expressing cells in the tube feet of *S. purpuratus* thus provides the first evidence for a distinct photoreceptor in an echinoid. However, it takes more for an organism than opsin expression to develop and maintain a functioning photoreceptor cell. A gene that became famous for its involvement in photoreceptor specification in bilaterian animals is *pax6*. (Gehring and Ikeo 1999, Gehring 2002, Fernald 2006, Arendt 2003, Arendt et al. 2004, Vopalensky and Kozmik 2009). The collaborating working group of M.I. Arnone (SZN) provided evidence for *Sp-pax6* (the sea urchin *pax6* ortholog) expression within *S. purpuratus* tube feet stalk, disc and a very proximal tube foot region (M.I. Arnone, personal communication). The expression pattern varies in that the stalk region shows a relatively strong *Sp-pax6* expression compared to a weaker and more diffuse expression within the disc. In the stalk, *Sp-pax6* seems to be present in deeper tissue layers whereas in the disc region *pax6* expression is present in deeper regions as well but also in the epidermis. The findings of Arnone and co-workers corroborate former findings of *pax6* expression in *Paracentrotus lividus* tube feet (Czerny and Busslinger 1995). The r-opsin positive cells at the base of the *S. purpuratus* tube feet are embedded in a region of strong *Sp-pax6* expression (M.I. Arnone, personal communication). The disc PRCs on the other hand show localization of Sp-opsin4 protein and expresssion of *Sp-pax6* RNA in close vicinity, but a co-localization on cellular level could not be observed so far. In the juvenile, the whole region of developing tube feet shows very strong *pax6* expression indicating that both photoreceptor types, basal and disc ones arise from a *pax6* dependend tissue.

Sp-pax6 and *Sp-opsin4* expression in the *S. purpuratus* tube foot PRCs indicate the presence of a conserved molecular apparatus that serves PRC formation in echinoderms as in many other bilaterian animals (Gehring and Ikeo 1999, Gehring 2002, Fernald 2006, Arendt 2003, Arendt et al. 2004, Vopalensky and Kozmik 2009). This view of conservation of at least part of an upstream gene regulatory network deploying “eye-relevant” genes in echinoderms is further supported by the findings of Burke et al. (2006). The authors demonstrate expression of other well known upstream regulators of eye formation, as well as expression of genes playing a role in later events of cell type specification and differentiation, such as members of the *six* gene family, *rx*, *atonal*, *neuroD*, and *barh1* within *S. purpuratus* tube feet.

4.2. Morphological structure of r-opsin positive PRCs

Despite decades of dedicated research in echinoids, no distinct optic organ or eye has been documented. Not even the simplest “proto-eye” is present in form of a PRC being partially shielded by pigment and thus allowing for directional vision (Gehring and Ikeo 1999, Arendt and Wittbrodt 2001, Land and Nilsson 2002). This led to the hypothesis of a so called diffuse “dermal light sense” in echinoids and echinoderms in general (for review see Yoshida 1966). This dermal light sense was thought to deploy morphologically unconspicious neurons of the superficial basiepidermal nerve net for photoreception. Although Yoshida emphasizes in his 1966 review (p. 440) “... that it has not yet been shown that the superficial nerve fibres are photosensitive” this hypothesized mode of photoperception became readily accepted among echinoderm researchers. For this reason the finding of distinct photoreceptor cells contrasting to that long proposed hypothesis sets a completely new basis for evaluating former experiments on echinoid photobehavior.

The photoreceptor cells localized via immunostaining against the rhabdomeric opsin Sp-Opsin4 could be classified as microvillar receptor cells by observation and schematic reconstruction of TEM serial sections. The overall morphology of the examined r-opsin expressing receptor cell type resembles that of the microvillar photoreceptors deployed by the only two described echinoderm eye-organs, namely the optic cushions of five asteroid species: *Asterias rubens* (Vaupel-von Harnack 1963) *Patiria miniata*, *Leptasterias pusilla* and *Henricia leviuscula* (Eakin and Brandenburger 1979) and *Nepanthia belcheri* (Penn and Alexander 1980) as well as the ocelli of the synaptid holothurian *Opheodesoma spectabilis* (Yamamoto and Yoshida 1978). Common features of their photoreceptors shared with the newly discovered ones in echinoids comprise the apical microvilli that show an irregular arrangement in light adapted specimens as well as the presence of a cilium projecting from the cell apex. Some of the cilia of the optic cushion PRCs as well as of the optic tentacle ones show modifications of the ciliary axoneme as compared to locomotory or sensory cilia (Eakin and Brandenburger 1979, Yamamoto and Yoshida 1978) but others do not (Penn and Alexander, 1980). The majority of the examined cilia show an unmodified outer morphology, comparable to that of the observed echinoid PRC cilia. The cilium present in the echinoid PRCs due to its lack of membrane enlargement is not proposed to function in photoreception. This is supported by the finding of many rhabdomeric PRCs possessing unmodified cilia (Eakin 1979, Purschke et al. 2006). The most striking resemblance of the asteroid and holothuroid PRCs is the unusual high content of different sized vesicles within the cell cytoplasm of light adapted PRCs that matches the condition in the echinoid PRCs. Dark adapted PRCs in all examined species in contrast do show a fine granular cytoplasm structure. Potential photoreceptor candidate

cells showing a similar smooth granular cytoplasm in tube feet of dark adapted *S. purpuratus* have been documented, but could not undoubtedly be assigned as PRCs due to the loss of TEM serial sections showing the apical cell region. Although differing in the hypothesized detailed mechanisms, Yamamoto and Yoshida (1978) as well as Eakin and Brandenburger (1979) proposed the prominent vesicles present in the photoreceptors to comprise part of a membrane turnover cycle that is typical for many microvillar photoreceptors (Blest 1988) and it is highly likely that the vesicles observed in the echinoid PRCs serve a similar purpose.

PRCs in echinoids thus morphologically equal those of other echinoderms to a certain degree. An important difference is the lack of pigment within or surrounding the echinoid photoreceptor cells. In asteroid optic cushions the PRCs are flanked by pigment cells providing light shielding through dark pigment (Vaupel-von Harnack 1963, Eakin and Brandenburger 1979, Penn and Alexander, 1980) and in the holothuroid *Opheodesoma spectabilis* the ocellus is enveloped and thus shielded by pigment cells of the tentacular nerve (Yamamoto and Yoshida 1978). For an eye or PRC organ that is used in directional vision, a limitation of the angle of the light reaching it is essential to determine the direction of the light source. This is achieved in the majority of PRCs deployed for directional vision via dark shielding pigment within the PRCs or in cells adjacent to them (Land and Nilsson 2002) as e.g. realized in asteroids and holothuroids. But despite thorough investigations of the echinoid tube feet, no such shielding pigment could be detected in *S. purpuratus*. The deep purple pigment that is incorporated within this and many other echinoids' epidermis (Goodwin and Srisukh 1950) is located within epidermis cells all over the animal's body and does not provide a directional shielding comparable to that provided by the black pigment containing cells within asteroid or holothuroid eyes.

The lack of echinoid photoreceptors associated with shielding pigment is certainly the main reason why these cells have been overlooked for so long. Additionally, the question arises how the animals are capable of directed phototaxis. As *S. purpuratus* lacks pigment cells associated with its PRCs, the animal must have evolved an alternative mechanism, which provides screening of light. A referring model adressing this prerequisite will be discussed later in this chapter.

The lack of associated screening pigment is not the only feature distuingishing echinoid from asteroid and holothuroid PRCs. Whereas on cellular level similarities can be recognized, the morphological arrangement of the echinoid photoreceptors contrasts strongly to that of PRCs in the other two echinoderm phyla. Whereas in asteroids and holothuroids the PRCs constitute typical “eye-organs” the echinoid PRCs show a much more dispersed pattern within the tube foot disc with a maximum of 3-4 cells per epidermal bulge clustering together. The PRC cluster at the base of locomotory tube feet

is comprised of a much higher number of single PRCs. Nevertheless they are not part of a distinct “eye-organ”, but simply group together in close association and connect to the nervous system.

Interestingly, this ganglion has been described by Millott and Coleman (1969) in the context of the tube foot base being the most photosensitive region of the sea urchin epidermis (Millott 1954) The authors describe a glandular pit (podial pit) associated with a ganglion to form the so called “podial organ”. From the presented histological and TEM data it is unfortunately not possible to assess, whether the described structure in fact represents the PRC cluster at the base of the tube feet, or not. However, the reported localization of this “podial ganglion” fits precisely to the obtained CLSM data on *S. purpuratus* basal PRCs. Yoshida in his 1966 review presents an unpublished TEM picture by Kawaguti and Ikemoto that clearly displays an array of neighboring thin cell projections within a cross section of a podial organ cell that might well belong to a microvillar receptor cell.

4.3. R-opsin positive PRCs in optic cushions of *A. rubens*

Classifying a photoreceptor type through its morphology adds one important piece to the puzzle while exploring an unknown photoreceptor system. The fact that echinoid PRCs comprise a morphologically very similar photoreceptor type to the one being present in asteroid and holothuroid optic organs already hints on a shared origin and function for these PRCs in the three echinoderm phyla. To determine the function of the newly discovered echinoid PRCs turned out to be rather complicated. The enormous amount of tube feet present in the adult animal and the relatively bad accessibility of the PRC clusters within them hampered direct investigation of the PRC function.

Attempts were made to check if an operated adult sea urchin, deprived of tube feet within a certain epidermal area and then illuminated exclusively in the operated area with the same light source that otherwise elicited negative phototaxis, would react differently from unoperated ones. For this purpose, all tube feet of a certain area were cut off as close to the skeleton as possible and a black foil cone was glued around this operated zone with surgical tissue glue. Unfortunately, while operating all tube feet, the remaining epidermis and spines were destroyed in such a way that the experimental outcome would have shown reaction of the animal upon removal of the whole epidermis that might involve other receptors then the tube feet alone. Additionally the standard procedures in such an experimental design include recovery of operated animals for a couple of days before experiment performance. But the operated sea urchins all managed to strip off the glued foil cones within a maximum of two days, possibly due to the remaining humidity of their epidermis that effects the surgical tissue glue effectivity.

Molecular experiments examining the function of the tube feet PRCs were not realizable as these would typically include some kind of gene knockdown process using an anti *Sp-opsin4* RNA directed morpholino. These morpholinos (complementary RNA strands, that block translation of the corresponding protein) can only be injected into the freshly fertilized egg of the echinoids. The *Sp-opsin4* expressing PRCs first develop with the start of larval rudiment formation which in *S. purpuratus* sets on after several weeks of development of the free swimming larvae (Hyman 1955, Davidson et al. 1998, Smith et al. 2008). As to my knowledge, there is no description of a successful experiment knocking down a RNA transcript that is expressed a couple of weeks after injection of the complementing morpholino which subsequently degrades after injection.

Thus the attempt to find out something about the *S. purpuratus* PRC function was bound to rely on indirect evidence from experiments with other echinoderms.

As mentioned earlier, asteroid optic cushions are the only echinoderm optic organs that have been demonstrated to play a role in phototaxis (Yoshida and Ohtsuki 1968). The authors performed behavioral experiments on *Asterias rubens*, in which phototaxis in the animals was tested with and without dissection of the optic cushions. After optic cushion removal, the animals show a strongly reduced phototaxis but are still responsive and able to detect the direction of incoming light. The authors thus draw the conclusion that whereas the optic cushions are the main receptor units regarding phototaxis, a second, extra- or non-ocular photoreceptor system must coexist in this species. These findings substantiate earlier findings of Yoshida and Othsuki (1966) on relative efficiency of light in inducing downward movements of isolated arm tips of *Asterias amurensis*. Their findings of different maxima in operated versus non operated armtips also show the optic cushions to be the primarly, but not the only receptor organ used for phototaxis. Takasu and Yoshida (1983) added evidence to the hypothesis of a light related function of the optic cushions by showing that not only the microvillar length and arrangement of the receptor cells changed considerably in dark versus light adapted specimen, a fact that had already been shown earlier by Eakin and Brandenburger (1979), but also that the amount of intramembranous particles of the receptive microvilli changed strongly under different light regimes in contrast to the constant amount of those particles within other portions of the presumed photoreceptor.

Asteroid optic cushions therefore constituted a promising target for attempting a first cross-species immunohistochemical experiment deploying the Sp-Opsin4 antibody. Indeed, optic cushions of juvenile *Asterias rubens* turned out to show a positive immunoreaction to the *S. purpuratus* specific r-opsin antibody. The stainings appeared not as brilliant as those in echinoid tube feet but this may be due to the arrangement of the photoreceptor cells within the optic cushions, where they are deeply embedded and

covered by a layer of 12 or more “corneal cells” and an additional mucoid coat or cuticle (Eakin and Brandenburger 1979).

Clear immunoreaction against the echinoid rhabdomeric opsin in an asteroid optic organ that on various occasions has been shown to mediate phototaxis strongly indicates a similar function of rhabdomeric opsin positive PRCs in echinoids, too.

These results also corroborate the finding of Johnsen (1997) who demonstrated immunoreactivity of a bovine rhodopsin within the optic cushions of *Asterias forbesi*. The bovine rhodopsin stainings yielded very diffuse immunostainings which is probably due to the fact that (i) the vertebrate species (*Bos bos*) against which this opsin antibody was designed is only very distantly related to echinoderms, and (ii) because bovine rhodopsin belongs to the ciliary opsins being expressed within vertebrate rod photoreceptors.

Bearing in mind that a certain cross reactivity of antibodies (e.g. between r-opsins and c-opsins) applied in animals that are only distantly related to the immunizing species is likely to occur, I tested the *A. rubens* optic cushions for immunoreactivity against the echinoid ciliary opsin Sp-Opsin1. The results documented function of the ciliary opsin antibody in *A. rubens* by showing c-opsin presence in spine cells (see later section of this chapter), but the asteroid optic cushions showed no staining after Sp-Opsin1 incubation. As the control experiments show that only the r-opsin is present within *A. rubens* optic cushions it is most likely that the r-opsin expressing PRCs mediate the phototaxis.

The Sp-Opsin4 antibody stainings in *A. rubens* also confirmed the results of earlier authors that an additional PRC system is present in this species. The labeling of additional Sp-Opsin4 positive cells in the aboral epidermis as well as in tube feet discs of the juvenile starfish substantiate the proposed second PRC system of Yoshida and Ohtsuki (1966, 1968) but also the findings of Rockstein (1956) p. 341, who demonstrated the presence of a similar “photosensitive chemical component” within optic cushion PRCs and cells of the aboral epidermis.

With its cross species reactivity, the Sp-Opsin4 antibody thus provides an excellent tool for future investigations not only on echinoid, but also on asteroid PRC systems.

4.4. Echinoid PRCs and their connection to the nervous system

Former studies regarding the nervous system of echinoderms have shown them to possess a huge variety of what was interpreted as primary sensory neurons, distributed within the epidermis (Bullock and Horridge 1965, Cobb 1970, Cobb and Pentreath 1977, Cameron and Mackie 1996). As a result, the echinoderm nervous system was often described to be of a simple nerve net type, comparable to that in cnidarians (Hyman 1955, Smith 1965, for review see Burke 2011). Recent studies deploying molecular tools for tracking neuron specific proteins and RNA do not provide evidence for that view (Burke et

al. 2006, Diaz-Balzac et al. 2007, Nomaksteinsky et al. 2009). On the contrary, from the emerging data it can be concluded that the sea urchin nervous system is much more centralized and sophisticated then previously assumed (Burke 2011).

The microvillar photoreceptors described within echinoid tube feet are all connected to the animal`s nervous system. The disc PRCs project axons into branches of the distal tube foot nerve whereas the basal PRCs project axons into the most proximal portion of the tube foot nerve and its extension, the lateral nerve, leading towards the radial nerve through the tube foot ampulla. In early juveniles the basal PRCs have been demonstrated to project axons as far as into the developing radial nerves. With regard to the nervous system this PRC arrangement is unique among metazoans. Whereas many PRCs in Bilateria are directly connected to the central nervous system (CNS), the axons of echinoids seem to project into a more peripheral part of the nervous system. However, the evaluation of echinoid PRCs integrating into the animals nervous system largely depends on homology hypotheses regarding the echinoderm nervous system. In general, the echinoderm nervous system as well as the whole adult animal organization is considered to show extremely derived characters compared to a hypothesized deuterostome ancestor (Cameron et al. 2000, Smith 2008). Many authors for more then 100 years have doubted that these animals possess anything comparable to a CNS and have described their nervous and sensory system to be of a rather primitive type (for review see Burke 2011) All the more interesting is a scenario recently proposed by Burke (2011) in which he concludes from newly emerged molecular data, that echinoderms share a centralized nervous system with all other deuterostomes as a heritage from their last common ancestor. His conclusion is amongst other recent findings based on the model drawn by Raff and Popodi (1996) and Smith (2005) that an originally single axial nervous system was present within the echinoderm stem group, which later duplicated via a radial metamerism. That means that each of the five radial nerves would comprise a functional CNS (unit).

According to this hypothesis, the former statement of echinoid PRCs integrating into a more peripheral part of the animals nervous system has to be re-evaluated. At least in the case of the basal tube foot PRC cluster shown to project axons directly into the radial nerves during their development, these PRCs would then indeed directly connect to the animal`s “CNS”. Given this direct connection, an integrational mode beyond local short circuits must be hypothesized for these PRCs. Taking into account the more distal position of the tube foot disc PRCs which have been shown to lack any connection to the radial nerves throughout development, it is tempting to suggest a different function for these PRCs. If one assumes a CNS function for the echinoderm radial nerves, an

interesting question is if and how the oral nerve ring which interconnects the radial nerves is involved in photobehavior.

Burke (2011) states that the radial nerves are connected at their proximal ends with a set of comissures that form a ring surrounding the mouth, citing Cobb (1970), p. 112, who demonstrated “that these are simple tracts of connecting axons lacking neuronal cell bodies and do not constitute a neuronal integration centre”.

Although Burke´s model comprises an attractive hypothesis on deuterostome CNS evolution, applied to the indeed scarce knowledge on photobehavior it bears some critical points.

Physiological studies showed that radial nerves as well as the oral nerve ring are essential for phototaxis in asteroids and echinoids. Millott and Yoshida (1959) thus showed that dissection of the radial nerve abolishes light elicited spine reactions in *Diadema antillarum*. Yoshida and associates (unpublished but reviewed in Yoshida 1966) show that in *Temnopleurus toreumaticus* separation of the radial nerve from the nerve ring abolishes phototaxis in that sector. Yoshida and Othsuki (1968) demonstrated phototaxis in the asteroid *Asterias amurensis* to depend on the presence of the oral nerve ring, and Holmes (1912) showed that the oral nerve ring is essential for negative phototaxis in *Arbacia punctulata*.

The latter three findings conflict with the model proposed by Burke (2011): in the context of photoreception there must at least be some integrational function within the oral nerve ring. Alternatively, the oral nerve ring mediates data processing that depends on interaction of more than one radial nerve cord.

4.5. An alternative PRC shielding mechanism in echinoids

When not attached to a surface, sea urchin tube feet are highly mobile and constantly sway around. Thus the PRCs in the rim of the tube foot disc will receive light from almost all directions. As the EM studies showed, they lack any screening pigment, i.e. even a minimum spatial resolution accounting for directed phototaxis cannot be inferred from the existing data. Nevertheless, some of the reported photoreactions within tube feet may not require a sophisticated shading mechanism to e.g. simply differentiate between local light intensities. This could apply for the rapid tube foot shortening reported either upon illumination as in *Arbacia punctulata* (see Holmes 1912) and *Asterias* sp. (see Moore 1921) or upon shading as in *Diadema antillarum* (Millott 1954) and *Psammechinus miliaris* (Millott and Yoshida 1956). Such local reflex responses, probably occuring in the context of predator avoidance, could potentially be mediated by the tube foot disc PRCs.

After cancelling the tube foot disc PRCs from the list of phototaxis related PRC candidates in echinoids, the attention shifted to the second PRC cluster. Contrasting to the disc PRCs, the PRCs at the tube foot base are not subjected to such intense movements but keep their position close to the animal skeleton. The calcite skeleton of *S. purpuratus* provides shielding to one side of this basal PRC cluster. Depending on the position of the tube foot protruding from an oral, lateral or aboral part of the skeleton, the skeleton provides a varying shading angle to the basal tube foot PRC cluster. With the idea of the skeleton comprising a light shielding device at hand, I examined the area of tube foot attachment to the skeletal surface. It was interesting to observe that the tube foot pore bearing the tube foot nerve always shows an additional depression where the tube foot nerve enters the skeleton. Although this structure is well documented e.g. by Smith (1978, 1980) for many different echinoid species, it has so far not attracted any attention in the context of photoreception. Although Millott and Coleman (1969) already examined the tube foot base of *Diadema antillarum* in regard to a potentially photosensory organ (“the podial organ”), the skeletal depression within the investigated area was obviously not noticed. The overlay projection of a decalcified piece of *S. purpuratus* epidermis showing an Sp-opsin4 immunostaining on top of a SEM picture of the corresponding area of a piece of intact skeleton shows that a reasonable portion of the basal tube foot PRCs seems to fit into the invagination that is formed by the upper tube foot nerve channel portion. Certainly some PRCs are located outside of this depression, but it has to be kept in mind that (i) there are tissue artefacts resulting from specimen treatment during decalcification, general fixation and the immunostaining procedure, (ii) two different specimens were used for the experiment.

According to Land and Nilsson (2002) there are two features of an eye´s function that reciprocally determine its performance. These two features are resolution and sensitivity. Sensitivity refers to the ability of an eye to get enough light to the photoreceptors to make full use of the eyes potential resolution. This ability partly depends on the deployed photoreceptor cell type (Fain et al. 2010) and also on potential eye components like e.g. lenses which focus light onto the receptor cells (Land 2005).

Sensitivity will not be evaluated any further in this thesis since apart from the deployed PRC type no structures that might function as “lenses” or optical filters were detected in the vicinity of the basal tube foot clusters.

In fact, the idea arising from the SEM observations on the tube foot insertion area focussed on the “resolution” component of the PRC cluster. Land and Nilsson (2002) again defined resolution as the precision with which an eye splits up light in respect to the direction of its origin. This precision is defined by the quality of the image provided by the optics, and the fineness of the mosaic of the retinal detectors.

Although many of the above listed components for optical performance so far remain unclear in echinoids, the question was whether the skeletal depression would provide a sufficient screening off angle for the *S. purpuratus* basal PRC cluster to allow the animal to detect the direction of incoming light and thus to perform phototaxis?

X-ray microtomography was thus used to exactly determine the 3D morphology of the skeletal pore depression. The smallest opening angle of the tube foot nerve channel depression measured within several tube foot pores of seven virtual cross sections was 88°. This minimum opening angle thus results within a maximum shading angle of up to 272° for the majority of PRCs within the basal tube foot cluster. This unusual combination of a skeletal component which embeds epidermal PRCs within a shading cavity might functionally resemble the PRC/shading arrangement within single-chambered simple pit eyes of flat worms (Plathelminthes), annelids, molluscs and many invertebrate larvae (Land 2005). According to Land's definition, the echinoid basal PRC arrangement does fulfill the definition of an “eye”: “At its simplest, an eye might consist of a small number of light-responsive receptors in a pigmented pit, which shadows some receptors from light in one direction, and others from a different direction” (Land 2005: p. R319). Even spatial vision (to a certain degree) could be achieved through such an eye-organ as spatial vision does require “the simultaneous comparison of light intensities in different directions (Land 2005: p. R319, see also Land and Nilsson 2002). I therefore hypothesize that the basal PRC clusters in the echinoid *S. purpuratus* fulfill the minimum requirements needed for directional vision and phototaxis .

Additional support for the skeleton comprising an essential component of the photoreceptive system in echinoids comes from data regarding the onset of phototaxis in juvenile *S. purpuratus* and *Paracentrotus lividus* (M.I. Arnone, personal communication). In both species, presence of Sp-Opsin4 protein has been detected as early as within the future adult rudiment when it was still enclosed in the larvae. However, despite presence of the photopigment in tube foot disc and basal PRCs even before metamorphosis, tested freshly metamorphosed juveniles do not show phototactic behavior. The skeleton of juvenile sea urchins develops following a complicated mechanism termed “Lovén´s rule”, named after Sven Lovén who first unraveled this intricate pattern (David et al. 1995, Märkel 1975, 1976). Simply speaking, Lovén's rule says that new coronal plates always arise at the oral side of the juvenile, pushing the older ones to a more aboral portion of the developing echinoid. After a certain time thus a round and closed skeleton has formed to which later more and more plates are added and the existing plates elongate laterally to account for proportional growth of the animal. The phototaxis experiments of Arnone et al. (personal communication) demonstrate that neither *S. purpuratus* nor *P. lividus* show any phototaxis until their skeletogenesis is complete with a sufficient number of skeletal plates

having formed to build a closed, roundish skeleton. From this time (around 1 month in both species), the animals show clear negative phototaxis when exposed to full spectrum artificial light.

To exclude as many alternative factors causing the late onset of phototaxis as possible, Arnone et al. (personal communication) also tested the sea urchins for presence and/or lack of the ciliary opsin Sp-Opsin1 in the non-photoreactive echinoid juveniles. Sp-Opsin1 is the second opsin that might potentially be involved in vision as it clusters with the ciliary opsins that mediate chordate vision (Raible et al. 2006). But a late onset of Sp-Opsin1 expression can be excluded as potential reason for the late onset of phototaxis, since this opsin protein, similar to the rhabdomeric opsin, is already present in the future adult rudiment in late larval stages of both tested echinoid species.

It is thus reasonable to speculate that the echinoid skeleton comprises an integral component necessary to realise the animal's phototactic behavior.

4.6. The visual PRC system - a resulting model for echinoid phototaxis

Analysis of the previously presented data results in a model of the echinoid visional photoreceptor system to function like a huge compound eye. A large amount of unusual “detector units” composed of r-opsin positive microvillar photoreceptor cells embedded in a “shadowing pit” of the echinoid skeleton detects differences in light intensity relative to the animal's body position. Light input from the basal PRCs conducted and processed via the radial nerves and most probably the oral nerve ring interconnecting them, would then enable the echinoid to perform directed movement when illuminated from a certain direction.

4.7. A different “compound eye” model in echinoids

In the past, although lacking any structural evidence for distinct PRCs, different authors have already suggested a “compound eye model” for echinoderm vision.

Woodley (1982) studying photobehavior of the tropical echinoid *Diadema antillarum* first suggested that the entire animal functions as a compound eye, with the spines screening off light from certain angles. Similarly, Blevins and Johnsen (2004) introduced their model for two different echinoid species of the genus *Echinometra* (*E. lucunter* and *E. viridis*) which they showed to possess a certain degree of spatial vision. To test for spatial vision they placed individual echinoids in a round tank with diffuse overhead illumination and presented dark objects of different sizes at the periphery of this tank. The ability to detect and move towards those different targets was taken as indication of spatial vision. In this experimental design, the two *Echinometra* species showed significant orientation towards the presented object with a minimum positively tested angular width of 33°. Subsequent

work on *S. purpuratus* led to the hypothesis that this echinoid species might have a higher spatial resolution than the *Echinometra* species, because the *S. purpuratus* body bears approximately 2-3 times more spines (Yerramilli and Johnsen 2010). By deploying the same experimental design, the authors recorded movement of the animals to smaller objects than in *E. lucunter* and *E. viridis*, interpreted as spatial vision with an even higher optical resolution (minimum positively tested angular width that elicited orientation towards dark target being 10°) than in *Echinometra*.

Both studies were based on the assumption that, according to the long hypothesized "diffuse" dermal light sense in echinoderms (Hyman 1955, Millot 1975, Yoshida et al. 1984), the whole body surface of the echinoids would be equally photosensitive. The spatial resolution of the PRC system would then depend on the spacing of spines that function, similarly to pigment cells in insect ommatidia, by shading defined parts of the sea urchin's skin.

Contrasting to this hypothesis, the findings of well separated clusters of distinct PRCs contradict the prerequisite of the model proposed by Blevins and Johnsen (2004) and Yerramilli and Johnsen (2010). The documented morphological arrangement of r-opsin positive microvillar PRCs in the bases of locomotory tube feet indicates a much higher photosensitivity in the ambulacral regions where the tube feet are protruding. This is in accordance with the findings of Millott (1954) that photosensitivity in *Diadema antillarum* is greatest at the ambulacral margins and decreases towards the ambulacral center. The interambulacrum comprises the least sensitive body area of this species. Millott's findings thus nicely correlate with the location of the tube feet (at the ambulacral margins) and are even further supported by his later findings demonstrating that the podial bases in echinoids comprise the most photosensitive part of their skin (Millott and Coleman 1969).

The findings of Millott (1954) and Milott and Coleman (1969) are not considered in the "compound eye" model of Blevins and Johnsen (2004). Instead, by using the average spine number of 100-150 as supposed to be present within the two *Echinometra* species , a mean angular distribution of 12-16° for the spines in regard to the skeletal surface is calculated. In the following it is inferred from signal theory that details can be observed over angles that are double the angular resolution of the detector. Thus the predicted spatial resolution is 24-32°, suggesting that the spines may be responsible for the observed resolution." (Blevins and Johnsen 2004, p. 4253). The authors show a figure depicting light reaching the body surface within the "acceptance angle" between two spines that are located horizontally next to each other and thus include the ambulacral portion in between two vertically arranged tube foot rows. The measured spine angles in both analyses (Blevins and Johnsen 2004, Yerramilli and Johnsen 2010) do only include the spine angles measured within the ambulacrum and within the interambulacrum, but

not the angle between ambulacral and interambulacral spines, which, according to my findings, would be the basis for an accurate measurement of the spines shading the photoreceptors. In *Echinometra*, this angle (see Fig. 4A in Blevins and Johnsen 2004) measure around 20° and thus does not add to the author's arguments for spine shading determining resolution in echinoid spatial vision.

Nevertheless, the role of spine shading and its potential influence on certain visional abilities in echinoids cannot be ruled out completely. However, the finding that the echinoid basal PRC cluster is embedded in a “shading-pit” formed by the skeleton challenges the “compound eye” model of Johnsen and co-workers by clearly disproving the prerequisite of their model, i.e. the existence of an overall dermal light sense. If and how the basal PRC clusters might account for the experimental findings of Yerramilli and Johnsen (2010) has to be shown with a new model, which implements the new structural data and additional parameters like e.g. the species specific number and arrangement of tube feet.

It was demonstrated via the Sp-Opsin4 antibody that other echinoid species possess the same type of photoreceptor cells. Arnone et al. (personal communication) showed presence of the basal Sp-Opsin4 tube foot cluster in the two mediterranean echinoid species *P. lividus* and *Arbacia lixula*. Furthermore, they report different phototaxis speed rates for *P. lividus* and *A. lixula* tested within the same experimental setting as used for *S. purpuratus*. While *P. lividus* shows a much faster phototactic reaction than *S. purpuratus*, *A. lixula* displays a considerably slower response under the same illumination regime. Although phototaxis is not necessarily correlated with spatial vision, both photobehaviors prerequisite the ability to differentiate the direction of incoming light (Land and Nilsson 2002). Obviously, the morphology of *P. lividus* and *A. lixula* is different. *A. lixula* has only a small number of tube feet compared to *P. lividus*, and their arrangement within the skeleton is considerably different. It is obvious that these positional data have to be implemented in a new model for echinoid spatial vision. Additionally, the differences in skeletal composition have to be considered.

Preliminary SEM results show differences in stereom composition between *S. purpuratus* and *E. lucunter*. The stereom trabeculae of *S. purpuratus* are more solid resulting in a rather massive corona. Although in the living animal the intercalcite spaces of the skeleton are filled with cells and do not form “empty spaces”, it can be assumed that the more massive calcite structure of the *S. purpuratus* corona has better shielding properties then the more delicate skeleton of *E. lucunter*. From the existing data it is impossible to evaluate the direct impact of those skeletal differences for echinoid directional vision, but it will be interesting to include these structural stereom parameters into a future predictive model for echinoid photosensitivity.

4.8. R-opsin protein localization in ophiuroid tube feet

Interestingly, a third “compound eye” model for an echinoderm is based on the proposed photoreceptor system of certain ophiuroids (Hendler 1984, Aizenberg et al. 2001). Aizenberg and co-workers experimentally demonstrated that specialized calcite skeletal structures in the armplates of light sensitive *Ophiocoma wendtii* guide and focus light onto deeper tissues of the animal. Two closely related species that are light-indifferent were shown to lack such structures. The PRCs deployed in that scenario remained completely unknown except for their assumed position within a bundle of nerve cells underlying the arm ossicles in the focal plane of the “microlenses”. The actual “compound eye” was hypothesized to be comprised of a huge array of such lens- and photosensitive nerve cell units within the animal’s arms.

Immunostainings against the *S. purpuratus* specific rhabdomeric opsin in the ophiuroid *Amphiura filiformis* so far did not show any immunoreaction substantiating the findings of Aizenberg et al. (2001). However, it is important to note here that *A. filiformis* (i) is not closely related to any of the ophiuroid species examined by (Hendler 1984, Aizenberg et al. 2001), (ii) has a different morphology, and (iii) exhibits a completely different lifestyle. Whereas *O. wendtii* is a highly mobile species inhabiting rocky areas, *A. filiformis* is dug into the sediment, exposing only two or three of its arm tips into the water column above the substratum. It would thus not be surprising if the morphological arangement of PRCs varies between those two spieces.

The obtained Sp-Opsin4 immunostainings in *A. filiformis* show presence of an r-opsin within the tube feet of the ophiuroid. Two distinct regions show immunoreactivity, one in the very tip of the tube foot showing a cone shaped morphology and the second one in a more basal area of the tube foot. These findings coincide with the finding of r-opsin in two regions of the echinoid tube feet, although it is of course not possible to evaluate distinct ultrastructural PRC features from the immunostainings. The third albeit weaker r-opsin staining was detected within the radial nerve of *A. filiformis*. This staining is the only one that might possibly be associated with a photoreceptor system as proposed by Aizenberg et al. (2001). Through the decalcification procedure and the relatively large size of the examined adult arm it is unfortunately not possible to determine the exact localization of the Sp-Opsin4 staining within the radial nerve. Analyses of z-stacks of the recorded r-opsin staining indicate its presence within a central portion of the radial nerve cord that would thus not coincide with the localization of the presumed PRCs of *O. wendtii.* According to the model, the PRCs of *O. wendtii* would have to be embedded in a nerve bundle located at the focal plane of the microlenses (Aizenberg et al. 2001). This nerve bundle is localized below the dorsal arm plates and thus clearly aboral and distinct from the radial nerve (Biressi et al. 2010). It can be concluded that, in *A. filiformis* the r-opsin

positive PRCs are unlikely to be the ones necessary for the Aizenberg model, since they are situated in a different region of the ophiuroid arms..

Rosenberg and Lundberg (2004) demonstrate that the activity pattern of *A. filiformis* is clearly related to photoperiodicity. The animals show low or no activity at daytime and high activity at night. Although the authors assume a possible existence of a kind of PRC system as proposed by Aizenberg et al. (2001), the question remains, whether the different behavioral patterns, namely changing diurnal activity in *A. filiformis versus* flight reaction upon shading in *O. wendtii* depend on the same photoreceptor system, or not. Based on the first localizations of the ciliary opsin Sp-Opsin1 in echinoids, asteroids and ophiuroids presented here, a different interpretation will be discussed in one of the following sections.

Rosenberg and Lundberg (2004), besides recording the mentioned diurnal activity difference of *A. filiformis* arms in their natural habitat, also performed laboratory experiments within which they demonstrated that the arms of *A. filiformis* start changing activity within the first 15 minutes after the light was switched on and off, respectively. This activity change was shown to continue over a period of 1—2 hours.

According to these results, the deployed PRCs do not necessarily have to show a very fast response. In fact, they do not even have to be capable of determining the direction of illumination and thus would not depend on a shading “device”. A scenario as described by the authors could simply rely on a PRC type that is able to measure the intensity of illumination. *A. filiformis* was studied in the wild at a water depth of 30 meters. Thus, light intensities reaching this depth are relatively low compared to terrestrial conditions. The functional advantage of rhabdomeric PRCs over ciliary PRCs with regard to determination of light intensities in this kind of environment is nicely reviewed in Fain et al. (2010). According to these authors, microvillar PRCs do show an extremely high sensitivity and, in contrast to ciliary PRCs, are able to detect single photons. This is an advantage for differentiating diurnal cycles in the ambient dim light conditions found in deeper water. As a result, the detected Sp-Opsin4 positive PRCs in the tube feet of *A. filiformis* are potential candidate PRCs mediating the photoactivity pattern described by Rosenberg and Lundberg (2004).

4.9. C-opsin protein localization in echinoid pedicellaria and tube feet

Since it was known from the *S. purpuratus* genome analysis (Sodergren et al. 2006) and different expression analyses (Burke et al. 2006, Raible et al. 2006) that this echinoid species possesses more than one expressed opsin protein it could be assumed that the animals possess more then one PRC type. It was thus not surprising to detect c-opsin positive cells in different tissues of *S. purpuratus*; however, the morphological characters of the Sp-Opsin1 positive PRCs revealed by CLSM leave many questions open and demand further investigation deploying additional molecular markers and ultrastructural analyses.

In *S. purpuratus*, the most prominent localization of the ciliary opsin is within tridentate pedicellaria, but it is also present in locomotory tube feet and radial nerves. M.I. Arnone (personal communication) furthermore reports presence of Sp-Opsin1 in buccal tube feet and spine bases. Except for the radial nerves, the Sp-Opsin1 immunolabeled cells share a common structural feature - they show a distinct striated morphology.

For echinoid globiferous pedicellaria it has been demonstrated that a neuropil is present within each valve of the pedicellarian head. It recieves input from primary sensory cells and in turn sends a pair of nerve tracts into the stalk. As bifurcation may occur, those neuropils supply the stalk with up to 12 longitudinal nerves. Interestingly, these longitudinal nerves bypass the echinoderm typical basiepidermal nerve plexus and instead project to a neuropil encircling the base of the pedicellaria (Peters and Campbell 1987, Ghyoot and Jangoux 1988, reviewed in Cavey and Märkel 1994). Although these observations were obtained from globiferous pedicellaria, the description of neuronal projections fits precisely to the acetylated-alpha-tubulin immunolabelings of the *S. purpuratus* tridentate pedicellarian head neuropil and the nerve strands within the neck region.

The staining pattern within the pedicellarian head does not reveal a clear picture on cellular level, but it shows striated Sp-Opsin1 positive structures within the same region as the nerve strands of the neuropil. In contrast, examination of CLSM z-stacks reveals the Sp-Opsin1 labeling of striated fibres in the pedicellarian neck to be clearly more internal compared to the acetylated alpha-tubulin stained nerve strands. A prominent cell type present within both regions of ciliary opsin localization are muscle cells. In fact, the documented striated patterns of the immunostaining fit the position of adductor and abductor muscles within the pedicellarian valves, and of longitudinal flexor muscles in the pedicellarian neck region (Scheme by M. Stauber, cited in Cavey and Märkel 1994).

Similar striated, fibre-like Sp-Opsin1 positive cells occur in the locomotory tube feet of adult *S. purpuratus*. The overall staining shows much background due to the high amplification gain deployed while recording the CLSM pictures. Nevertheless, when amplified, the stainings seem to be specific as they show similar striated structures like

those present in pedicellaria. The weakness of these immunostaining intensities compared to the very clear and prominent labelings of the rhabdomeric opsin possibly mirrors different quantitative diferences in protein content. In adult tube feet of S. purpuratus *Sp-opsin1* expression has shown to be low in comparison to that of *Sp-opsin4* (Burke et al. 2006, Raible et al. 2006). Comparable to the situation in pedicellaria, muscles are present within the region of ciliary opsin detection in tube feet (Coleman 1969a, Florey and Cahill 1980). In the tube foot stalk these muscle fibres reside internally compared to the basiepithelial nerve plexus (see Florey and Cahill 1980). This non-epidermal location correlates with the Sp-Opsin1 immunostaining recorded for the adult locomotory tube foot stalk in *S. purpuratus*. The morphology of the Sp-Opsin1 positive region in the tube foot disc also nicely correlates with the arrangement of muscles documented in the tube foot sucker of *Diadema antillarum* (Fig.1, Coleman 1969b) and *Sphaerechinus granularis* (Flammang and Jangoux 1993). The latter authors document two different muscle systems within the tube foot disc of coronal (= locomotory) tube feet, i.e. the retractor and the levator system. The retractor muscle consists of the end of the podial stem retractor muscle which anchors to the connective layer of the rosette (the distal part of the disc- supporting skeleton). The levator muscle connects the frame (proximal portion of the disc-supporting skeleton) with the median part of the central area of the disc. The ciliary opsin stainings documented in the *S. purpuratus* tube foot disc show a considerable correspondence to this described disc muscle system.

M.I. Arnone (personal communication) documented Sp-Opsin1 positive cells in spine bases. These stainings again correlate with the muscle arrangement documented at the spine base of *Diadema antillarum* by Millott and Takahashi (1963) and several other Mediterranean echinoid species (see Stauber and Märkel 1988).

At the first glance, presence of a ciliary opsin within muscle cells is an unexpected result, given the fact that so far opsin proteins have never been found in muscle cells of any animal. However, light triggered muscle reactions have been documented in the literature, e.g. within the lantern muscles of echinoids (Boltt and Ewer 1963). The question remained, whether these reactions were indeed triggered by some photopigment incorporated within the muscle cells themselves or by nerve cells associated with them. Recent findings of Diaz-Balzac et al. (2010) might shed a new light on this question and might also be interesting in the context of the observed ciliary opsin localization in *S. purpuratus*. The authors used a whole set of antibodies directed against various nervous system components to study the neuroanatomy of the holothuroid *Holothuria glabberima* and found labeling of different muscular tissues. They interpreted this as presence of a large number of nerve fibres that appear to be innervating the muscle fibres and thus for the

first time described the possible motor pathway responsible for the innervation of the echinoderm muscle system.

At the current state of knowledge it is impossible to decide whether the ciliary opsin protein is localized in extremely fine nerve cells pervading the musculature or rather by the muscle cells themselves. It is nevertheless interesting to consider the general possibility of a set of muscle cells being intrinsically photosensitive, or alternatively being directly innervated by light sensitive neurons in close vicinity in the context of the long proposed diffuse “dermal light sense” in echinoderms. Many echinoderms show reactions upon shading of their body or certain areas of it. Many of the resulting behavioral patterns have been described as local reflex responses (for review see Yoshida 1966). Tube foot withdrawel upon shading (Millott 1954, Millott and Yoshida 1956) falls into that category, so do local muscle contractions upon shading as reported e.g. in holothuroids (Hess 1915, Crozier 1915). In these cases a direct and local interaction of receptors and effectors that are either located closely together or indeed combined within a single cell type, would be advantageous to mediate fast and direct response to local stimuli.

4.10. Presence of c-opsin in the echinoid radial nerve

At this point the detection of Sp-Opsin1 in the radial nerves of *S. purpuratus* shall be discussed. Within the radial nerves, distinct clusters of Sp-Opsin1 positive PRCs were found. Their morphology does not equal the external stainings within the echinoid appendages. Instead, a whole cell complex - with the dark areas most presumably being the embedded nuclei - seems to exhibit broad immunoreactivity to the applied c-opsin antibody.

Millott (1963) and Millott and Yoshida (1960a) demonstrated that illumination and especially shading of defined spots of the radial nerve in *Diadema antillarum* elicits spine erections in a defined area. Their findings demonstrate presence of a functioning PRC system within the radial nerves of this sea urchin. To date, there is no proof that the presence of the Sp-Opsin1 protein within radial nerves correlates with the PRC system that was stimulated in the above mentioned experiments. Nevertheless the hypothesis of the echinoid ciliary opsin mediating the documented shadow reactions is attractive. Concluding from the phylogenetic opsin analysis of Raible et al. (2006) the *S. purpuratus* c-opsin clusters with other c-opsins expressed by animals belonging to different phyla and their c-opsins serving different functions. Interestingly, Kusakabe and Tsuda (2007), reviewing the photoreceptor systems of ascidian tadpole larvae, report on typical “shadow responses” in which an abrupt decrease in light intensity elicits active larval swimming. The visual pigment of the larval ocellus of *Ciona intestinalis* is Ci-Opsin1 (Kusakabe and Tsuda 2007) which in phylogenetic analyses also clusters within the group of c-opsins

(Terakita 2005, Kusakabe and Tsuda 2007). A similar shadow response is present in larvae of teleosts and amphibians (Blaxter 1969, Roberts 1978) and (Kusakabe and Tsuda 2007) state that the shadow response in young *Xenopus* larvae is mediated by the pineal eye.

If c-opsins of other animals and/or their larval stages, which phylogenetically cluster with the echinoid c-opsin, do elicit shadow reactions, a similar function in echinoids and even echinoderms in general can possibly be assumed.

It has been a matter of long debate (for detailed review see Yoshida (1966) and Millott (1975)), why an internal echinoid tissue, that is shielded from incoming light by opaque skeletal plates and a pigmented epidermis should deploy functioning PRCs. A possible explanation might arise from the potential similarity of the echinoid c-opsin deploying PRC system to those in ascidian larval ocelli and in pineal eyes of teleost and amphibian larvae. Kusakabe and Tsuda (2007: p. 251) state that “both the ascidian ocellus and the pineal eye are the first photoreceptor organs that become functional during ontogeny”. Accordingly, in the *Xenopus* tadpole the pineal eye triggers the shadow response at a time when its developing lateral eyes are not yet capable of responding to the light stimulus (Foster and Roberts 1982).

The responsiveness to shading within the radial nerves inside the corona of echinoids may thus be a result of the ontogeny of the PRC system. Within the first weeks of juvenile development, echinoids do not possess a closed skeleton and they do not perform phototaxis (see above). During this period the young echinoid juveniles thus can not seek for shelter deploying phototactic abilities. But as long as their calcite skeleton is not closed, light can reach the animal's radial nerves. When suddenly shaded by an approaching predator, a spine erection of the tiny and relatively unprotected young juvenile can be imagined as a potential defensive behavior to avoid predation.

4.11. C-opsin protein localization in ophiuroid and asteroid spines

Presence of a ciliary opsin has also been demonstrated for spines of *A. rubens* and *A. filiformis*. The obtained immunolabeling patterns differ from those observed for Sp-Opsin1 in *S. purpuratus*. Contrasting to the striated c-opsin positive fibers in the echinoid, the asteroid and ophiuroid representatives show distinct Sp-Opsin1 labeling within their spines. The immunolabeling in spines of *A. rubens* corresponds to the bovine rhodopsin staining documented for *Asterias forbesi* spine tips by Johnsen (1987). In *A. rubens* the c-opsin immunopositive PRCs seem to be located within the spine epidermis, whereas in *A. filiformis* they are located deeper within the spine tissue. Many ophiuroids possess spines that show a “conspicious hollow” (Byrne 1994: p. 284) with the central space occupied by the axial nerve. The co-labeling of acetylated-alpha-tubulin and ciliary opsin might well

correspond to a position inside the calcite spine cylinder. For echinoids that also posess hollow spines in many species, it has been demonstrated that the long anatomical spine axis and the optical axis (c-axis) coincide (Raup 1966). PRCs embedded within those spines, as in the ophiuroid *A. filiformis*, may provide some focussing mechanism through the spine ossicle. This is reminiscent of the results of Aizenberg et al. (2001) who (i) also propose a light focussing mechanism provided by specialized structures of the ophiuroid sceleton and (ii) assume that the hypothesized PRCs in their photoreception scenario mediate a shadow response in *O. wendtii*, a potential feature of c-opsin PRCs hypothesized for echinoids in the previous section of this discussion. As *A. filiformis* and *O. wendtii* exhibit a completely different lifestyle, the absence of c-opsin protein from the arm ossicles of *A. filiformis* does not exclude that this PRC type might be deployed associated with the arm ossicles *of O. wendtii*.

4.12. Evolutionary implications within Echinodermata

Echinoderm phylogeny has challenged many researchers in the past (Ax 2001). The five major echinoderm subgroups show a variety of derived characters, probably due to a long time of divergent evolution dating back as far as the Cambrian (Nielsen 2001). Morphological (Nielsen 2001, Brusca and Brusca 2003) and molecular approaches (Littlewood et al. 2007, Mallatt and Winchell 2007) thus still come up with different sistergroup relationships depending on the mode of analysis. The traditional view based on morphological data proposes a sistergroup relationship of Crinoidea and Eleutherozoa, the latter comprising the Monophyla Echinoidea + Holothuroidea and Asteroida + Ophiurida. Alternatively, Asteroidea are proposed as sistergroup of the remaining eleutherozoan taxa (Ax 2001).

The presence of r-opsin positive PRCs within tube feet of representatives of Echinoidea, Asteroidea and Ophiuroidea indicates that the association of the characterized PRC type with podia is a more general phenomenon in echinoderms. Presence of the examined r-opsin positive PRC types may thus be hypothesized for the ground pattern of Eleutherozoa sensu Ax (2001). Additionally, ontogenetic data point in this direction: The asteroid optic cushions are situated at the basis of the animal's terminal tentacles, which arise from the first developing primary podia (Morris et al. 2009, Atwood 1973) Homology of the respective r-opsin expressing asteroid PRCs to the echinoid PRCs is evidenced by a similar microvillar design and the positive immunoreactivity to the anti Sp-Opsin4 antibody. The microvillar PRCs in the eyes of synaptid holothurians reside in the feeding tentacles, which also arise from the first developing primary podia (Yamamoto and Yoshida 1978). However, with immunohistochemical data on holothuroid ocelli still

missing, the hypothesis of the r-opsin positive PRC types for the eleutherozoan ancestor still remains to be tested.

The presence of pigmented supporting cells in Asteroidea as well as in Holothuroidea reflects the starndard design of simple pigmented eyes and may represent the ancestral condition. Pigmentation of the “eye-organ” would then have been lost in Echinoidea where shading pigment was functionally replaced by the underlying calcite skeleton.

4.13. Evolutionary implications within Deuterostomia

Compared with r-opsin positive PRCs of protostome animals, which usually form part of cerebral eyes, the echinoid tube foot PRCs stand out by their patchy distribution across the body. However, as recent molecular data led to hypothesize a CNS like function for the echinoid radial nerves (Burke 2011), at least at the echinoid basl tube foot r-opsin positive PRCs show a close association with a (very derived) kind of “brain”. The expression of a whole set of genes involved in patterning vertebrate retinal development also in the tube feet of *S. purpuratus* (Burke et al. 2006) plus the fact that the r-opsin positive tube foot PRCs form within an expression domain of *pax6* (M.I. Arnone, personal communication), is an argument for an evolutionary link between the newly discovered r-opsin positve PRC in sea urchin tube feet and r-opsin positive PRCs of other animals.

The former view that microvillar PRCs are exclusively present in protostome eyes (Eakin 1979, 1982) has been qualified by molecular photoreceptor research (Arendt 2003). While vertebrates have lately been shown to possess r-opsin expressing PRCs in their retina (Provencio et al. 2000, Hattar et al. 2002, Rollag et al. 2003, Fu et al. 2005, Bellingham et al. 2006), deuterostome animals have been generally thought to deploy ciliary type PRCs for vision (Eakin 1982). In morphological research, vertebrate r-opsin expressing PRCs have been overlooked for a long time due to their lack of any specialized membrane enlargement and they are clearly not deployed for vision. Instead, they mediate the pupillar reflex and entrain the circadian clock. The few known examples of deuterostome animals possessing microvillar PRCs comprise tornarian larvae of the enteropneust *Ptychodera flava* (Brandenburger et al. 1973) and *Balanoglossus proterogonius* (Nezlin and Yushin 2004), *Branchiostoma* with its Joseph cells and Hesse eyecups (Lacalli 2004, Koyanagi et al. 2005, Nasi and del Pilar Gomez 2009, Gomez et al. 2009), the tunicate salp *Salpa democratia* (Gorman et al. 1971) and the asteroids with their optic cushions (Eakin and Brandenburger 1979, Penn and Alexander 1980). With the single exception of asteroid optic cushions, none of the other microvillar PRCs has been shown to be involved in vision. This unavoidably leads to the question of when during evolution, the functional shift between microvillar PRCs used for vision (as in most protostomes and in asteroids) and their non-visual function in vertebrates, might have taken place.

The presented and discussed data provide evidence of microvillar, r-opsin expressing PRCs acting as visual photoreceptors in a deuterostome, non-vertebrate animal. It is thus proposed that the visual function of the r-opsin positive type of PRCs has to be considered ancestral not only for protostomes, but also for deuterostomes and the bilaterian ancestor. Due to similar gene regulatory networks in protostome and vertebrate eye development, this type of PRC most probably already formed part of a cerebral eye system in their last common ancestor. In deuterostomes, visual function was maintained in the lineage leading to echinoderms, but at least in sea urchins the cells were considerably re-organized and a unique compound-eye-like mode of data processing emerged. In the lineage leading to vertebrates, the PRCs kept their position in cerebral eyes, but now became involved in circadian rhythms. According to the presented data, this dramatic functional shift occurred no earlier than during the emergence of chordates.

5. References

Aizenberg J, Tkachenko A, Weiner S, Addadi L, Hendler G (2001) Calcitic microlenses as part of the photoreceptor system in brittlestars. Nature 412: 819-822.

Arboleda Herrera E (2008) Photoreception in the purple sea urchin *Strongylocentrotus purpuratus*: insights into opsin evolution. Unpublished PhD-Thesis, Open University of London, 123 pp.

Arendt D (2003) Evolution of eyes and photoreceptor cell types. International Journal of Developmental Biology 47: 563-571.

Arendt D (2008) The evolution of cell types in animals: emerging principles from molecular studies. Nature Reviews Genetics 9: 868-882.

Arendt D, Tessmar-Raible K, Snyman H, Dorresteijn AW, Wittbrodt J (2004) Ciliary photoreceptors with a vertebrate-type opsin in an invertebrate brain. Science 306: 869-871.

Arendt D, Wittbrodt J (2001) Reconstructing the eyes of Urbilateria. Philosophical Transactions of the Royal Society London B 356: 1545-1563.

Atwood DG (1973) Larval development in the asteroid *Echinaster echinophorus*. Biological Bulletin 144:1-11.

Ax P (2001) Das System der Metazoa III. Spektrum, Heidelberg.

Bellingham J, Chaurasia SS, Melyan Z, Liu C, Cameron MA, Tarttelin EE, Iuvone PM, Hankins MW, Tosini G, Lucas RJ (2006) Evolution of melanopsin photoreceptors: discovery and characterization of a new melanopsin in nonmammalian vertebrates. PLOS Biology 4: 1334-1343.

Biressi ACM, Zou T, Dupont S, Dahlberg C, Di Benedetto C, Bonasoro F, Thorndyke M,·Candia Carnevali, MD (2010) Wound healing and arm regeneration in *Ophioderma longicaudum* and *Amphiura filiformis* (Ophiuroidea, Echinodermata): comparative morphogenesis and histogenesis. Zoomorphology 129: 1-19.

Blaxter, J. H. S. (1969) Visual thresholds and spectral sensitivity offlatfish larvae. J. Exp. Biol. 51, 221–230.

Blest AD (1988) The turnover of phototransductive membrane in compound eyes and ocelli. Advanced Insect Physiology 20: 1-54.

Blevins E, Johnsen S (2004) Spatial vision in the echinoid genus Echinometra. Journal of Experimental Biology 207: 4249-4253.

Boltt RE, Ewer DW (1963) Studies on the myoneural physiology of Echinodermata. Journal of Experimental Biology 40:713-726.

Brandenburger JL, Woollacott LM, Eakin RM (1973) Fine structure of eyespots in tornarian larvae (Phylum: Hemichordata). Cell and Tissue Research 142: 89-102.

Brusca RC, Brusca GJ (2003) Invertebrates, 2nd ed. Sinauer, Sunderland.

Bullock T, Horridge G (1965) Structure and function in the nervous systems of invertebrates. W.H. Freeman, San Francisco, USA.

Burke RD (1980) Podial sesory receptors and the induction of metamorphosis in echinoids. Journal of Experimental Marine Biology and Ecology 47: 223-234.

Burke RD (2011) Deuterestome neuroanatomy and the body plan paradox. Evolution and Development 13: 110-115.

Burke RD, Angerer LM, Elphick MR, Humphrey GW, Yaguchi S, Kiyama T, Liang S, Mu X, Agca C, Klein WH, Brandhorst BP, Rowe M, Wilson K, Churcher AM, Taylor JS, Chen N, Murray G, Wang D, Mellott D, Olinski R, Hallböök F, Thorndyke MC (2006) A genomic view of the sea urchin nervous system. Developmental Biology 300: 434-460.

Byrne M (1994) Ophiuroidea. In: Harrison FW, Chia FS (eds) Microscopic Anatomy of Invertebrates, Vol. 14: Echinodermata. Wiley-Liss, New York, pp. 274-343.

Cameron CB, Mackie GO (1996) Conduction pathways in the nervous system of *Saccoglossus* sp. (Enteropneusta). Canadian Journal of Zoology 74: 15-19.

Cameron CB, Garey JR, Swalla BJ (2000) Evolution of the chordate body plan: new insights from phylogenetic analyses of deuterostome phyla. Proceedings of the National Academy of Sciences USA 97: 4469-4474.

Campbell AC, Laverick MS (1968) The responses of pedicellaria from *Echinus esculentus* L. Journal of Experimental Marine Biology and Ecology 2: 191-214.

Cavey MJ, Märkel K (1994) Echinoidea In: Harrison FW, Chia FS (eds) Microscopic Anatomy of Invertebrates, Vol. 14: Echinodermata. Wiley-Liss, New York, pp. 345-400.

Cobb JLS (1970) Significance of radial nerve cords in asteroids and echinoids. Cell and Tissue Research 108: 457-474.

Cobb JLS, Pentreath VW (1977) Anatomical studies of simple invertebrate synapses utilizing stage rotation electron-microscopy and densitometry. Tissue and Cell 9: 125-135.

Cobb JLS (1987) Neurobiology of Echinodermata. In: Ali MA (ed) Nervous systems of invertebrates. Plenum Press, New York, pp. 483-525.

Coleman R (1969a) Ultrastructure of the tube foot wall of a regular echinoid, *Diadema antillarum* Philippi. Cell and Tissue Research 96: 162-172.

Coleman R (1969b) Ultrastructure of the tube foot sucker of a regular echinoid, *Diadema antillarum* Philippi, with a special reference to secretory cells. Cell and Tissue Research 96: 151-161.

Cowles RP (1909) The movement of the starfish, *Echinaster*, toward the light. Zoologischer Anzeiger 35: 193-195.

Cowles RP (1910) Stimuli produced by light and by contact with solid walls as factors in the behavior of ophiuroids. Journal of Experimental Zoology 9: 387-416.

Cowles RP (1911) Reaction to light and other points in the behavior of the starfish. Publications of the Carnegian Institutions 3: 95-110.

Crozier WJ (1915) The sensory reactions of *Holothuria surinamensis* Ludwig. Zoologischer Jahrbücher, Abt. Systematik, Geographie und Biologie der Tiere 35: 233-297.

Czerny T, Busslinger M (1995) DNA-binding and transactivation properties of Pax-6: three amino acids in the paired domain are responsible for the different sequence recognition of Pax-6 and BSAP (Pax-5). Molecular and Cellular Biology 15: 2858-2871.

David B, Mooi R, Telford M (1995) The ontogenetic basis of Lovén's rule clarifies homologies of the echinoid peristome. In: Emson , Smith, Campbell (eds) Echinoderm Research, Balkema, Rotterdam, pp. 155-164.

Davidson EH, Cameron RA, Ransick A (1998) Specification of cell fate in the sea urchin embryo: summary and some proposed mechanisms. Development 125: 3269-3290.

Diaz-Balzac CA, Santacana-Laffitte G, San Miguel-Ruíz JE, Tossas K, Valentín-Tirado G, Rives-Sánchez M, Mesleh A, Torres II, García-Arrarás JE (2007) Identification of nerve plexi in connective tissues of the sea cucumber *Holothuria glaberima* by using a novel nerve-specific antibody. Biological Bulletin 213: 28-42.

Diaz-Balzac CA, Lasaro-Pena MI, Garcia-Arraras JE (2010) Subdivision of the echionoderm nervous system as defined by antibody probes. FASEB Journal 24: 642.6.

Diebschlag E (1938) Ganzheitliches Verhalten und Lernen bei Echinodermen. Zeitschrift für vergleichende Physiologie 25: 612-654.

Eakin RM (1979) Evolutionary Significance of Photoreceptors: In Retrospect. American Zoologist 19: 647-653.

Eakin RM (1982) Continuity and diversity in photoreceptors. In Westfall J (ed) Visual Cells in Evolution, Raven Press, New York, pp 91-105.

Eakin RM, Brandenburger JL (1979) Effects of light on ocelli of seastars. Zoomorphology 92: 191-200.

Fernald RD (2006) Casting a genetic light on the evolution of eyes. Science 29: 1914-1918.

Fain GL, Hardie R, Laughlin SB (2010) Phototransduction and the evolution of photoreceptors. Current Biology 20: R114-R124.

Flammang P, Jangoux M (1993) Functional morphology of coronal and peristomeal podia in *Sphaerechinus granularis* (Echinodermata, Echinoida). Zoomorphology 113: 47-60.

Florey E, Cahill MA (1980) Cholinergic motor control of sea urchin tube feet: evidence for chemical transmission without synapses. Journal of Experimental Biology 88: 281-292.

Foster RG, Roberts A (1982) The pineal eye in *Xenopus laevis* embryos and larvae: A photoreceptor with a direct excitatory effect on behaviour. Journal of Comparative Physiology 145: 413–419.

Fredriksson R, Lagerström MC, Lundin L-G, Schiöth HB (2003) The g-protein-coupled receptors in the human genome form five main families. Phylogenetic nalysis, paralogon groups, and fingerprints. Molecular Pharmacology 63: 1256-1272.

Fu Y, Liao HW, Tri H Do M, Yau KW (2005) Non-image-forming ocular photoreception in vertebrates. Current Opinion in Neurobiology 15: 415–422.

Gehring WJ (2002) The genetic control of eye development and its implications for the evolution of the various eye-types. International Journal of Developmental Biology 46: 65-73.

Gehring WJ, Ikeo K (1999) Pax 6: mastering eye morphogenesis and eye evolution. Trends in Genetics 15: 371-377.

Ghyoot M, Jangoux M (1988) The fine structure of the globiferous pedicellariae of Shpherechinus granularis (Echinoidea): Innervation of the stalk. In Burke RD, Mladenov PV, Lambert P, Parsley RL (eds) Echinoderm Biology. Balkema, Rotterdam, pp. 713-717.

Ghyoot M, De Ridder C, Jangoux M (1987) Fine structure and presumed functions of the pedicellariae of *Echinocardium cordatum* (Echinodermata, Echinoida). Zoomorphology 106: 279-288.

Giese AC, Farmanfarmaian A (1963) Resistance of the purple sea urchin to osmotic stress. Biological Bulletin 124: 182-192.

Goldschmid A (2007) Echinodermata. In Westheide W, Rieger R (eds) Spezielle Zoologie, Bd.1 Einzeller und Wirbellose Tiere. Spektrum, Heidelberg, pp. 778-827.

Gomez M, Angueyra JM, Nasi E (2009) Light-transduction in melanopsin-expressing photoreceptors of amphioxus. Proceedings of the National Academy of Sciences USA 106: 9081-9086.

Goodwin TW, Srisukh S (1950) A study of the pigments of the sea-urchins, *Echinus esculentus* L.and *Paracentrotus lividus* Lamarck. Biochemical Journal 47: 69-76.

Gorman ALF, McReynolds JS, Barnes SN (1971) Photoreceptors in primitive chordates: fine structure, hyperpolarizing receptor potentials, and evolution. Science 172: 1052-1054.

Hattar S, Liao HW, Takao M, Berson DM, Yau KW (2002) Melanopsin-Containing Retinal Ganglion Cells: Architecture, Projections, and Intrinsic Photosensitivity. Science 295: 1065-1070.

Hayat MA (2000) Principles and techniques of electron microscopy: biological applications. 4th edition. Cambridge University Press, Cambridge.

Hendler G (1984) Brittle star color-change and phototaxis (Echinodermata, Ophiuroidea, Ophiocomidae). PSZNI Marine Ecology 5: 379-401.

Hendler G, Byrne M (1987) Fine structure of the dorsal arm plate of *Ophiocoma wendti*: evidence for a photoreceptor system (Echinodermata, Ophiuroidea). Zoomorphology 107: 261-272.

Hess C (1915) Untersuchungen über den Lichtsinn bei Echinodermen. Pflügers Archiv für die gesamte Physiologie des Menschen und der Tiere 160: 1-26.

Holmes SJ (1912) Phototaxis in the sea urchin *Arbacia*. Journal of Animal Behaviour 2: 126-136.

Hyman LH (1955) The Invertebrates Vol. IV: Echinodermata. Mc-Graw-Hill, New York.

Johnsen S (1994) Extraocular sensitivity to polarized light in an echinoderm. Journal of Experimental Biology 195: 281-291.

Johnsen S (1997) Identification and localization of a possible rhodopsin in the echinoderms *Asterias forbesi* (Asteroidea) and *Ophioderma brevispinum* (Ophiuroidea). Biological Bulletin 193: 97-105.

Johnsen S, Kier WM (1999) Shade-seeking behaviour under polarized light by the brittle star *Ophioderma brevispinum* (Echinodermata: Ophiuroidea). Journal of the Marine Biological Association of the UK 9: 761-763.

Koyanagi M, Kubokawa K, Tsukamoto H, Shishida Y, Terakita A (2005) Cephalochordate Melanopsin: Evolutionary Linkage between Invertebrate Visual Cells and Vertebrate Photosensitive Retinal Ganglion Cells. Current Biology 15: 1065–1069.

Kleinholz LH (1938) Color changes in echinoderms. Pubblicazzione de la Stazione Zoologica di Napoli 17: 53-57.

Kusakabe T, Tsuda M (2007) Photoreceptive systems in ascidians. Photochemistry and Photobiology 83: 248-252.

Lacalli TC (2004) Sensory Systems in *Amphioxus*: A Window on the Ancestral Chordate Condition. Brain, Behavior and Evolution 64: 148–162.

Land MF (2005) The optical structures of animal eyes. Current Biology 15: R319-R323.

Land MF, Nilsson DE (2002) Animal Eyes. Oxford University Press, New York.

Littlewood DTJ, Smith AB, Clough KA, Emson RH (1997) The interrelationships of the echinoderm classes: morphological and molecular evidence. Biological Journal of the Linnean Society 61: 409-438.

Märkel K (1975) Wachstum des Coronarskelettes von *Paracentrotus lividus* Lamarck (Echinodermata, Echinoidea). Zoomorphology 82: 259-280.

Märkel K (1976) Struktur und Wachstum des Coronarskelettes von Arbacia lixula Linné (Echinodermata, Echinoidea). Zoomorphology 84: 279-299.

Mallatt J & Winchell CJ 2007 Ribosomal RNA genes and deuterostome phylogeny revisited: more cyclostomes, elasmobranchs, reptiles, and a brittle star. Molecular Phylogenetics and Evolution 43: 1005–1022.

Mangold E (1909) Sinnesphysiologische Studien an Echinodermen. Zeitschrift für allgemeine Physiologie 9: 112-146.

Millott N (1952) Colour change in the echinoid *Diadema antillarum* Philippi. Nature 170: 325-326.

Millott N (1953) Light emission and light perception in species of *Diadema*. Nature 171: 973-973.

Millott N (1954) Sensitivity to light and the reactions to changes in light intensity of the echinoid, *Diadema antillarum* Philippi. Philosophical Transactions of the Royal Society London B 238: 187-220.

Millott N (1960) The photosensitivity of sea urchins. In: Allan MB (ed) Comparative biochemistry of photoreactive systems. Academic Press, New York, pp. 279-293.

Millott N (1963) Spine movements in response to photic stimuli and their implications, in the echinoid *Diadema*. Proceedings of the 16th International Congress of Zoology 3: 118-119.

Millott N (1966) Co-ordination of spine movement in echinoids. In: Boolootian RA (ed) Physiology of Echinodermata. Interscience, New York, pp. 465-485.

Millott N (1975) The Photosensitivity of Echinoids. Advances in Marine Biology 13: 1-52.

Millott N, Coleman R (1969) The Podial Pit- a new Structure in the Echinoid *Diadema antillarum* Philippi. Cell and Tissue Research 95: 187-197.

Millott N, Manly BM (1961) Iridophores of the echinoid *Diadema antillarum*. Quarterly Journal of Microscopical Science 102: 181-194.

Millott N, Takahashi K (1963) The shadow reaction of *Diadema antillarum* Philippi. IV. Spine movements and their implications. Philosophical Transactions of the Royal Society London B 246: 437-469.

Millott N, Yoshida M (1956) Reactions to Shading in the Sea Urchin *Psammechinus miliaris* (Gmelin). Nature 178: 1300.

Millott N ,Yoshida M (1959) The photosensitivity of the sea urchin *Diadema antillarum* Philippi: responses to increases in light intensity. Proceedings of the Zoological Society London 133: 67-71.

Millott N, Yoshida M (1960a) The shadow reaction of *Diadema antillarum* Philippi. I. The spine response and its relation to the stimulus. Journal of Experimental Biology 37: 363-375.

Millott and Yoshida (1960b) The shadow reaction of *Diadema antillarum* Philippi. II. Inhibition by light. Journal of Experimental Biology 37: 376-389.

Mooi R, David B, Ray GA (2005) Arrays in rays: Terminal addition in echinoderms and its correlation with gene expression. Evolution and Development 7: 542-555.

Moore AR (1921) Stereotropic orientation of the tube feet of starfish (*Asterias*) and its inhibition by light. Journal of General Physiology 4: 163-169.

Moore A, Cobb JLS (1985) Neurophysiological studies on photic responses in *Ophiura ophiura*. Comparative Biochemistry and Physiology 80A: 11-16.

Morris VB, Selvakumaraswamy P, Whan R, Byrne M (2009) Development of the five primary podia from the coeloms of a sea star larva: homology with the echinoid

echinoderms and other deuterostomes. Proceedings of the Royal Society London B 276: 1277-1284.

Nakajima Y, Kaneko H, Murray G, Burke RD (2004) Divergent patterns of neural development in larval echinoids and asteroids. Evolution and Development 6: 95-104.

Nasi E, del Pilar Gomez M (2009) Melanopsin-mediated light-sensing in *Amphioxus*: a glimpse of the microvillar photoreceptor lineage within the deuterostomia. Communicative and Integrative Biology 2: 441-443.

Nezlin LP, Yushin VV (2004) Structure of the nervous system in the tornaria larva of *Balanoglossus proterogonius* (Hemichordata: Enteropneusta) and its phylogenetic implications. Zoomorphology 123: 1–13.

Nielsen C (2001) Animal evolution – interrelationships of the living phyla. Oxford University Press, New York.

Nomaksteinsky M, Röttinger E, Dufour HD, Chettouh Z, Lowe CJ, Martindale MQ, Brunet JF (2009) Centralization of the deuterostome nervous system predates chordates. Current Biology 19: 1264-1269.

O'Connell MG, Alender CB, Wood EM (1974) A fine structure study of venom gland cells in globiferous pedicellariae from *Strongylocentrotus purpuratus* (Stimpson). Journal of Morphology 142: 411-432.

Passamaneck YJ, Furchheim N, Hejnol A, Martindale MQ, Lüter C (2011) Ciliary photoreceptors in the cerebral eyes of a protostome larva. EvoDevo 2: 6.

Pearse JS, Pearse VB, Davis KK (1986) Photoperiodic regulation of gametogenesis and growth in the sea urchin *Strongylocentrotus purpuratus*. Journal of Experimental Zoology 237: 107-118.

Penn PE, Alexander CG (1980) Fine structure of the optic cushion in the asteroid *Nepanthia belcheri*. Marine Biology 58: 51-256.

Peters BH, Campbell AC (1987) Morphology of the nervous and muscular systems in the heads of pedicellariae from the sea urchin *Echinus esculentus* L. Journal of Morphology 193: 35-51.

Provencio I, Rodriguez R, Jiang G, Pär Hayes W, Moreira EF, Rollag MD (2000) A Novel Human Opsin in the Inner Retina. Journal of Neuroscience 20: 600-605.

Purschke G, Arendt D, Hausen H, Müller MCM (2006) Photoreceptor cells and eyes in Annelida. Arthropod Structure and Development 35: 211-230.

Raff RA, Popodi EM (1996) Evolutionary approaches to analysing development. In: Ferraris JD, Palumbi SR (eds) Molecular Zoology: Advances, Strategies, and Protocols. Wiley Liss, New York, pp. 245-265.

Raible F, Tessmar-Raible K, Arboleda E, Kaller T, Bork P, Arendt D, Arnone MI (2006) Opsins and clusters of G-protein coupled receptors in the sea urchin genome. Developmental Biology 300: 461-475.

Raup DM (1966) The endoskeleton. In: Boolootian RA (ed) Physiology of Echinodermata. Interscience, New York, pp. 379-395.

Reynolds ES (1963) The use of lead citrate at high pH as an electron-opaque stain in electron microscopy. Journal of Cell Biology 17: 208-212.

Rockstein M (1956) Role of the terminal pigment spots of the starfish, *Asterias forbesi*, in light orientation. Nature 177: 341-342.

Roberts A (1978) Pineal eye and behavioiur in *Xenopus* tadpoles. Nature 273: 774-775.

Rollag MD, Berson DM, Provencio I (2003) Melanopsin, Ganglion-Cell Photoreceptors, and Mammalian Photoentrainment. Journal of Biological Rhythms 18: 227-234.

Rosenberg R, Lundberg L (2004) Photoperiodic activity pattern in the brittle star *Amphiura filiformis*. Marine Biology 145: 651-656.

Salwini-Plawen L v (1982) On the polyphyletic origin of photoreceptors. In: Westfall JE (ed) Visual cells in evolution. Raven Press, New York, pp. 137-154.

Salvini-Plawen L v, Mayr E (1977) On the evolution of photoreceptors and eyes. In: Hecht MK, Steere WC, Wallace B (eds) Evolutionary Biology. Plenum Press, New York, pp. 207-263.

Sarasin PB, Sarasin CF (1887) Die Augen und das Integument der Diadematiden. Ergebnisse naturwissenschaflicher Forschung auf Ceylon. C.W. Kreidel, Wiesbaden, pp. 1-18.

Sharp DT, Gray IE (1962) Studies on factors effecting the local distribution of two sea urchins, *Arbacia punctulata* and *Lytechinus variegatus*. Ecology 43: 309-313.

Smith JE (1965) Echinodermata. In Bullock TH, Horridge GA (eds) Structure and function in the nervous systems of invertebrates, Vol. II. W.H. Freeman, London, pp. 1519-1558.

Smith AB (1978) A functional classification of the coronal pores of regular echinoids. Palaeontology 21: 759-789.

Smith AB (1980) The structure, function, and evolution of tube feet and ambulacral pores in irregular echinoids. Palaeontology 23: 39-83.

Smith AB (2005) The pre-radial history of echinoderms. Geological Journal 40: 255-280.

Smith MM, Smith LC, Cameron RA, Urry LA (2008) The larval stages of the sea urchin *Strongylocentrotus purpuratus*. Journal of Morphology 269: 713-733.

Sodergren E, Weinstock GM, Davidson EH, Cameron RA, Gibbs RA, Angerer RC, Angerer LM, Arnone MI, Burgess DR, Burke RD, Coffman JA, Dean M, Elphick MR, Ettensohn CA, Foltz KR, Hamdoun A, Hynes RO, Klein WH, Marzluff W, McClay DR, Morris RL, Mushegian A, Rast JP, Smith LC, Thorndyke MC, Vacquier VD, Wessel GM, Wray G, Zhang L, Elsik CG, Ermolaeva O, Hlavina W, Hofmann G, Kitts P, Landrum MJ, Mackey AJ, Maglott D, Panopoulou G, Poustka AJ, Pruitt K, Sapojnikov V, Song X, Souvorov A, Solovyev V, Wei Z, Whittaker CA, Worley K, Durbin KJ, Shen Y, Fedrigo O, Garfield D, Haygood R, Primus A, Satija R, Severson T, Gonzalez-Garay ML, Jackson AR, Milosavljevic A, Tong M, Killian CE, Livingston BT, Wilt FH, Adams N, Bellé R, Carbonneau S, Cheung R, Cormier P, Cosson B, Croce J, Fernandez-Guerra A, Genevière AM, Goel M, Kelkar H, Morales J, Mulner-Lorillon O, Robertson AJ, Goldstone JV, Cole B, Epel D, Gold B, Hahn ME, Howard-Ashby M, Scally M, Stegeman JJ, Allgood EL, Cool J, Judkins KM, McCafferty SS, Musante AM, Obar RA, Rawson AP, Rossetti BJ, Gibbons IR, Hoffman MP, Leone A, Istrail S, Materna SC, Samanta MP, Stolc V, Tongprasit W, Tu Q, Bergeron KF, Brandhorst BP, Whittle J, Berney K, Bottjer DJ, Calestani C, Peterson K, Chow E, Yuan QA, Elhaik E, Graur D, Reese JT, Bosdet I, Heesun S, Marra MA, Schein J, Anderson MK, Brockton V, Buckley KM, Cohen AH, Fugmann SD, Hibino T, Loza-Coll M, Majeske AJ, Messier C, Nair SV, Pancer Z, Terwilliger DP, Agca C, Arboleda E, Chen N, Churcher AM, Hallböök F, Humphrey GW, Idris MM, Kiyama T, Liang S, Mellott D, Mu X, Murray G, Olinski RP, Raible F, Rowe M, Taylor JS, Tessmar-Raible K, Wang D, Wilson KH, Yaguchi S, Gaasterland T, Galindo BE, Gunaratne HJ, Juliano C, Kinukawa M, Moy GW, Neill AT, Nomura M, Raisch M, Reade A, Roux MM, Song JL, Su YH, Townley IK, Voronina E, Wong JL, Amore G, Branno M, Brown ER, Cavalieri V, Duboc V, Duloquin L, Flytzanis C, Gache C, Lapraz F, Lepage T, Locascio A, Martinez P, Matassi G, Matranga V, Range R, Rizzo F, Röttinger E, Beane W, Bradham C, Byrum C, Glenn T, Hussain S, Manning G, Miranda E, Thomason R, Walton K, Wikramanayke A, Wu SY, Xu R, Brown CT, Chen L, Gray RF, Lee PY, Nam J, Oliveri P, Smith J, Muzny D, Bell S, Chacko J, Cree A, Curry S, Davis C, Dinh H, Dugan-Rocha S, Fowler J, Gill R, Hamilton C, Hernandez J, Hines S, Hume J, Jackson L, Jolivet A, Kovar C, Lee S, Lewis L, Miner G, Morgan M, Nazareth LV, Okwuonu G, Parker D, Pu LL, Thorn R, Wright R (2006) The genome of the sea urchin *Strongylocentrotus purpuratus*. Science 314, 941-952.

Stauber M, Märkel K (1988) Comparative morphology of uscle-skeleton attachments in the Echinodermata. Zoomorphology 108: 137-148.

Takasu N, Yoshida M (1983) Photic effects on photosensory microvilli in the seastar Asterias amurensis (Echinodermata: Asteroida). Zoomorphology 103: 135-148.

Tan E, Wang Q, Quiambao AB, Xu X, Qtaishat NM, Peachey NS, Lem J, Fliesler, SJ, Pepperberg DR, Naash MI, Al-Ubaidi MR (2001) The relationship between opsin overexpression and photoreceptor degeneration. Investigative Ophtalmology & Visual Science 42: 589-600.

Terakita A (2005) The opsins. Genome Biology 6:213.1-213.9.

Uexküll, J v (1897a) Über Reflexe bei den Seeigeln. Zeitschrift für Biologie 34: 298-318.

Uexküll, J v (1897b) Vergleichend sinnesphysiologische Untersuchungen II. Der Schatten als Reiz für *Centrostephanus longispinus*. Zeitschrift für Biology 34: 319-339.

Uexküll, J v (1900) Die Wirkung von Licht und Schatten auf die Seeigel. Zeitschrift für Biologie 40: 447-476.

Vaupel-von Harnack M (1963) Über den Feinbau des Nervensystems des Seesterns (*Asterias rubens* L.). Cell and Tissue Research 60: 432-451.

Vopalensky P, Kozmik Z (2009) Eye evolution: common use and independent recruitment of genetic components. Philosophical Transactions of the Royal Society London B 364: 2819-2832.

Weel, PB v (1935) Über die Lichtempfindlichkeit der Ambulacralfüßchen des Seesterns (*Asterias rubens*). Archiv Néerlandaises de Zoologie 1: 347-353.

Williams DS (2002) Transport to the photoreceptor outer segment by myosin VIIa and kinesin II. Vision Research 42: 455-462.

Wolfrum U, Schmitt A (2000) Rhodopsin transport in the membrane of the connecting cilium of mammalian photoreceptor cells. Cell Motility and the Cytoskeleton 46: 95-107.

Woodley J D (1982). Photosensitivity in *Diadema antillarum*: does it show scototaxis? In Lawrence JM (ed) Proceedings of the International Echinoderm Conference, Tampa Bay. Balkema, Rotterdam, pp. 61.

Yerramilli D, Johnsen S (2010) Spatial vision in the purple sea urchin *Strongylocentrotus purpuratus* (Echinoidea). Journal of Experimental Biology 213: 249-255.

Yamamoto M & Yoshida M (1978) Fine structure of the ocelli of a synaptid holothurian, *Opheodesoma spectabilis*, and the effects of light and darkness. Zoomorphology 9: 1-17.

Yoshida M (1956) On the light response of the chromatophore of the sea urchin *Diadema setosum* (Leske). Journal of Experimental Biology 33: 119-123.

Yoshida M (1957) Positive phototaxis in *Psammechinus microtuberculatus* (Blainville). Pubblicazione de la Stazione Zoologica di Napoli 30: 260-262.

Yoshida M (1966) Photosensitivity. In Boolootian RA (ed) Physiology of Echinodermata. John Wiley and Sons, New York, pp 435-464.

Yoshida M, Millott N (1959) Light sensitive nerve in an echinoid. Experimentia 15: 13-14.

Yoshida M, Ohtsuki H (1966) Compound ocellus of a starfish: its function. Science 153: 197-198.

Yoshida M, Ohtsuki H (1968) The phototactic behaviour of the starfish *Asterias amurensis* Lütken. Biological Bulletin 134: 516-532.

Yoshida M, Takasu N, Tamotsu S (1984) Photoreception in Echinoderms. In Ali MA (ed) Photoreception and Vision in Invertebrates. Plenum Press, New York, pp 743-772.

6. Summary

Echinodermata is a group of marine non-chordate Deuterostomia with an unusual pentameric adult body plan. Photosensitivity within many species of echinoderms has been documented over the last 150 years but corresponding photoreceptor cells (PRCs) or organs in most cases remained enigmatic. Especially in the case of Echinoidea, which display a huge variety of photo elicited behaviors, no distinct PRC was ever identified. The genome sequencing of the echinoid *Strongylocentrotus purpuratus* and subsequent expression analyses of genes known to be involved in PRC development and differentiation, provided the first time opportunity to investigate echinoid PRCs deploying a new molecular approach. The aim of this study is to localize and characterize PRCs within echinoids and other echinoderms using a combined molecular and morphological approach. Protein and RNA localization of a rhabdomeric opsin (r-opsin), which comprises an essential component in phototransduction and which is expressed in *S. purpuratus* (Sp-opsin4), led to the discovery of two disctinct PRC clusters in the tube feet of this echinoid. Using scanning electron microscopy, transmission electron microscopy plus deployment of anti-Sp-Opsin4 immunogold labeling, the PRC type could be classified as microvillar/ rhabdomeric. Antibody labelings against nervous system (NS) components demonstrated connection of the two echinoid tube foot PRC clusters to the animal's NS. The PRCs lack any associated shielding pigment, but one of the two PRC clusters is embedded in a depression of the echinoid's opaque skeleton that is hypothesized to act as a shielding device for these PRCs. Based on (i) a detailed examination of this skeletal depression deploying x-ray microtomography, (ii) immunoreaction of the echinoid specific r-opsin antibody in asteroid optic cushions known to function in phototaxis, and (iii) onset of phototaxis in *S. purpuratus* juveniles depending on complete skeletogenesis, a model of echinoid vision is proposed, in which the animal functions as a huge “compound eye”. The skeleton shielding the PRCs arranged at the base of tube feet all around the echinoid body causes a limited illumination angle of each PRC cluster. Processing the different photic input of each PRC cluster thus enables the animal to detect the direction of incoming light and perform phototaxis. This study provides first evidence of distinct PRCs in an echinoid and thus challenges the long proposed diffuse “dermal light sense” that was hypothesized to deploy unspecialized neurons of the echinoderm epidermal nerve net. The finding of r-opsins in tube feet PRCs of echinoids, asteroids and ophiuroids indicates homology of the r-opsin positive PRC type throughout these echinoderm groups. Asteroids and most certainly echinoids deploying a microvillar, r-opsin expressing PRC type for vision (phototaxis) as usually realized in protostomes thus contrast to most other deuterostomes in which visional functions are based on ciliary, c-opsin expressing PRCs. The findings of this study thus suggest that the functional shift from rhabdomeric to ciliary PRC systems might have happened as late as in the chordate stemline.

7. Zusammenfassung

Echinodermata (Stachelhäuter) sind eine ausschließlich marine Gruppe wirbelloser Deuterostomia. Im Gegensatz zu den Chordaten besitzen sie als Adulti einen stark abgewandelten, pentameren Körperbau. Photosensitivität in Echinodermen ist seit über 150 Jahren gut dokumentiert, aber die korrespondierenden Augenorgane bzw. Photorezeptorzellen blieben bis heute in den meisten Fällen unbekannt. Dies trifft insbesondere auf Seeigel zu, bei denen trotz einer Vielzahl verschiedener Verhaltensreaktionen auf Lichtreize kein verantwortlicher Photorezeptor gefunden werden konnte. Die Sequenzierung des Genoms von *Strongylocentrotus purpuratus* und anschließende Expressionsanalysen von Genen, die an der Entwicklung und Differenzierung von Photorezeptoren beteiligt sind, bot daher erstmals die Gelegenheit, diese Sinneszellen von Echinodermen mittels molekularbiologischer Methoden zu untersuchen. Das Ziel dieser Arbeit ist dabei, mit Hilfe molekularer und morphologischer Methoden, Photorezeptoren von Echinoiden und anderen Echinodermen zu lokalisieren und zu charakterisieren. Die Protein- und RNA-Lokalisierung eines rhabdomerischen Opsins (r-Opsin: Sp-Opsin4), welches eine essentielle Komponente der Phototransduktion darstellt und in *S. purpuratus* nachweislich exprimiert wird, führte zur Identifizierung zweier Ansammlungen von Photorezeptoren in den Ambulacralfüßchen dieses Seeigels. Mittels raster- und transmissionselektronenmikroskopischer Untersuchungen, sowie Immunfärbungen mit Goldpartikel-konjugierten Antikörpern gegen Sp-Opsin4 auf Ultradünnschnitten, konnte der Photorezeptortyp als microvillär/rhabdomerisch klassifiziert werden. Mittels weiterer Antikörperfärbungen des Nervensystems konnte eine Anbindung der Photorezeptoren an das Nervensystem dokumentiert werden. Die Photorezeptoren besitzen kein assoziiertes Pigment zur gerichteten Abschattung ihrer lichtsensitiven Membranen, stattdessen liegen die Rezeptoren im basalen Teil des Ambulacralfüßchens eingesenkt in eine Vertiefung des Skeletts, für das eine Beschattungsfunktion hypothetisiert wird. Basierend auf Untersuchungen der Morphologie dieser Skelettvertiefung mittels Micro-Computertomographie, sowie dem Nachweis von r-Opsin in den Ocelli von nachgewiesen phototaktisch aktiven Seesternen und der Tatsache, dass der Beginn der Phototaxis in juvenilen Seeigeln mit der vollständigen Skelettbildung korreliert, wird hier ein Modell zum Sehvermögen von Seeigeln postuliert. Das gesamte Tier funktioniert im Kontext von Photosensitivität wie ein großes „Komplexauge“. Das Skelett schattet die Photorezeptoren an der Basis der Ambulacralfüßchen dahingehend ab, dass sich für diese Lichtsinneszellen ein eingeschränkter möglicher Lichteinfallswinkel ergibt. Indem die Information über (unterschiedlich starke) Beleuchtung jeder einzelnen Ansammlung von Sinneszellen über die Oberfläche des gesamten Tieres verrechnet wird, ist der Seeigel in der Lage, die Richtung der Lichtquelle zu ermitteln und entsprechend Phototaxis auszu-

führen. Die vorliegende Untersuchung erbringt den ersten Nachweis distinkter Photozeptoren bei einem Seeigel und stellt damit den seit langem postulierten, diffusen dermalen Lichtsinn in Frage, bei dem unspezialisierte Neurone des epineuralen Nervennetzes als Photorezeptoren vermutet wurden. Da der untersuchte, r-Opsin exprimierende Photorezeptorzelltyp in den Ambulacralfüßchen sowohl von Echinoidea, als auch von Asteroidea und Ophiuroidea nachgewiesen wurde, liegt eine Homologie dieses Zelltyps bei diesen Echinodermengruppen nahe. Die Untersuchung zeigt, dass sowohl Asteroiden als auch sehr wahrscheinlich Echinoiden einen microvillären, r-Opsin exprimierenden Photorezeptorzelltyp zur gerichteten Lichtwahrnehmung nutzen, wie dies die meisten Protostomia tun. Im Gegensatz dazu wurde innerhalb der Deuterostomia Richtungssehen nur über ciliäre, c-Opsin exprimierende Photorezeptoren nachgewiesen. Der Funktionswechsel von microvillären zu ciliären Photorezeptoren im Zusammenhang mit gerichtetem Sehen hat daher wahrscheinlich erst innerhalb der Stammlinie der Chordaten stattgefunden.